

ISTANBUL TECHNICAL UNIVERSITY ★ GRADUATE SCHOOL OF SCIENCE
ENGINEERING AND TECHNOLOGY

**FABRICATION AND CHARACTERIZATION OF POLYETHERSULFONE
(PES)/MULTIWALLED CARBON NANOTUBE HOLLOW FIBER
ULTRAFILTRATION MEMBRANES**

M.Sc. THESIS

Reyhan ŞENGÜR

Department of Nanoscience & Nanoengineering

Nanoscience & Nanoengineering Programme

JANUARY 2013

ISTANBUL TECHNICAL UNIVERSITY ★ GRADUATE SCHOOL OF SCIENCE
ENGINEERING AND TECHNOLOGY

**FABRICATION AND CHARACTERIZATION OF POLYETHERSULFONE
(PES)/MULTIWALLED CARBON NANOTUBE HOLLOW FIBER
ULTRAFILTRATION MEMBRANES**

M.Sc. THESIS

Reyhan ŐENGÜR
(513101017)

Department of Nanoscience & Nanoengineering

Nanoscience & Nanoengineering Programme

Thesis Supervisor: Prof. Dr. İsmail KOYUNCU

JANUARY 2013

İSTANBUL TEKNİK ÜNİVERSİTESİ ★ FEN BİLİMLERİ ENSTİTÜSÜ

**ÇOK DUVARLI KARBON NANOTÜP KATKILI POLİETERSÜLFON (PES)
İÇİ BOŞLUKLU ULTRAFİLTASYON MEMBRAN ÜRETİMİ VE
KARAKTERİZASYONU**

YÜKSEK LİSANS TEZİ

**Reyhan ŞENGÜR
(513101017)**

Nanobilim & Nanomühendislik Anabilim Dalı

Nanobilim & Nanomühendislik Programı

Tez Danışmanı: Prof. Dr. İsmail KOYUNCU

OCAK 2013

To my family and all beloved ones,

FOREWORD

First of all, I would like to thank my thesis supervisor Prof. Dr. İsmail KOYUNCU who shared his knowledge, supported me throughout my thesis and also made me possible to work in MEM-TEK which is a great laboratory. I really enjoyed work in such a great laboratory as MEM-TEK.

I would also like to thank TUBITAK 2210 National Scholarship Programme for MSc Students for their financial support throughout my master programme.

Finally, I would like to say I'm grateful to my co-worker Türker TÜRKEN, Serkan GÜÇLÜ, Dr. Derya KÖSEOĞLU İMER, all other MEM-TEK workers, my friends and of course my great family who are always with me in my whole life.

December 2012

Reyhan ŞENGÜR
(Environmental Engineer)

TABLE OF CONTENTS

	<u>Page</u>
FOREWORD	ix
TABLE OF CONTENTS	xi
ABBREVIATIONS	xiii
LIST OF TABLES	xv
LIST OF FIGURES	xvii
SUMMARY	xxi
ÖZET	xxv
1. INTRODUCTION	1
1.1 Importance of the Study	1
1.2 Mission and Scope of the Study	2
2. LITERATURE REVIEW	3
2.1 Membrane Separation Technology	3
2.1.1 Historical development of membranes	3
2.1.2 Some basic membrane terms.....	3
2.2 Membrane Classification.....	4
2.2 Membrane Fabrication Methods	7
2.3 Fabrication of Hollow Fiber Membranes by Phase Inversion Method	8
2.3.1 Phase inversion membranes fabrication.....	8
2.3.2 Features of hollow fiber membranes.....	10
2.3.3 Phase inversion fabrication methods for hollow fiber membranes.....	11
2.3.3.1 Wet spinning	11
2.3.3.2 Dry Spinning	11
2.3.3.3 Dry-wet spinning.....	12
2.3.3.4 Melt extrusion	13
2.3.4 Theory of hollow fiber spinning by phase inversion	13
2.3.5 Spinning parameters.....	14
2.3.5.1 Type of polymer.....	15
2.3.5.2 Type of solvents	15
2.3.5.3 Type of additives.....	15
2.3.5.4 Air gap length.....	16
2.3.5.5 Viscosity.....	16
2.3.5.6 Dope extrusion rate	17
2.3.5.7 Coagulation bath temperature and composition.....	17
2.3.5.8 Take-up speed	18
2.3.5.9 Bore and outer fluid type.....	18
2.4 Carbon Nanotubes	18
2.5 Polymer/Nanocomposite Hollow Fiber Membrane Studies.....	21
3. MATERIALS & METHODS	23
3.1 Materials	23
3.2 Preparation of Spinning Solution	23

3.2.1 Preparation of dope solutions without MWCNT	23
3.2.2 Prepaion of dope solution with MWCNTs.....	24
3.3 Spinning of Hollow Fiber Membranes	24
3.4 Treatment & Post-treatment of Hollow Fiber Membranes.....	26
3.5 Preparation of Hollow Fiber Test Modules	27
3.6 Membrane Characterization	28
3.6.1 Filtration experiments	28
3.6.1.1 Permeability test.....	28
3.6.2 Fouling experiments.....	29
3.6.5 Stereo microscopy	31
3.6.6 Mechanical stability	32
3.6.7 Scanning electron microscopy (SEM).....	33
3.6.8 Porosity measurements.....	34
3.6.9 Zeta potential of membranes	34
3.6.10 Fourier transformation infrared spectroscopy (FTIR).....	34
3.6.11 Growth of <i>Escherichia Coli</i> (<i>E.Coli</i>) on hollow fiber membranes	35
4. RESULTS & DISCUSSIONS.....	37
4.1 Deciding Dope Solution Recipe	37
4.2 Spinning Conditions	38
4.3 Effect of Viscosity	39
4.4 Morphology of the Membranes	39
4.5 Permeability of Hollow Fiber Membranes	55
4.6 FTIR Spectra	58
4.7 Contact Angle Results	60
4.8 Porosity of Membranes.....	62
4.9 Surface Charge of Fabricated Membranes	64
4.10 Fouling of Membranes	67
4.11 Mechanical Properties of the Membranes	73
4.12 Growth of <i>E.Coli</i> on Hollow Fiber Membranes	75
5. RECOMMENDATIONS & CONCLUSIONS	77
REFERENCES	81
APPENDICES	87
CURRICULUM VITAE.....	101

ABBREVIATIONS

AFM	: Atomic Force Microscopy
BSA	: Bovine Serum Albumin
CNT	: Carbon Nanotube
DMAc	: Dimethylacetamide
DMF	: N,N-dimethylformamide
ε	: Porosity
<i>E. Coli</i>	: <i>Escherichia Coli</i>
FTIR	: Fourier Transformation Infrared
HF	: Hollow Fiber
LiCl	: Lithium Chloride
MD	: Membrane Distillation
MWCNT	: Multiwalled Carbon Nanotube
MWCNT-COOH	: Carboxyl Functionalized Multiwalled Carbon Nanotube
MWCNT-OH	: Hydroxyl Functionalized Multiwalled Carbon Nanotube
MWCO	: Molecular Weight Cut-off
NaOCl	: Sodium Hypochloride
NF	: Nanofiltration
NMP	: 1-methyl-2-pyrrolidone
PAN	: Polyacrylonitrile
PEO	: Polyethyleneoxide
PEG	: Polyethyleneglycol
PES	: Polyethersulfone
PS	: Polysulfone
PVDF	: Polyvinylidenedifluoride
PVP	: Polyvinylpyrrolidone
PWP	: Pure Water Permeability
RO	: Reverse Osmosis
SEM	: Scanning Electron Microscopy
T_g	: Glass Transition Temperature
TiO₂	: Titanium Dioxide
UF	: Ultrafiltration

LIST OF TABLES

	<u>Page</u>
Table 2.1 : Membrane classification.	5
Table 3.1 : Filtration cell specifications.....	28
Table 4.1 : Spinning solution composition trials to optimize hollow fiber spinning process.	37
Table 4.2 : Spinning solution of chosen composition.	38
Table 4.3 : Spinning parameters.....	38
Table 4.4 : Outer and inner diameters of fabricated membranes.	51
Table 4.5 : Elongation at break percentages of fabricated membranes.....	75
Table 5.1 : Membranes were chosen as the best optimized membranes considering all dope solutions and spinning parameters and their properties.....	79

LIST OF FIGURES

	<u>Page</u>
Figure 1.1 : Freshwater availability – current and future	1
Figure 2.1 : Cross-flow and Dead end filtration setup	4
Figure 2.2 : Concentration Polarization.	4
Figure 2.3 : Pressure driven membrane processes.	6
Figure 2.4 : Diffusion induced phase separation methods a) water vapor induced, b) evaporation of solvent, c) immersion precipitation	9
Figure 2.5 : Hollow fiber membrane module.....	10
Figure 2.6 : Different hollow fiber membrane types.	11
Figure 2.7 : Dry/wet phase inversion spinning line.	12
Figure 2.8 : (I)Phase diagram for ternary system : polymer/solvent/non-solvent. (II) Schematic of composition change	13
Figure 2.9 : Schematic phase diagram for quaternary system	14
Figure 2.10 : Types of carbon nanotubes	19
Figure 3.1 : Chemical formula of PES and PVP.....	23
Figure 3.2 : Dispersion of MWCNTs within solvent.....	24
Figure 3.3 : Sonication of dope solution.	24
Figure 3.4 : Hollow fiber membrane system.	25
Figure 3.5 : Schematic of spinning line.	26
Figure 3.6 : Schematic view of triple spinneret.	26
Figure 3.7 : Membrane flushing system.	27
Figure 3.8 : Prepared test modules.....	27
Figure 3.9 : (a) normal sterlitech setup, (b) modified sterlitech setup for hollow fiber membrane.	28
Figure 3.10 : Spectrophotometer used for BSA absorbance.	30
Figure 3.11 : Viscosimeter.	31
Figure 3.12 : Contact angle measurement setup.	31
Figure 3.13 : Stereo Microscope.	32
Figure 3.14 : Mechanical stability testing equipment.	33
Figure 3.15 : (a) SEM setup, (b) ion sputtering setup.....	33
Figure 3.16 : Electrokinetic analyzer cell.	34
Figure 3.17 : FTIR spectrophotometer.....	35
Figure 3.18 : Insertion of modules on agar medium for growth of <i>E.Coli</i>	35
Figure 4.1 : Dope viscosity change vs. concentration.....	39
Figure 4.2 : Cross section stereo microscope pictures of #1 membranes. a) pristine 1, b) 0.2COOH 1, c) 0.4COOH 1, d) 0.8COOH 1, e) 0.2OH 1, f) 0.4OH 1, g) 0.8OH 1.	40
Figure 4.3 : Cross section stereo microscope pictures of #2 membranes. a) pristine 2, b) 0.2COOH 2, c) 0.4COOH 2, d) 0.8COOH 2, e) 0.2OH 2, f) 0.4OH 2, g) 0.8OH 2.	41

Figure 4.4	: Cross section stereo microscope pictures of #3 membranes. a) pristine 3, b) 0.2COOH 3, c) 0.4COOH 3, d) 0.8COOH 3, e) 0.2OH 3, f) 0.4OH 3, g) 0.8OH 3.	42
Figure 4.5	: Cross sectional view of #1 membranes. a) Pristine 1, b) 0.2COOH 1, c) 0.4COOH 1, d) 0.8COOH 1, e) 0.2OH 1, f) 0.4OH 1, g) 0.8OH 1.	44
Figure 4.6	: Cross sectional view of #2 membranes. a) Pristine 2, b) 0.2COOH 2, c) 0.4COOH 2, d) 0.8COOH 2, e) 0.2OH 2, f) 0.4OH 2, g) 0.8OH 2.	45
Figure 4.7	: Cross sectional view of #3 membranes. a) Pristine 3, b) 0.2COOH 3, c) 0.4COOH 3, d) 0.8COOH 3, e) 0.2OH 3, f) 0.4OH 3, g) 0.8OH 3.	46
Figure 4.8	: Detailed cross sectional view of #1 membranes. a) Pristine 1, b) 0.2COOH 1, c) 0.4COOH 1, d) 0.8COOH 1, e) 0.2OH 1, f) 0.4OH 1, g) 0.8OH 1.	48
Figure 4.9	: Detailed cross sectional view of #2 membranes. a) Pristine 2, b) 0.2COOH 2, c) 0.4COOH 2, d) 0.8COOH 2, e) 0.2OH 2, f) 0.4OH 2, g) 0.8OH 2.	49
Figure 4.10	: Detailed cross sectional view of #3 membranes. a) Pristine 3, b) 0.2COOH 3, c) 0.4COOH 3, d) 0.8COOH 3, e) 0.2OH 3, f) 0.4OH 3, g) 0.8OH 3.	50
Figure 4.11	: MWCNT in membrane matrix (0.8 % MWCNT-COOH).	51
Figure 4.12	: Outer surface images of #1 membranes. a) Pristine 1, b) 0.2COOH 1, c) 0.4COOH 1, d) 0.8COOH 1, e) 0.2OH 1, f) 0.4OH 1, g) 0.8OH 1.	52
Figure 4.13	: Outer surface images of #2 membranes. a) Pristine 2, b) 0.2COOH 2, c) 0.4COOH 2, d) 0.8COOH 2, e) 0.2OH 2, f) 0.4OH 2, g) 0.8OH 2.	53
Figure 4.14	: Outer surface images of #3 membranes. a) Pristine 3, b) 0.2COOH 3, c) 0.4COOH 3, d) 0.8COOH 3, e) 0.2OH 3, f) 0.4OH 3, g) 0.8OH 3.	54
Figure 4.15	: Permeation rate values for spinning condition 1 (Air gap: 15cm, take-up speed : 8.4m).	56
Figure 4.16	: Permeation rate values of spinning condition 2 (Air gap: 15cm, take-up speed : 4.2m).	57
Figure 4.17	: Permeation rate values of spinning condition 3 (Air gap: 0cm, take-up speed : 4.2m).	57
Figure 4.18	: FTIR spectra of all dopes.	59
Figure 4.19	: Contact angle results of spinning #1 (Air gap: 15cm, take-up speed : 8.4m).	60
Figure 4.20	: Contact angle results of spinning #2 (Air gap: 15cm, take-up speed : 4.2m).	61
Figure 4.21	: Contact angle results of spinning #3 (Air gap: 0cm, take-up speed : 4.2m).	61
Figure 4.22	: Porosity values of spinning 1 (Air gap: 15cm, take-up speed : 8.4m).	62
Figure 4.23	: Porosity values of spinning 2 (Air gap: 15cm, take-up speed : 4.2m).	62
Figure 4.24	: Porosity values of spinning 3 (Air gap: 0cm, take-up speed : 4.2m).	63
Figure 4.25	: Zeta potential values of pristine membranes in mV.	64
Figure 4.26	: Zeta potential values of 0.2 % MWCNT-COOH membranes in mV.	64
Figure 4.27	: Zeta potential values of 0.4 % MWCNT-COOH membranes in mV.	65
Figure 4.28	: Zeta potential values of 0.8 % MWCNT-COOH membranes in mV.	65
Figure 4.29	: Zeta potential values of 0.2 % MWCNT-OH membranes in mV.	65
Figure 4.30	: Zeta potential values of 0.4 % MWCNT-OH membranes in mV.	66
Figure 4.31	: Zeta potential values of 0.8 % MWCNT-OH membranes in mV.	66
Figure 4.32	: Water flux recovery (FR%) of spinning condition #1 (Air gap: 15cm, take-up speed : 8.4m).	67

Figure 4.33 : Water flux recovery (FR%) of spinning condition 2 (Air gap: 15cm, take-up speed : 4.2m).....	68
Figure 4.34 : Water flux recovery (FR%) of spinning condition 3 (Air gap: 0cm, take-up speed : 4.2m).....	68
Figure 4.35 : Total fouling (Rt), reversible fouling (Rr) and irreversible fouling (Rir) ratios of spinning condition #1(Air gap: 15cm, take-up speed : 8.4m).69	
Figure 4.36 : Total fouling (Rt), reversible fouling (Rr) and irreversible fouling (Rir) ratios of spinning condition #2(Air gap: 15cm, take-up speed : 4.2m).70	
Figure 4.37 : Total fouling (Rt), reversible fouling (Rr) and irreversible fouling (Rir) ratios of spinning condition #3 (Air gap: 0cm, take-up speed : 4.2m). 70	
Figure 4.38 : BSA rejection of spinning #1 (Air gap: 15cm, take-up speed :8.4m).71	
Figure 4.39 : BSA rejection of spinning #2 (Air gap: 15cm, take-up speed :4.2m).72	
Figure 4.40 : BSA rejection of spinning #3 (Air gap: 0cm, take-up speed : 4.2m). 72	
Figure 4.41 : Young's modulus values (MPa) of membranes of spinning #1 (Air gap: 15cm, take-up speed : 8.4m).....	73
Figure 4.42 : Young's modulus values (MPa) of membranes of spinning #2 (Air gap: 15cm, take-up speed : 4.2m).....	74
Figure 4.43 : Young's modulus values (MPa) of membranes of spinning #3 (Air gap: 0cm, take-up speed : 4.2m).....	74
Figure 4.44 : Growth of <i>E.Coli</i> on hollow fiber membranes on agar medium.	76
Figure A.1 : Cross section stereo microscope pictures of #1 membranes without post treatment. a) pristine 1, b) 0.2COOH 1, c) 0.4COOH 1, d) 0.8COOH 1, e) 0.2OH 1, f) 0.4OH 1, g) 0.8OH 1.....	88
Figure A.2 : Cross section stereo microscope pictures of #2 membranes without post treatment. a) pristine 2, b) 0.2COOH 2, c) 0.4COOH 2, d) 0.8COOH 2, e) 0.2OH 2, f) 0.4OH 2, g) 0.8OH 2.	89
Figure A.3 : Cross section stereo microscope pictures of #3 membranes without post treatment. a) pristine 3, b) 0.2COOH 3, c) 0.4COOH 3, d) 0.8COOH 3, e) 0.2OH 3, f) 0.4OH 3, g) 0.8OH 3.	90
Figure A.4 : Cross sectional view of #1 membranes without post treatment. a) Pristine 1, b) 0.2COOH 1, c) 0.4COOH 1, d) 0.8COOH 1, e) 0.2OH 1, f) 0.4OH 1, g) 0.8OH 1.....	91
Figure A.5 : Cross sectional view of #2 membranes without post treatment. a) Pristine 2, b) 0.2COOH 2, c) 0.4COOH 2, d) 0.8COOH 2, e) 0.2OH 2, f) 0.4OH 2, g) 0.8OH 2.....	92
Figure A.6 : Cross sectional view of #3 membranes without post treatment. a) Pristine 3, b) 0.2COOH 3, c) 0.4COOH 3, d) 0.8COOH 3, e) 0.2OH 3, f) 0.4OH 3, g) 0.8OH 3.....	93
Figure A.7 : Detailed cross sectional view of #1 membranes without post treatment. a) Pristine 1, b) 0.2COOH 1, c) 0.4COOH 1, d) 0.8COOH 1, e) 0.2OH 1, f) 0.4OH 1, g) 0.8OH 1.....	94
Figure A.8 : Detailed cross sectional view of #2 membranes without post treatment. a) Pristine 2, b) 0.2COOH 2, c) 0.4COOH 2, d) 0.8COOH 2, e) 0.2OH 2, f) 0.4OH 2, g) 0.8OH 2.....	95
Figure A.9 : Detailed cross sectional view of #3 membranes without post treatment. a) Pristine 3, b) 0.2COOH 3, c) 0.4COOH 3, d) 0.8COOH 3, e) 0.2OH 3, f) 0.4OH 3, g) 0.8OH 3.....	96
Figure A.10 : Outer surface images of #1 membranes without post treatment. a) Pristine 1, b) 0.2COOH 1, c) 0.4COOH 1, d) 0.8COOH 1, e) 0.2OH 1, f) 0.4OH 1, g) 0.8OH 1.....	97

Figure A.11 : Outer surface images of #2 membranes without post treatment. a) Pristine 2, b) 0.2COOH 2, c) 0.4COOH 2, d) 0.8COOH 2, e) 0.2OH 2, f) 0.4OH 2, g) 0.8OH 2..... 98

Figure A.12 : Outer surface images of #3 membranes without post treatment. a) Pristine 3, b) 0.2COOH 3, c) 0.4COOH 3, d) 0.8COOH 3, e) 0.2OH 3, f) 0.4OH 3, g) 0.8OH 3..... 99

FABRICATION AND CHARACTERIZATION OF POLYETHERSULFONE (PES)/MULTIWALLED CARBON NANOTUBE HOLLOW FIBER ULTRAFILTRATION MEMBRANES

SUMMARY

Water is the most significant thing in the world for all living things. Already 2.7 billion people are lack of water, however before this scarcity enlarges to more people, some ways have to be found.

Membrane technology has gained attention for the treatment of process and drinking water and wastewater in recent years. Membranes are suffering because of fouling and concentration polarization. Optimal membranes must have high permeate flux with high solute rejection and low capital, operational cost with low fouling ratios. With developments in technology, we can cope with this fouling problem. Nanotechnology increases the range of applications related to membrane technologies in a better way. Pristine polymers show different and generally improved properties when they are fabricated with nanoparticles.

Objectives of this study are the characterization of polyethersulfone (PES) ultrafiltration hollow fiber membranes fabricated with different functional carbon nanotubes and investigating their effects to membrane fouling. To reach our target carboxyl (-COOH) and hydroxyl (-OH) functionalized multiwalled carbon nanotubes were used.

Hollow fiber membranes were spun by using phase inversion method. To choose optimum dope recipe, some trials were done with pristine membranes. After choosing optimum recipe (20 % PES, 5 % PVP K30, 2 % PVP K90, 73 % DMF), 7 different dopes were spun with this recipe. 0.2 % , 0.4 % , 0.8 % both hydroxyl and carboxyl multiwalled carbon nanotube membranes and a pristine membrane were fabricated. And for each dope, 3 different spinning parameters were used. Air gap, take-up speed were changed in these spinning parameters. After spinning, all membranes were flushed. Half of the membranes were post treated with NaOCl for 2 days. Then all membranes were put into 10/90 % glycerol/water solution for 12 hours. All experiments were done after these processing steps.

For characterizing these membranes some experiments were done. Dope viscosity, permeability, contact angle, water flux recovery, total fouling ratio, BSA rejection rate, surface functionalization, surface charge, mechanical stability of the membranes were measured and calculated. To investigate structure of the membranes, scanning microscopy and stereo microscopy images were taken. Also antibacterial effect of membranes was checked.

According to the results, viscosity of dope were increased when carboxyl functionalized multiwalled carbon nanotubes were used, however for hydroxyl functionalized multiwalled carbon nanotubes were used, dope viscosity first decreased and then increased as the concentration of the nanotubes was increased.

According to microscopy images, membranes had circular structure, cross sections of the membranes were between finger-like to sponge-like. Effects of increasing or

decreasing take-up speed or air gap were clearly seen in cross sections, outer layers and diameters of the membranes.

Permeabilities of both post-treated and non-treated membranes were calculated to show the effects of post treatment. Post-treated membranes had high permeate fluxes. Using carboxyl functionalized multiwalled carbon nanotubes, permeability first decreased and then increased as concentration was increased. However for hydroxyl functionalized multiwalled carbon nanotubes, as concentration increased, permeability was also increased. At high take up speed (8.4m) and air gap (15cm), high permeability values were obtained. At 0 cm air gap and low take-up speed (4.2m) low permeability values were obtained. From this point, experiments were done with post treated membranes except contact angle values.

In contact angle results, it was seen that in post treated membranes effect of washing of hydrophilic PVPs can be clearly seen as an increment in contact angle values of post treated membranes. Increasing the both functional carbon nanotubes content in dopes, resulted in generally discordant contact angle changes.

The overall porosity values were also found. The highest porosity was observed at 0.4 % carboxyl functionalized multiwalled carbon nanotubes, 8.4m take-up speed and 15cm air gap as 69 % whereas the least porosity observed at 0.2 % hydroxyl functionalized multiwalled carbon nanotubes, 4.2m take-up speed and 15cm air gap as 12,5 %.

Surface charge values of the membranes were found between pH 3-10. Surface charge parameter was an important parameter for fouling. Since BSA which has a negative charge was used for fouling measurements, pH of 6.8-7.0 was important. According to surface charge values of pristine membranes, membranes showed negative charge. When negativity increased, fouling rates decreased and vice versa.

Water flux recoveries which show recycling properties of membranes were also measured. Due to the results carboxyl functionalized multiwalled carbon nanotubes showed better water flux recovery values. As concentration of carbon nanotubes increased, generally recovery decreased. The best results were obtained at 8.4m take-up speeds and 15cm air gap. For hydroxyl functionalized multiwalled carbon nanotubes, water flux recovery values generally were lower than pristine membranes. Increasing of the concentration of hydroxyl functionalized multiwalled carbon nanotubes, changed recovery values discordantly except 4.2m take-up speed and 0 cm air (increment in concentration, increased recovery and then decreased).

When calculating total fouling ratios both reversible and irreversible fouling ratios were calculated. Different spinning parameters affected membrane fouling rates different. Carboxyl functionalized multiwalled carbon nanotubes generally showed lower fouling ratios whereas hydroxyl functionalized multiwalled carbon nanotubes had higher fouling ratios over pristine membranes. Main fouling mechanisms of the membranes were found as irreversible fouling. BSA rejections were decreased as permeability of the membranes increased.

Addition of carbon nanotubes into membrane matrix enhanced mechanical stabilities of the membranes. Generally, membranes spun with carbon nanotubes (both functionality) had higher young's modulus values over pristine membranes. For different spinning parameters, obtained young's modulus values were changed. The best young's modulus values were obtained at 8.4m take-up speeds and 15cm air gap due to greater molecular orientation. Increasing the concentration of both functional carbon nanotubes led to discordant changes in young's modulus values of the membranes. Elongation at break percentages showed also discordant trends for different spinning parameters.

Antibacterial properties of the membranes were found using *Escherichia Coli*. After 1 day incubation, degree of the growth of *Escherichia Coli* was investigated. According to the results, both carboxyl functionalized multiwalled carbon nanotubes and hydroxyl functionalized multiwalled carbon nanotubes showed no antibacterial properties.

ÇOK DUVARLI KARBON NANOTÜP KATKILI POLİETERSÜLFON (PES) İÇİ BOŞLUKLU MEMBRAN ÜRETİMİ VE KARAKTERİZASYONU

ÖZET

Su, bütün dünya üzerinde yaşayan canlılar için en önemli maddedir. Su bu kadar önemliyken yaklaşık 2.7 milyar kişinin hâli hazırda içilebilir su kaynaklarına ulaşamaz durumda olması, bu sayı daha da artmadan bizleri bu duruma çare olabilecek yeni yöntemler bulmaya itmektedir.

Son yıllarda membran teknolojileri, su, atıksu ve proses suyunu arıtmada önemli bir yer almıştır. Membranlarda sıkça karşılaşılan sorunlar kirlenme ve konsantrasyon polarizasyonudur. En iyi özelliklere sahip bir membranda olması gerekenler yüksek bir geçirgenlik değeriyle birlikte yüksek bir giderim veriminin de olması, ayrıca düşük kirliliğe ve ilk yatırım maliyetiyle işletim maliyetinin de düşük olmasıdır. Teknolojideki gelişmeler sayesinde membran kirlenmesiyle başa çıkabilecek yeni teknolojiler ortaya çıkmıştır. Nanoteknoloji sayesinde membranların kullanımını daha geniş bir çerçeveye yaymak mümkün olacaktır. Çünkü nanoparçacık katılarak üretilen membranların saf membranlara göre üstün özellikler sergilediği ve membran performansını da iyileştirdiği gözlemlenmiştir.

Bu çalışmada polietersülfon ultrafiltrasyon membranına farklı fonksiyonelliğe sahip çok duvarlı karbon nanotüp eklenip, membranların karakterizasyonu yapılmıştır ve bu nanotüplerin membran kirlenmesi üzerine etkileri incelenmiştir. Bu amaçla kullanılan farklı fonksiyonelliğe sahip çok duvarlı karbon nanotüpler, karboksil ve hidroksil çok duvarlı karbon nanotüpleri olmuştur.

İçi boşluklu membranlar faz ayrımı metodu kullanılarak üretilmiştir. En uygun çözelti reçetesini bulana kadar birçok farklı konsantrasyon ve farklı malzemeler katılarak membran üretilmiştir. Bunların sonucunda %20 PES, %5 PVP K30, %2 PVP K90 ve %73 DMF kullanılmasına karar verilmiştir. Daha sonra bu reçete kullanılarak 7 farklı membran dökülmüştür. Döküm çözeltisine % 0.2, %0.4, %0.8 oranında hem karboksil hem de hidroksil çok duvarlı karbon nanotüp eklenmiş ve membranlar üretilmiştir. Her çözelti dökülürken 3 farklı işletim parametresiyle oynanıp 3 farklı membran örneği alınmıştır. Parametrelerdeki değişkenler çekme hızı ve hava boşluğu olmuştur. Membranlar üretildikten sonra 12 saat boyunca suda yıkanmıştır. Üretilen membranların yarısı üretim sonrası prosese tabi tutulmuştur. Bu proste membranlar 4000ppm lik sodyum hipoklorit çözeltisine konmuş ve 2 gün bekletilmiştir. Sonrasında bütün membranlar %10/90'lık gliserol/su çözeltisine konmuştur. Membran modülleri hazırlanmıştır ve bütün deneyler bu aşamaların sonunda yapılmaya başlanmıştır.

Membranların karakterizasyonu için birçok yöntem kullanılmıştır. Çözelti viskozitesi, membran geçirgenliği, temas açısı, su geri kazanımı, toplam kirlilik oranı, BSA giderimi, yüzey fonksiyonelliği, yüzey yükü, mekanik dayanımı gibi özellikleri ölçülüp hesaplanmıştır. Membranın dış yüzeyi, çapı ve yanal yüzeyinin yapısı hakkında bilgi sahibi olmak için taramalı elektron mikroskopu ve stereo

mikroskop görüntüleri çekilmiştir. Ayrıca membranların antibakteriyel özellik gösterip göstermediği de kontrol edilmiştir.

Sonuçlara göre çözelti viskozitesi karboksil çok duvarlı karbon nanotüp eklendiğinde sürekli artmıştır. Fakat hidroksil çok duvarlı karbon nanotüp eklendiğinde viskozite ilk önce düşmüştür. Karbon nanotüp konsantrasyonu arttıkça bir artış gözlemlenmiştir.

Taramalı elektron mikroskopu ve stereo mikroskopla çekilen fotoğraflar sonucunda membranların yuvarlak bir yapıda olduğu gözlemlenmiştir. Yan kesiti incelendiğinde ise membranlarda genel olarak süngerimsi ve parmağımsı yapılar görülmüştür. Çekme hızıyla oynanması, hava boşluğunun değiştirilmesi gibi parametrelerin etkileri membranın dış yüzeyinde, yan kesitinde, ve membranlar çaplarında açıkça gözlemlenmektedir.

Üretim sonrası prosesinin membranları ne şekilde etkilediğini görebilmek için hem proses görmüş hem de görmemiş membranların geçirgenlik oranları hesaplanmıştır. Bunun sonucunda prostesten geçen membranların daha yüksek geçirgenlik oranlarına sahip olduğu gözlemlenmiştir. Karboksil çok duvarlı karbon nanotüp kullanıldığında, geçirgenlik oranı karbon nanotüp yüzdesi arttıkça ilk önce düşmüş, daha sonrasında artmıştır. Fakat hidroksil çok duvarlı karbon nanotüp kullanıldığında, karbon nanotüp yüzdesi artışıyla birlikte geçirgenlik değeri de artmıştır. 8.4m çekme hızı ve 15cm hava boşluğunda daha geçirgen membranlar elde edilmiştir. 0 cm hava boşluğunda ve 4.2m çekme hızında daha düşük geçirgenlik oranı elde edilmiştir.

Temas açısı sonuçlarına göre, üretim sonrası prosese tabi tutulan membranlarda, hidrofilik PVPnin membranlardan yıkanması sonucu, temas açısı değerleri artmıştır. Her iki fonksiyonel karbon nanotüpte de nanotüp yüzdesinin artışıyla birlikte temas açılarında genel olarak düzensiz bir değişim olmuştur. Bu noktadan sonra yapılan bütün deneyler üretim sonrası proses gören membranlar üzerinden yapılmıştır.

Membranların toplam gözeneklilik değerleri incelendiğinde en yüksek gözeneklilik % 0.4 karboksil çok duvarlı karbon nanotüpte ve 8.4m çekme hızında ve 15cm hava boşluğu kullanıldığında % 69 olarak elde edilmiştir. En düşük gözeneklilik ise % 0.2 hidroksil çok duvarlı karbon nanotüp, 4.2m çekme hızı ve 15cm hava boşluğunda % 12,5 olarak elde edilmiştir.

Yüzey yükleri değerlendirilirken farklı pH aralıkları seçilmiştir. Bu aralık pH 3-10'dur. Membran kirlenmesi için yüzey yükü parametresi oldukça önemlidir. BSA proteini pH 6.8-7.0 arasında negatif yüke sahiptir. Üretilen membranlarda bu aralıktaki pH değerleri incelenmiştir ve bu pH değeri arasında negatiflik ne kadar fazlaysa membran kirlenmesinin o kadar düşük, ne kadar azsa membran kirlenmesinin o kadar fazla olduğu görülmüştür.

Membranların tekrar kullanılabilirlik özelliklerini gösteren geri kazanım oranları da hesaplanmıştır. Sonuçlara göre karboksil çok duvarlı karbon nanotüp kullanılan membranlarda geri kazanım yüzdeleri daha fazla olmuştur. Nanotüp yüzdesinin artışıyla birlikte bu geri kazanım genel olarak düşüş göstermiştir. En iyi sonuçlar 8.4m çekme hızında ve 15cm hava boşluğunda elde edilmiştir. Hidroksil çok duvarlı karbon nanotüp eklenmesi genelde geri kazanım oranlarını saf membranlardan daha düşük olmuştur. Karbon nanotüp yüzdesinin artışıyla birlikte, 4.2m çekme hızı ve 0 cm hava boşluğu hariç (bu parametreler kullanıldığında konsantrasyon artışıyla birlikte geri kazanım artıp, azalmıştır.) bu oran düzensiz bir şekilde değişim göstermiştir.

Toplam membran kirlenme oranı hesaplanırken geri dönüştürülemez ve dönüştürülebilir kirlenme oranları hesaplanmıştır. Farklı üretim parametreleri kullanıldığında elde edilen membran kirlenmeleri de farklı olmuştur. Karboksil çok

duvarlı karbon nanotüp kullanıldığında genel olarak saf membrana göre daha düşük membran kirlenmesi olmuştur. Hidroksil çok duvarlı karbon nanotüp kullanıldığında ise saf membrana göre yüksek kirlenme oranları hesaplanmıştır. Geri dönüşsüz kirlenme, ana membran kirlenme mekanizması olmuştur. BSA giderimleri geçirgenlik oranı arttıkça düşmüştür.

Membran matrisine karbon nanotüp eklenmesiyle birlikte membranların mekanik dayanıklılığında artış gözlemlenmiştir. Genel olarak karbon nanotüp eklenmiş bütün membranların elastisite modülü değerleri saf membranlara göre yüksek çıkmıştır. Farklı üretim parametrelerinin kullanılması sonucu elastisite modülü değerleri de farklılık göstermiştir. En iyi elastisite modülü değeri daha iyi moleküler dizilimin gerçekleştiği yüksek çekme hızı (8.4m) ve 15cm hava boşluğunda elde edilmiştir. Her iki fonksiyonellikte de karbon nanotüp yüzdesinin artışıyla birlikte düzensiz bir değişim meydana gelmiştir. Ayrıca kopma anındaki uzama değerleri de farklı üretim parametreleri kullanıldığında düzensiz bir değişim göstermiştir.

Membranların antibakteriyel özelliklerini incelemek için *Escherichia Coli* kullanılmıştır. 1 günlük inkübasyon sürecinden sonra, *Escherichia Coli* büyümesinin ne kadar olduğu incelenmiştir. Sonuçlara göre hem karboksil çok duvarlı karbon nanotüp hem de hidroksil çok duvarlı karbon nanotüp hiç antibakteriyel özellik sergileyememiştir.

1. INTRODUCTION

1.1 Importance of the Study

Water is the most important thing in the world, without it, life itself cannot exist. Although it is that much important, fresh water resources are limited and cannot be reachable (30% is locked up in glaciers etc.) for humans or other living things. We have only 0.08-1% fresh water in our hands to continue our existence. It is estimated that by 2025, between 2.7 billion to 3.2 billion people will suffer from water scarcity. In Figure 1.1 current and future situation of water can be seen.

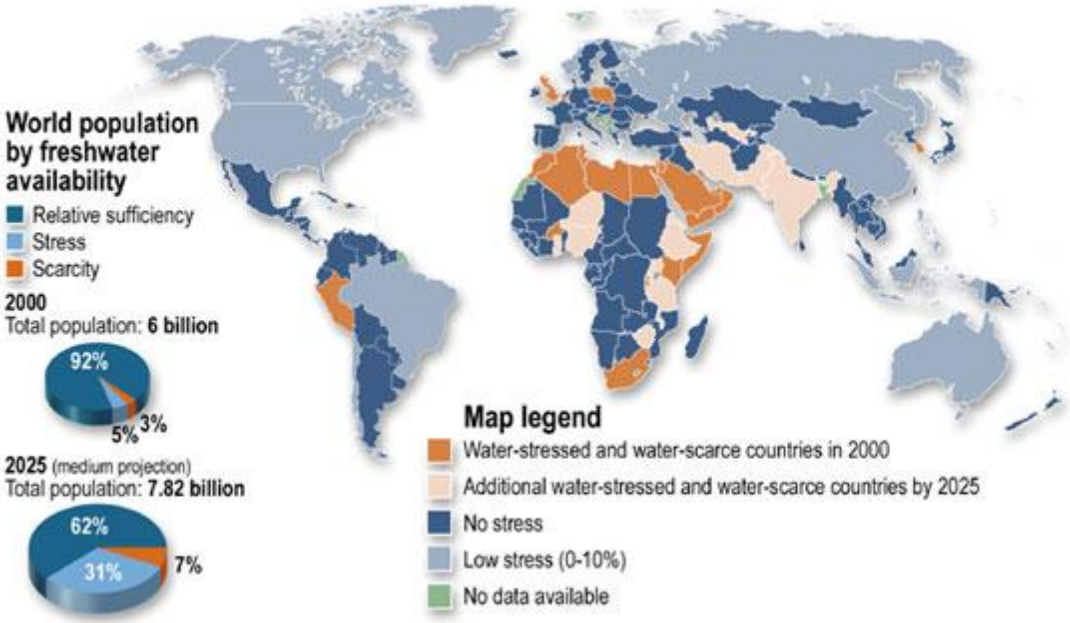


Figure 1.1 : Freshwater availability – current and future (url-1).

That being the case, non-conventional methods gain importance because conventional methods for water and wastewater treatment need huge footprints on land and for land use they are not so efficient. Two of the key technologies are nanotechnology as we can use it for so many environmental related purposes such as water and wastewater purification, remediation, sensing, pollution prevention etc. and membranes that used for water and

wastewater treatment. Therefore, combination of these two technologies complement each other to overcome water scarcity problem by solving challenges linked to the issue.

1.2 Mission and Scope of the Study

Membrane technology has gained attention for the treatment of process and drinking water and wastewater in recent years. Optimal membrane thought as having maximum permeate flow with maximum solute rejection and minimum amount of capital and operating cost (Vatanpour et al., 2011). The most significant factors affecting the properties of membranes are fouling and concentration polarization phenomena. With developments in technology, we can cope with this fouling problem. Nanotechnology increase the range of applications related to membrane technologies in a better way. Pristine polymers show different and generally improved properties when they are fabricated with nanoparticles. This results in drawing attention to polymer-nanocomposite membrane preparation (Merkel et al., 2002).

Objectives of this study are characterizing of polyethersulfone (PES) ultrafiltration hollow fiber membranes fabricated with different nanomaterials and investigating their effects to membrane fouling. To reach our target Carboxyl (-COOH) and hydroxyl (-OH) functionalized multiwalled carbon nanotubes were used. Detailed literature of nanocomposite hollow fiber membrane was given, results of our findings were given and finally what can be done for future researches were discussed respectively throughout the thesis.

2. LITERATURE REVIEW

2.1 Membrane Separation Technology

2.1.1 Historical development of membranes

First studies related to membranes can be found in eighteenth century as in the concept of “osmosis”. They were just used as laboratory tools back then, there was no industrial or commercial usage. First commercial use was after World War II. U.S army sponsored to improve filters used in to obtain clean drinking water sources. However, membrane processes were expensive. Before Loeb and Sourirajan were improved fabrication processes of membranes, membranes couldn't find a place in commercial and industrial use because they were slow, unselective, not reliable, and very expensive. They developed defect-free, high-flux membranes. After 1960s, they showed increasing trend and their cost decreased gradually (Baker, 2004). Now, membranes used in many industrial applications like water, wastewater treatment, pharmaceutical, beverage, semiconductor, desalination, gas separation, medicine (artificial kidneys, controlled drug delivery) etc. (Singh, 2006).

2.1.2 Some basic membrane terms

Membranes; are selective materials for filtration applications. Under a driving force like pressure or temperature difference; while small particles are passing from membrane filter, bigger particles are retained.

Cross-flow; When concentrate collected as a different stream from membrane, it is defined as cross-flow.

Dead-end filtration; When concentrate is not collected as a different stream, it is defined as dead-end flow.

Flux; flowrate which is passing through membrane's specific surface area in a specific time period.

Permeate; flow contains penetrants that leaves membrane modules

Fouling; deposition of suspended or dissolved substances on membrane surface which results in loss of performance. Main disadvantage of membrane processes is, when flux decreased, permeate productivity are also lowered. To prevent fouling, undesired adsorption and adhesion processes should be prevented because by this way accumulation of colloids on membrane will slow down. For overcoming this, advanced pretreatment, surface modification (increasing hydrophilicity by incorporating nanoparticles etc.), chemical or physical cleaning (backwashing etc.) can be done (Ng et al., 2010).

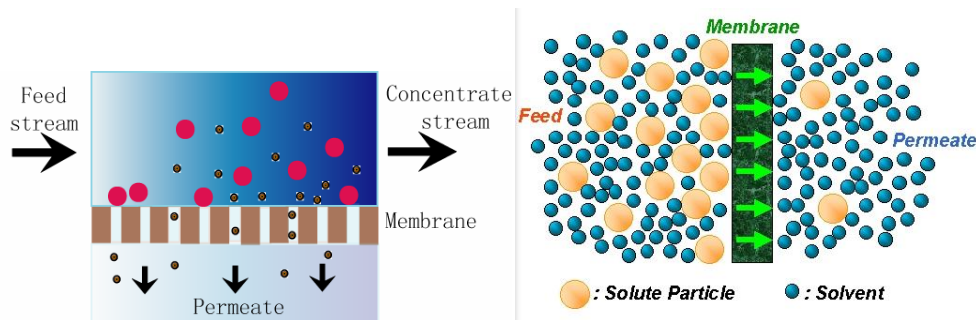


Figure 2.1 : Cross-flow and Dead end filtration setup (url-2, Ahmed S.F., 2010).

Recovery; rate of input flow to output flow.

Retentate; flow contains no penetrants that leaves membrane modules without passing through the membrane downstream.

Concentration polarization; accumulation of excess particles in a thin layer adjacent to the membrane surface, so this phenomena leads to increase in resistance and decrease in permeate flux after a period of time (Koros W.J, 1996).

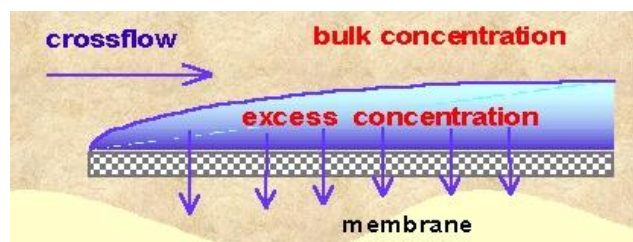


Figure 2.2 : Concentration Polarization (url-3).

2.2 Membrane Classification

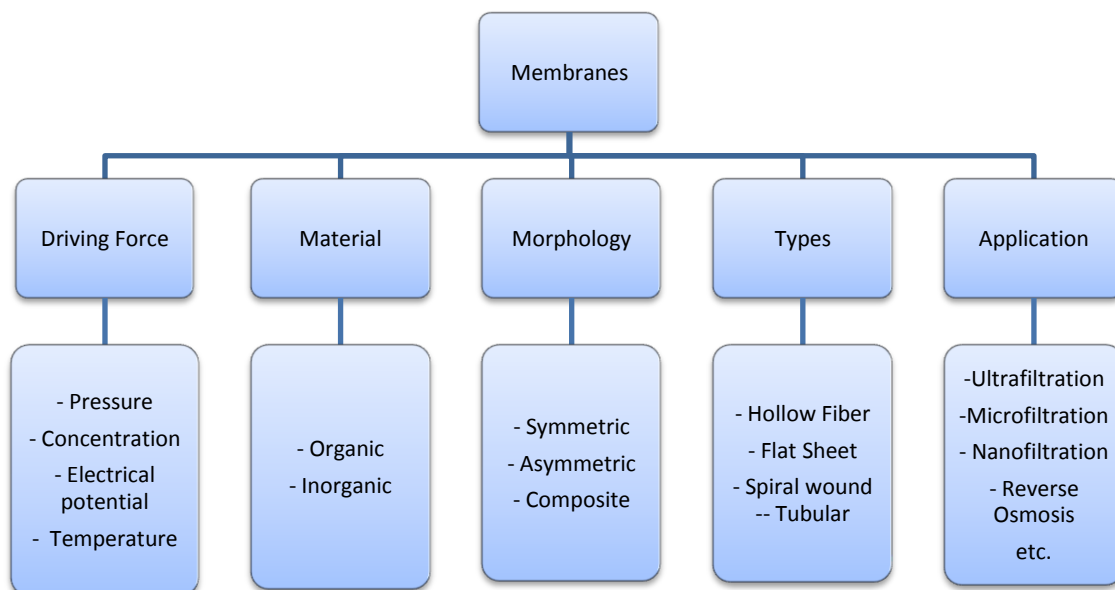
Membrane classification can be categorized as their 5 different properties (Table 2.1). All categorizes actually are engaged with each other.

Four important application of membranes use pressure as driving force whereas process like electro dialysis uses electrical potential or membrane distillation (MD) uses temperature as driving force.

Materials used in membranes can be organic or inorganic or both. Polymeric membranes are in more focus because of their easier pore forming control, and their lower costs according to inorganic materials (Ng et al,2010).

Membrane morphology can be categorized as in three different groups. Symmetric membranes have almost a constant diameter of pores along the cross section of the membrane where thickness causes resistance to mass transfer acting as a selective barrier. In asymmetric membranes, pore sizes are different between surface and bottom side. So, larger particles are eliminated from the beginning. Composite membranes have two different layers which are support or porous and skin or non-porous can be made different materials as well as different purposes. The support or porous layer have high porosity, no selectivity and a thickness between 50 to 150 mm (url-4).

Table 2.1 : Membrane classification.



To protect membranes from any collapse from outside, modules were developed. Type of these modules are hollow fiber, flat sheet, tubular or spiral wound. Hollow fiber (HF) membranes have very small diameters (<1mm), consists of large number of tiny tubes in a module and self supporting, water can be flow through inside to outside or vice versa. HF membrane modules result in more rapid mass transfer because of their large surface area per

volume. For instance liquid extraction is 600 times faster than conventional methods or 30 times faster when gas absorption is considered (Pabby, 2008). Fabrication of it can be made by using dry-wet inversion. It is advantageous because it needs modest energy requirement, has no waste products, low operational cost and larger surface area per volume, is flexible whereas it is expensive, can be easily undergo fouling and needs more researches (url-5). More detailed information about fabrication of hollow fiber will be given ongoing sections. Flat sheet membranes have an easy structure, so renewing is simpler than hollow fibers. They are placed like sandwich with feed sites looking each other, feed flows come from its sides and permeate through top and bottom of frames. A corrugated spacer is used to apart membranes. On the other hand spiral wound module is prepared from flat sheet membranes wrapped around a center collection pipe. It has really good features which are low concentration polarization, compact, low permeate flow which leads to less contamination and durability to high pressures (Baker, R.W. 2004; url-4).

Process classification was based on the size of particles and molecules removed (Figure 2.3).

	Reverse Osmosis	Nanofiltration	Ultrafiltration	Micro filtration
Membrane	Asymmetrical	Asymmetrical	Asymmetrical	Symmetrical Asymmetrical
Thickness	150 μm	150 μm	150 - 250 μm	10-150 μm
Thin film	1 μm	1 μm	1 μm	
Pore size	<0.002 μm	<0.002 μm	0.2 - 0.02 μm	4 - 0.02 μm
Rejection of	HMWC, LMWC sodium chloride glucose amino acids	HMWC mono-, di- and oligosaccharides polyvalent neg. ions,	Macro molecules, proteins, polysaccharides vira	Particles, clay bacteria
Membrane material(s)	CA Thin film	CA Thin film	Ceramic PSO, PVDF, CA Thin film	Ceramic PP, PSO, PVDF
Membrane Module	Tubular, spiral wound, plate-and-frame	Tubular, spiral wound, plate-and-frame	Tubular, hollow fiber, spiral wound, plate-and-frame	Tubular, hollow fiber
Operating pressure	15-150 bar	5-35 bar	1-10 bar	<2 bar

Figure 2.3 : Pressure driven membrane processes (Wagner, J. 2001).

Reverse osmosis (RO) is used for to desalinate seawater, Nanofiltration (NF) is pretty much the same with RO both in concept and in operation. Ultrafiltration (UF) uses a finely porous

membrane which has an average pore diameter of the membrane is in the 10–1000 °A range, to separate water and microsolute from macromolecules and colloids like proteins from small molecules like sugars and salts. They have usually anisotropic structures which is made up with a finely porous surface layer on a much more open microporous substrate. The finely porous surface layer performs the separation; the microporous substrate provides mechanical strength. Operating pressures are between 1 and 10 bar. Modules can be spiral wound, tubular or hollow fiber. It can be used in domestic or industrial wastewater treatment such as beverage, pharmaceutical ie., water treatment and reuse, as a pretreatment before RO and NF to decrease fouling (Baker R.W, 2004; url-2; Scott, K. (1999); url-6; Li, N.N., 2008).

2.2 Membrane Fabrication Methods

Wide range of fabrication methods exist however not all methods are used for every type of membranes. Preparation techniques can be classified considering morphology of the membrane. Hereunder, isotropic and anisotropic membrane fabrication will be scope of this part.

Isotropic membranes, can be porous or dense but their distinctive feature is their homogeneity and uniformity throughout the membrane while anisotropic membranes have non uniform structure, they have dense, thin top layer which provide selectivity to the membrane but thicker and more porous structure which gives mechanical strength to the membrane inside.

Solution casting, melt extruded film, track-etching, expanded film, template leaching, phase inversion processes is put to use for isotropic membranes whereas phase inversion, interfacial polymerization, solution coated composite processes are used for anisotropic membranes (Baker, R.W., 2004).

Solution casting generally used to prepare lab scale membranes, it uses phase inversion theory, a casting knife is used to cast films onto a glass substrate. Then glass is immersed into water, membrane film is obtained. Melt extrusion method is used generally polymers which can not dissolve in a solvent. Polymer is compressed between two heated plate which heated just below the melting point of the polymer used and membrane is extruded. Track-etch method uses radiation source to open porous membrane structure. Irradiated polymer have tracks on it when it is put into solution these tracks are etched which leads to porous structure. In expanded film method, crystalline polymer are used and main processes are orientation and

annealing. Extruding a polymer heating up to its melting point results in highly oriented films, then annealing and cooling processes come, and then film is stretched up to 300%. Because of this, amorphous regions in the stretched film are deformed which becomes pores of membrane structure. Logic behind the template leaching method is preparing a homogeneous structure with insoluble polymer like polyethylene and leachable component. After film is extruded leachable part of the film is leached by using a solvent.

Phase separation or phase inversion method will be covered throughoutly in the ongoing section but to be summarize, it involves changing one-phase solution into two different phase solution. Two phases consist of polymer rich phase which is the basis of dense, selective layer, and the other is polymer lean phase that forms membrane pores. It can be performed by several methods such as water precipitation, solvent extraction, thermal gelation, water vapor absorption. In interfacial polymerization method, a reactive prepolymer is deposited on a microporous support membrane, then this support membrane is immersed in a water-immiscible solvent which reacts at the membrane interface, so highly crosslinked, dense membrane structures are formed. These kind of membranes have high selectivity, high permeability. Solution casted composite membranes are fabricated by using two teflon rods and a water quench bath. Polymer solution is casted onto two teflon rods which moves apart to spread film. As film is spread water on the surface makes porous structure. Then film is transferred onto a support layer.

2.3 Fabrication of Hollow Fiber Membranes by Phase Inversion Method

2.3.1 Phase inversion membranes fabrication

Commercial membranes for general usage usually fabricated by this method. Various morphologies which are affected by both thermodynamic and kinetical parameters, can be produced by this method. First polymer dissolved in a solvent and solution is extruded in fiber format. Then this fiber coagulated either by changing temperature or solution composition. By this way final fiber form obtained (Wienk, 1993).

Phase inversion process can be made using two technics:

1. Thermally induced phase inversion
2. Diffusion induced phase inversion

In thermally induced phase inversion method, polymer solution is prepared at high degrees and is forced to cool down. When solvent evaporates at top layer of solution there can be an increase in polymer concentration, if that's occurred asymmetrical structure of the polymer is obtained (Wienk, 1993).

In diffusion induced phase inversion, polymer solution is getting into contact with either non-solvent vapor or another liquid, so film composition is locally undergo a diffusional change. So vitrification of polymer film is happened. Non-solvent vapor diffuses into the solution, exchange occurs between non-solvent and solvent. These technique can be categorized into 3 groups (Wienk,1993):

1. Vapour induced phase separation
2. Solvent evaporation
3. Immersion precipitation

In Figure 2.4, Diffusion and exchange of solvent and non-solvent can be seen.

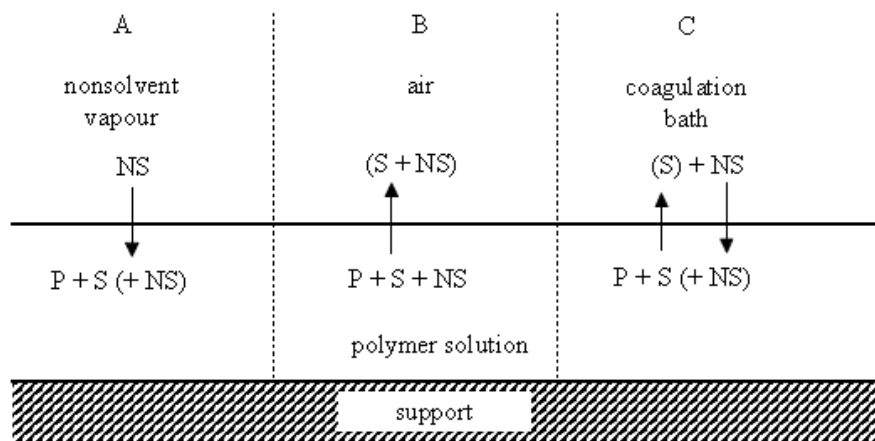


Figure 2.4 : Diffusion induced phase separation methods a) water vapor induced, b) evaporation of solvent, c) immersion precipitation (Kools, 1998).

Precipitation from vapour phase is a process where polymer solution is into contact with the vapour of non-solvent. Here, vapour penetrates into polymer solution that leads to precipitation of polymer and symmetric membrane formation (Wienk, 1993).

If one wants to fabricate dense homogeneous and porous membrane, solvent evaporation method is the appropriate precipitation method. In this process polymer dissolves in a mixture of non-solvent and solvent (Wienk, 1993).

Immersion precipitation case, polymer precipitates through either the diffusion of solvent into coagulation bath or the diffusion of non-solvent into polymer solution (Wienk, 1993).

2.3.2 Features of hollow fiber membranes

Hollow fiber membranes are the most preferred membranes in all other tubular membranes.

They have three main advantages over flat sheet membranes;

1. They have high surface area to volume ratio,
2. They don't need any support layer, they are self supported,
3. They have high recovery efficiencies. Due to having high surface area to volume ratio, modules can be compact and this increase recovery ratio and decrease energy consumption.

Hollow fiber membrane modules can have dead end flow or cross flow. Hollow fibers having diameters between 3mm to 0,5mm are called as capillary tube, between 50 μ m and fewer diameters are called hollow fibers.

In Figure 2.5, cross flow hollow fiber module working from lumen side to shell side can be seen. Here, retentate passes through membrane and exits from shell side whereas permeate can be collected from lumen side (url-7).

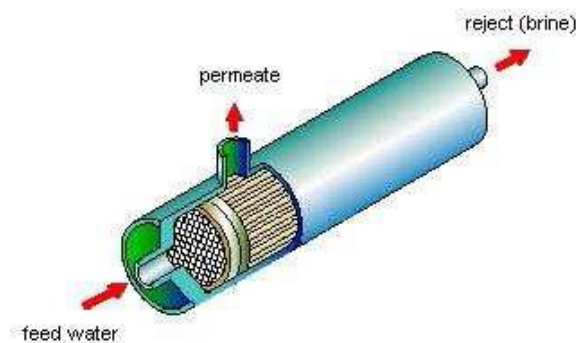


Figure 2.5 : Hollow fiber membrane module.

Due to fiber geometry feed solution can be given from either side (lumen to shell or shell to lumen). Hollow fibers having 50-200 μ m diameters generally used in high pressure processes. When fiber diameter is bigger than 200-500 μ m, feed solution generally is given from lumen side. Low pressurized gas separation, hemodialysis and ultrafiltration processes the best way is feeding from lumen side. In Figure 2.6 different types of hollow fiber membranes can be seen (Baker R.W, 2004).

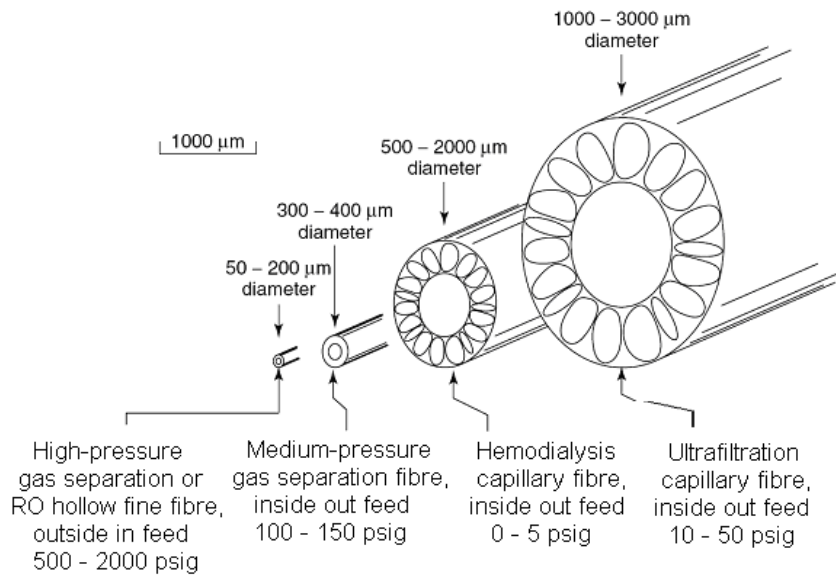


Figure 2.6 : Different hollow fiber membrane types (Baker R.W, 2004).

Most of cellulosic and synthetic fibers are fabricated by so-called “spinning” process. In this method, viscous polymer solution takes fiber form as solution goes through spinneret by using pressure (url-7).

2.3.3 Phase inversion fabrication methods for hollow fiber membranes

Four different fabrication methods exist for producing hollow fiber membranes. These are;

1. Wet spinning
2. Dry spinning
3. Dry-wet spinning
4. Melt extrusion

2.3.3.1 Wet spinning

Polymer dissolves in solvent and spinning solution is prepared. If spinning solution directly enters coagulation bath after leaving nozzle, it is called wet spinning (url-8). Wide, high porous UF and hemodialysis membranes are generally fabricated by this method (Baker R.W, 2004).

2.3.3.2 Dry Spinning

Polymer material like acetate, triacetate, acrylic, polypropylene etc. can be fabricated by dry spinning. Spinning solution is prepared like the same in other methods. However in dry

spinning after solution leaves nozzle, there is no coagulation bath, fibers form after solvent inside of spinning solution is starting to evaporate. Membrane solidification can be fastened by applying air flow (url-8).

2.3.3.3 Dry-wet spinning

This method and diffusion induced phase separation have the same 3 different processes.

1. Vapor diffusion through outer surface of membrane in the air gap
2. Coagulation of polymer solution by entering coagulation bath after leaving air gap region
3. Evaporation of the solvent in polymer solution

Coagulation process first has started in the air gap region which has higher amount of water vapor. In the air gap region, exchange of non-solvent to solvent has started and in the coagulation bath process continues and takes it final fiber form (Wienk, 1993). A simple dry/wet phase inversion system for hollow fiber membrane fabrication can be see in Figure 2.7.

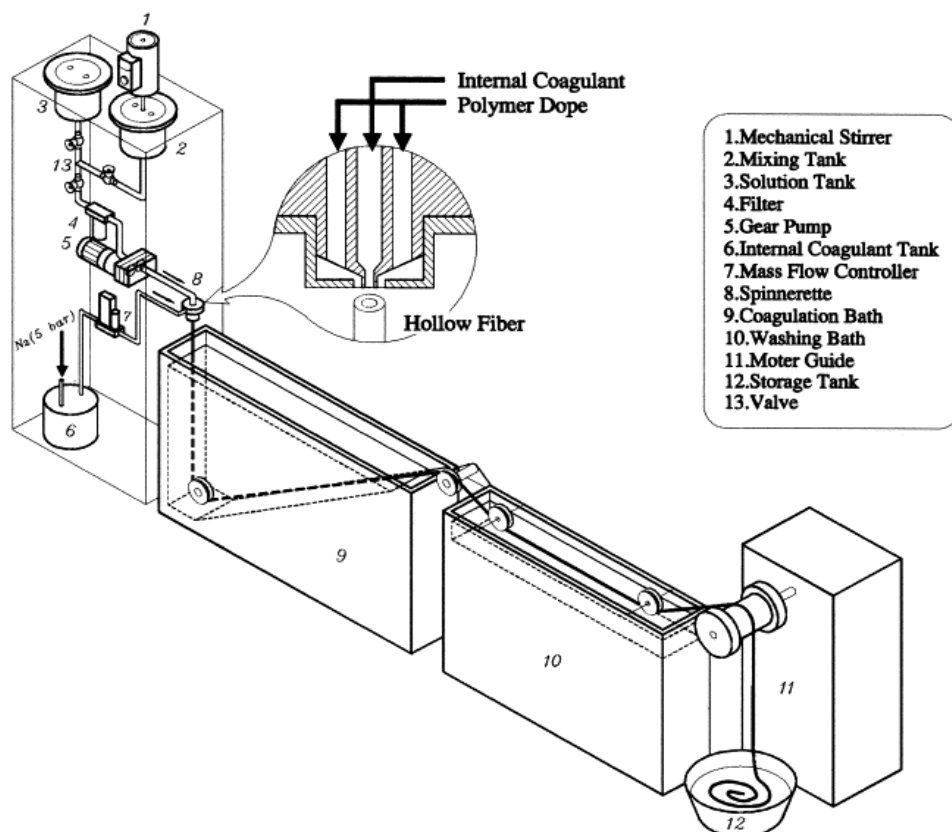


Figure 2.7 : Dry/wet phase inversion spinning line (Desmukh and Li, 1998).

2.3.3.4 Melt extrusion

Fiber formation occurs after melting polymer. Melt polymer is pumped to the nozzle and goes through nozzle. After leaving nozzle fiber starts to solidify by cooling down. In this method, neither solvent evaporized nor diffusion process occurs. Nylon and polyester are the most used polymers for this method to extrude fibers (url-8).

2.3.4 Theory of hollow fiber spinning by phase inversion

Dry/wet spinning process consists of phase separation of polymer rich phase and polymer lean phase which can be achieved by non-solvent, vapour or solution. The simplest systems can be explained by ternary diagram (Figure 2.8) which is formed by three components, polymer/solvent/non-solvent.

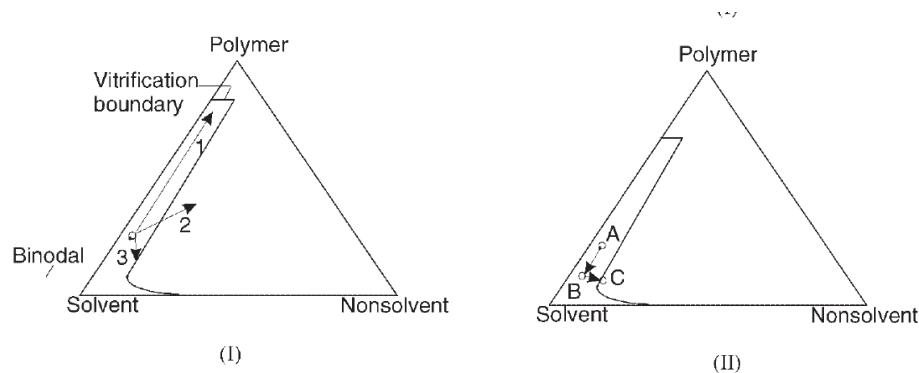


Figure 2.8 : (I)Phase diagram for ternary system: polymer/solvent/non-solvent. (II)Schematic of composition change (Li and He, 2007).

If there is high enough polymer concentration, and outflow of solvent to non-solvent is also higher, first route is followed and phenomena such as vitrification, gelation or crystallization occurs. Final form of the membrane will be asymmetric with a dense top layer. The second path will be followed if outflow of the solvent to the inflow of solvent is low. If second path is followed resulting membrane have porous structure with UF properties. Third path is followed if system has low polymer concentration or by using coagulation bath consists of solvent and non-solvent. Herein polymer lean phase is greater than polymer rich phase and when the solidification occurs, polymer lean phase is washed up from membrane matrix and results in a open porous membrane (Machado et al., 1999; Li and He, 2007; Ohya et al, 2009; Wienk, 1993).

When an additive is used in dope solution, phase diagram becomes a tetrahedron (Figure 2.9) however interpretation of a three dimensional diagram is very complex, so quaternary systems

can be explained by using pseudo-ternary phase diagrams (Ohya et al., 2009). In pseudo-ternary diagrams, it is thought that additive and polymer act as an one component. As cited in Ohya et al. 2009 and Machado et al. 1999, Boom et al explained this phenomena by using two time scales. In shorter scale exchange of solvent and non-solvent is valid. Herein polymer and additive act as one and real binodal line in ternary system is becoming virtual binodal line. In longer time scale two polymer can move relative to each other, therefore additive moves into polymer lean phase and virtual binodal shift into real binodal line.

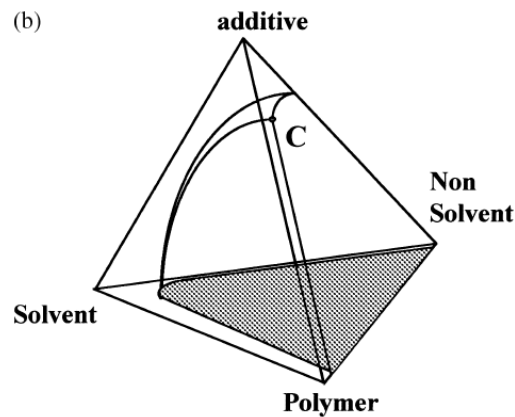


Figure 2.9 : Schematic phase diagram for quaternary system (Machado et al., 1999).

Also to guess how morphology is going to be change, after polymer solution contact with coagulation bath, instataneous and delayed mixing become significant. Phase separation through instataneous mixing happens immediately after precipitation whereas delayed mixing occurs when precipitation of polymer doesn't start after it is in contact with coagulation bath. One uses instataneous mixing can obtain membranes having porous top layer and can be usable in UF and MF processes whereas if one uses delayed mixing, membranes have denser skin and can be used in gas separation, pervaporation etc. (Machado et al., 1999).

2.3.5 Spinning parameters

By applying different spinning conditions and varying membrane material countless possibilities can be achieved for membrane properties. Hollow fiber spinning differs from flat sheet process due to its various spinning conditions. When spinning process begins all related factors must be optimized to have desired structure. Type of polymer, type of solvents, dope extrusion rate, viscosity, types of additives, air gap length, take-up speed, coagulation bath temperature, concentration of bore and outer liquids will be discussed in the forthcoming part.

2.3.5.1 Type of polymer

The choice of the membrane material has huge significance. Polymeric membranes have easy forming properties, inexpensive, wide range of applications (Ng et al., 2010). Separation process demands different resistance such as high thermal or chemical resistance or both (Wagner J., 2001; Baker, R.W. 2004). Hydrophilicity is also important due to its effect on permeability of membrane (Wienk, 1993). Generally used polymers for ultrafiltration processes are polyethersulfone (PES), polysulfone (PS), Polyvinylidenedifluoride (PVDF), polyacrylonitrile (PAN) and polyamide (Albrecht et al, 2005; Çulfaz et al., 2010; Liu et al., 2008).

2.3.5.2 Type of solvents

Solvents are used in membrane formation as they are the key for phase inversion process. Solvent and polymer should be miscible in each other to produce homogeneous spinning solution. Not all solvent dissolve exact type of polymers. Used solvent in spinning solution should be rapidly evaporates immediately after immersed in water. Mostly used solvents are dimethyl acetamide (DMAc), N,N-dimethylformamide (DMF), 1-methyl-2-pyrrolidone (NMP) (Baker, W.R, 2004).

2.3.5.3 Type of additives

Membrane separation performance is related to various parameters such as hydrophilicity, surface charge, porosity etc. Additives help to change hydrophilicity, porosity of the membranes. Increasing hydrophilicity acts as a fouling preventer. Polyvinylpyrrolidone (PVP), polyethyleneoxide (PEO), polyethyleneglycol (PEG) are mainly used pore additives, Lithium chloride (LiCl), ethanol, methanol, water are also used (Rugbani, 2009).

Wienk et. al (1995), have investigated how different PVP concentrations affect hollow fiber membrane morphology and performance. They found that high PVP concentrations favor water flux and lead to lower Bovine serum albumin (BSA) rejections. Wongchiphimon et al. (2011) have investigated the influence of PEG having different molecular weights. They concluded that as molecular weight of PEG increases and the weight amount of PEG is kept as the same, dimension of finger like macrovoids increased because PEG mobility decreases and viscosity increases, so more PEG is entrapped within membrane matrix during phase inversion process, also pure water permeability (PWP) increased. Loh et al. (2011) have concluded that usage of Pluronic F127 and F108 as additives in the spinning solution, pure

water permeation became higher and they obtained low molecular weight cut off (MWCO) hollow fiber membranes. Also Pluronic F127 increased pore size of the membranes which lead to better rejections. Xu and Qusay (2004) used different ethanol concentrations to observe its effects in pore formation and they found that as ethanol concentration increased morphology of the membranes were changed from wide finger like to thin finger like and then to sponge like structure. Also PWP was increased and up to some point rejections are increased and then it decreased.

2.3.5.4 Air gap length

Air gap is one of the most researched and important parameter for the formation of hollow fiber membranes because of its significant influence on the performance and morphology of the membrane.

Khayet (2003) have found that pore size, roughness parameters of inner and outer structure of PVDF membrane were affected as air length increases, which leads to lower permeation flux and high solute separation performance. As air gap increased, wall thicknesses, inner and outer diameters decreased. This attributes can be due to die swelling of polymer macromolecules and gravitational forces which introduces elongational stress on fibers and shear and elongational stresses within the spinneret. Flux and separation features generally is affected by active surface layer which are formed by the mechanism of non-solvent/solvent exchange during phase separation.

Zhang et al. (2008) observed that inner and outer diameters of PAN hollow fibers decreased while air gap increased. They attributed this result to the surface tension in the air gap. Chung et al. (1998) have investigated the effect of air gap for mechanical and thermal stability of polybenzimidazole/polyetherimide hollow fiber membranes and they found that air gap have dual effect on membrane properties. As air gap increased up to a point, tensile modulus increased and then decreased. Glass transition temperature (T_g) value decreased as air gap increased due to reduce in porosity of membrane because of molecular orientation and elongational stress.

2.3.5.5 Viscosity

To give membrane its hollow shape, viscosity is very important. Since too low viscosity value can result in irregular shapes whereas at too high viscosity values can cause large pressure drops in the spinneret (Kools, 1998). Increasing polymer concentration, non-solvent additives

increases viscosity while increasing solvent concentration decreases viscosity of the spinning solution. Raising dope viscosity extends the exchange time between non-solvent/solvent, so the time to reach coagulation composition. Therefore nucleation and growth of polymer-lean phase is favored, which cause larger pores (As cited in Ohya et. al 2009). Ohya et al. observed that as dope viscosity increases outer-surface pore size increases and there is a certain dope viscosity, after that limit, bore liquid can not be able to enter nascent membrane wall by using osmotic pressure and this situation affects macrovoid formation.

2.3.5.6 Dope extrusion rate

Dope extrusion rate is one of the important parameters for hollow fiber spinning since polymer solution will be subject to various stresses which may affect fiber formation and separation performance as they affect molecular orientation and relaxation through spinneret. Two mechanism affect fiber formation during phase inversion. One of them is elongation stresses (air gap etc.) caused by gravity and spinning line stresses. The other one is shear and elongation stresses result from inside the spinneret. Qin and Chung (1999) have investigated effect of dope flow rate on hollow fiber membranes using wet spinning to decrease the effect of elongation which is caused by air gap. They observed that at higher dope flow rates, they fabricated membranes having decreased pore size, water permeability, elongation whereas separation performance, tensile strength and Young's modulus increased. Wang et al. (2004) are observed the same results as Qin and Chung (1999). Ismail et al. (2006) also have investigated the effect of dope extrusion rate by using dry-wet phase inversion method. Their results show that flux was decreased whereas separation performance which is due to thicker and denser outer skin of membranes was increased.

2.3.5.7 Coagulation bath temperature and composition

Fiber morphology depends heavily on coagulation bath temperature. Since an increment in coagulation bath temperature leads to an increment of solvent - non-solvent exchange and solubility, so porous structure is achieved. Composition is also significant especially for demixing process (Peng et al, 2012). Wienk et al. (1995) have studied the effect of coagulation bath temperature on HF membranes. They found that if coagulation bath temperature increases pore sizes became bigger due to high exchange rates. Xu et al. (2008) have investigated the effects of coagulation bath temperature, and found that an increase in coagulation bath temperature, decreased outer and inner diameter of membranes increased

water flux, porosity, pore size and fiber morphology changed from finger like to sponge like. Desmukh and Li (1998) have investigated effect of ethanol coagulation bath on HF membranes and found that structure went from finger like to sponge like structure.

2.3.5.8 Take-up speed

Module productivity is increased when modules have higher surface areas/volume. To control this take-up speed is an important phenomena. Because smaller diameters can be formed at high draw ratios. Also at high take-up speeds due to higher orientation high tensile strength and modulus are obtained. Chou and Yang (2005) have investigated the effect of take-up speed on cellulose acetate hollow fiber membranes. They found that retention, inner and outer diameter were decreased, permeation, elongation and tensile strength were increased as take-up speed increased. Li et al. (2012) observed obvious changes on diameters of hollow fiber and mechanical strength however pure water flux and porosity were changed slightly.

2.3.5.9 Bore and outer fluid type

Bore and outer fluids alter membrane structure. Especially bore fluid gives a membrane its hollowness. Phase separation process is mainly affeted by exchange of non-solvent amd solvent, so if bore and outer fluid types and concentration are changed, structure of our membranes like selective layer or cross sectional morphology are also changed (Peng et al, 2012). Chen et al. (2010) used different concentration as bore liquid (100% water and, 75% DMAc : 25% water), they found that permeability was increased but rejection was decreased as solvent concentration increased.

2.4 Carbon Nanotubes

Carbon nanotube (CNT) can be viewed as a hollow cylinder formed by rolling graphite sheets. They can be synthesized as single wall CNT or multiwalled (consist of up to 10-100 carbon shells) CNT (Figure 2.4). Their diameters can be several nanometers whereas length can be varied longer. They have very interesting and usable features as high mechanical strength, high strength-to-weight ratio, large length to diameter ratio, high thermal stability, very smooth internal surface, precise diameter (Bruggen, 2012; Aroon et al, 2010).

They have many application areas which are field emission, reinforcing materials, energy storage and thermal interface materials, and also fluid separation (Goh et al., 2012), like

membrane separation. Membranes can be synthesized with organic or inorganic materials but just organic membranes are included in the scope of this thesis.

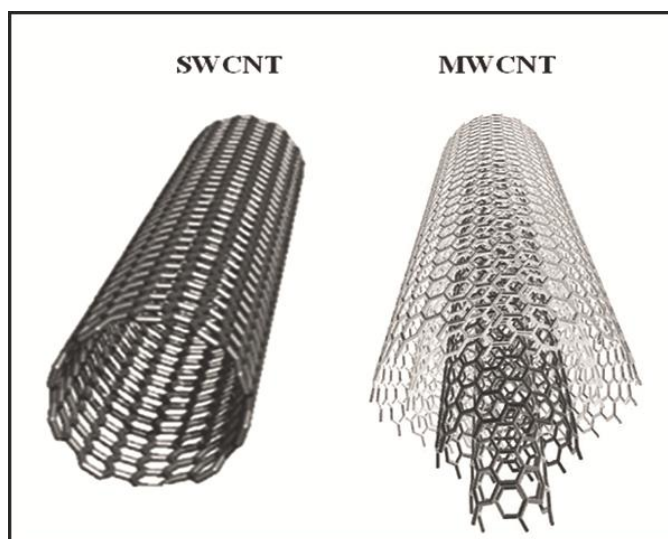


Figure 2.10 : Types of carbon nanotubes (Choudhary and Gupta, 2011).

CNTs are a model system used for water and ion transport due to their hydrophobicities and structural simplicities. Water transport mechanisms of CNTs have not fully understood but it is thought that water molecules interact with hydrophobic walls of CNTs and smooth nature of CNTs' walls enable almost frictionless water transport which leads to higher water flux (Goh et al, 2012).

Polymer material is easily processable, have medium mechanical strength, flexible and easily fouldable. For improving its properties, nanoparticles are used. One of them is CNTs. To use CNTs in polymer nanocomposites some struggles have to be overcome. By this way, true potential of CNTs can be achieved. "CNTs must have high purities, longer lengths, better integrities, larger amounts and at low cost. Besides orientation of CNTs, concentration, interfacial adhesion, distribution and dispersion must be considered." (Bruggen, 2012). Also, although CNTs are open-ended tubes, generally end are capped (Goh et al., 2012). It is also an obstacle for CNTs. Dispersion is the most significant part of these challenges as any aggregation in CNT/polymer composites results in inferior properties because of prevented efficient stress transfer of CNTs (Spitalsky et al., 2010). To control aggregation and dispersion behaviour, one has to overcome surface interaction like Van der Waals interaction, hydration force, depletion etc. (Ng et al., 2010) and better dispersion can be achieved by adding surfactants, with sonication or ultrasound. However, one has to be careful when using

sonication treatment because too high or long treatment can damage CNT (damage to wall or shortening etc.). Also surface functionalization can be used for preventing agglomeration, reagglomeration or for getting better dispersion. By functionalization, application of liquid flux in CNTs to attain selective and controlled transport can be achieved, besides selectivity and hydrophilicity of the surface increases (Goh et al., 2012).

Four types of CNT/polymer composite processing methods exist. These methods maximize the advantages of CNTs since they reinforce strength of CNTs effectively. Solution mixing, in situ polymerization, melt blending and chemical processing are these processing methods. In solution mixing method, all components are mixed within a certain solvent and then solvent is evaporated somehow. Bulk mixing (milling) is a mechanical process which uses high pressure and makes many collisions. This method is generally used for shortening CNT and satisfactory dispersion is obtained. Melt mixing method is generally used for polymers can not be dissolved in certain solvents. In this process blending polymers melt with CNT material by the help of shear forces. Main advantage of in situ polymerization is the higher homogeneity of CNT/polymer composite than solution mixing (Spitalsky et al., 2010).

Two types of carbon nanotubes membranes exist. One is CNT bucky papers, second is isoporous CNT membranes. CNT bucky papers are used for membrane distillation because of their high hydrophobicities, and high mechanical strengths, whereas isoporous membrane can be used for desalination etc. Isoporous CNT membranes are good candidates for gas or water purification. Carbon nanotube based membranes can be separated into 4 categories which are for gas separation, water treatment, drug delivery, and fuel cells. By using CNTs for gas separation, it is found that high selectivities and permeances can be obtained. For water treatment, using CNTs alter permeability, selectivity, mechanical properties, thermal properties, surface and much more etc. Usage of CNTs in fuel cell resulted from their good electrical and mechanical properties. Nanotube's advantage comes from their controllable pore diameter and thicknesses for drug delivery (Bruggen 2012). However these concepts are out of the scope of this thesis, so membrane usage in water or wastewater treatment will only be considered.

2.5 Polymer/Nanocomposite Hollow Fiber Membrane Studies

Wide varieties of polymeric material exist for membrane separation processes however performance of polymeric membranes are not suitable for commercial uses. Modifying them by adding nanoparticles increase their efficiencies like permeability, selectivity, mechanical, chemical and thermal stabilities and lower fouling. Titanium, silver, silica, aluminum, carbon nanotubes are main nanoparticles used in the most of the studies related to membranes. Generally titanium and silver based nanoparticles are used to decrease biofouling (Ng et al., 2010) and virus removal (Zodrow, 2009) of polymeric membranes and increase hydrophilicity and selectivity. Antibacterial mechanism for silver is related to its interaction with sulphur and phosphorus whereas for titanium it is related to photocatalytic effect which helps to decompose organic chemicals and kills bacteria. Silica nanoparticles are highly miscible, environmentally inert, have large surface area. Studies show that silica nanoparticles increase thermal stability, selectivity, permeability in polymeric membranes (Ng et al., 2010). Incorporating aluminum nanoparticles into polymeric membranes result in higher permeabilities, hydrophilicities. Up to some extent using aluminum based nanoparticle increased even mechanical strength. As already been said, CNTs are promising nanoparticles for membrane separation. Functionalized CNTs are especially used for polymer nanocomposite membranes due to their higher dispersibilities. So, functionalized CNTs can enhance permeability, flux, hydrophilicity of membranes, so better fouling resistance can be obtained (Vatanpour et al., 2011; Celik et al., 2011).

Razmjou et al. (2012) have studied the effect of TiO_2 nanoparticles on PES HF membranes. They used both mechanically modified and chemically and mechanically modified TiO_2 . Higher thermal resistance, higher permeability, higher hydrophilicity, porosity, pore size, lower elasticity and tensile strength were found for chemically and mechanically modified TiO_2 . Han et al. (2010) have spun hollow fiber membranes by adding aluminum, silica and titania nanoparticles at the same dope solution with different concentrations. They observed that higher flux, higher break strength values. BSA rejection changed discordantly. Morphology changed from macroporous structure to asymmetric structure, denser top layers were obtained and the most obvious effects on membrane morphology was on the inner surface. Goh et al. (2012) have studied the effects of multiwalled CNTs for polyimide HF membranes. Improvement in gas separation and permeability was observed, fast and smooth

transport of gas molecules enhanced. Aroon et al. (2010) have observed the effect of raw multiwalled carbon nanotube (MWCNT) on polyimide membranes. With the addition of raw MWCNTs gas separation factor increased whereas permeability decreased. Also glass transition temperature was increased with an increase in raw MWCNT content.

In addition, toxicity of nanoparticles should be considered before they are used in membranes for water and wastewater treatment. Besides optimum concentration must be found between polymer and nanoparticles to fabricate cost effective and higher performed membranes.

3. MATERIALS & METHODS

3.1 Materials

Polyethersulfone (PES) taken from BASF, the chemical company was used as membrane matrix, polymer. As pore formers, two types of polyvinylpyrrolidone (PVP) were bought from ISP (US) were used which were PVP-K30 (Mw=65000) and PVP-K90 (Mw=1,500,000). Dimethylformamide (DMF) was used as a solvent bought from Akkim Kimya Sanayi ve Ticaret A.Ş. (Turkey). Functionalized multiwalled carbon nanotubes (MWCNTs) were used. Carboxyl multiwalled carbon nanotubes (MWCNT-COOH) were purchased from Timesnano (China) and hydroxyl multiwalled carbon nanotubes (MWCNT-OH) were purchased from Cheaptubes (US). In Figure 3.1, structure of polyethersulfone and PVP can be seen.

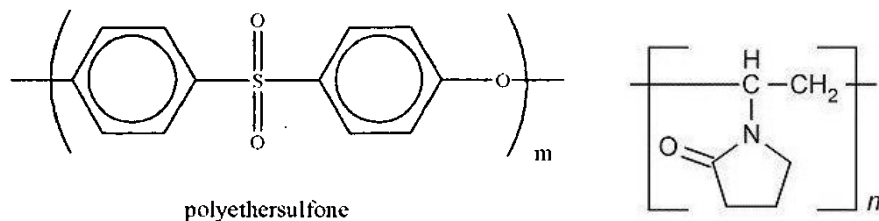


Figure 3.1 : Chemical formula of PES and PVP (url-9, url-10).

3.2 Preparation of Spinning Solution

Before choosing spinning solution composition and spinning parameters, lots of experiments were done to optimize the conditions.

3.2.1 Preparation of dope solutions without MWCNT

PES was dried for 2 hours at 100°C before it was dissolved in DMF at 90°C. After that PVP K90 and PVP K30 were dissolved in solution. Solution, then was mixed for 12 hours and it

became homogeneous. Before spinning, it was waited under vacuum condition for 30 min to get rid of bubbles.

3.2.2 Preperation of dope solution with MWCNTs

To be able to disperse functionalized MWCNTs homogeneously in spinning solution, first CNTs were mixed in Bandelin-Sonopuls (Germany) homogenizator Figure 3.2. Then, PES dried for 2 hours at 100°C, PVP K90 and PVP K30 were added and mixed for 12 hours at 90°C. Before spinning, for the removing of air bubble in dope solution, solution was sonicated for 30 min with Everest Ultrasonic sonicator (Figure 3.3) and then it was vacuumed.

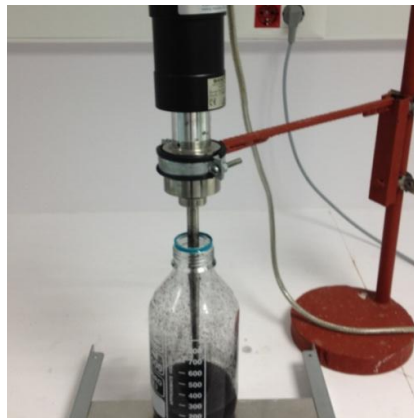


Figure 3.2 : Dispersion of MWCNTs within solvent.



Figure 3.3 : Sonication of dope solution.

3.3 Spinning of Hollow Fiber Membranes

Phase inversion by immersion precipitation was used to fabricate hollow fiber membranes. PHILOS (South Korea) hollow fiber membrane system (Figure 3.4) was used. Spinning line was used to fabricate hollow fiber membranes can be seen in Figure 3.5. Spinning line

consists of driving roll (8), godet roll (9) and take-up roll (10). Polymer solution (dope solution) (4), bore liquid (4) and outer liquid(4) was pumped into triple spinneret by the help of nitrogen gas pressure under 2 atm (1). There are valves before tanks (2,3) to control gas pressure and tanks. Detailed triple spinneret (6) schematic can be seen in Figure 3.6. Fiber extrusion rate and rate of bore liquid and outer liquids were adjusted according to the desired properties. All liquids and dope solution goes through spinning line (5) before they are met at the spinneret. As dope solution meets with bore liquid and outer liquid hollow structure occurs and nascent fibers goes to first coagulation bath (8), driving roll, second coagulation bath (9), godet roll and then take-up roll (10) respectively.

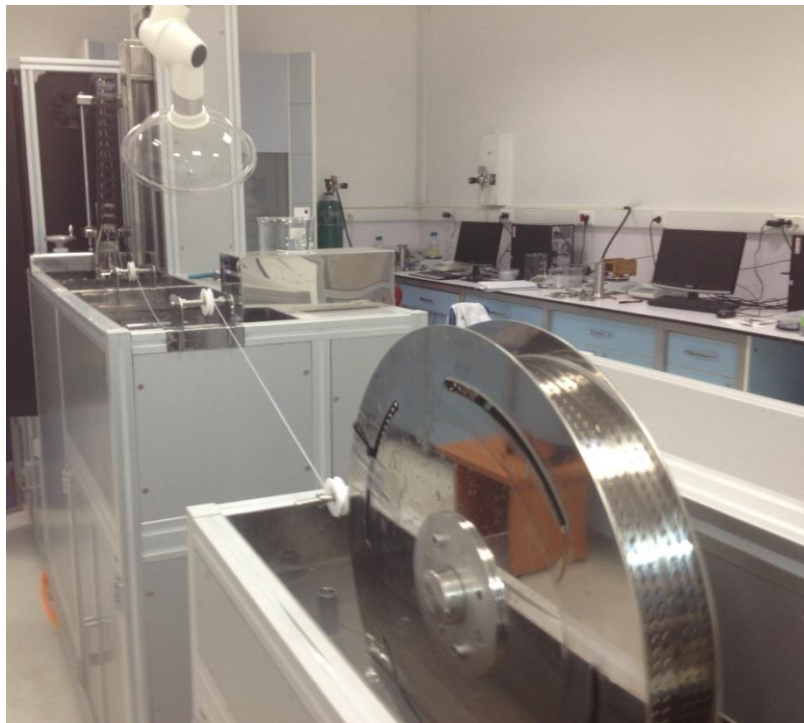


Figure 3.4 : Hollow fiber membrane system.

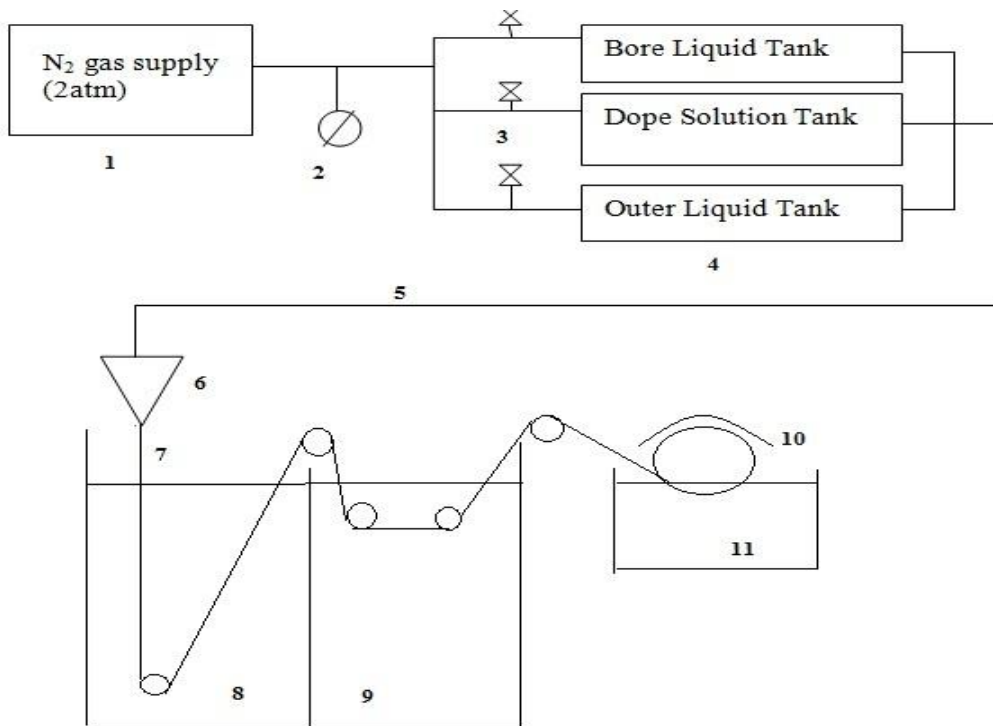


Figure 3.5 : Schematic of spinning line.

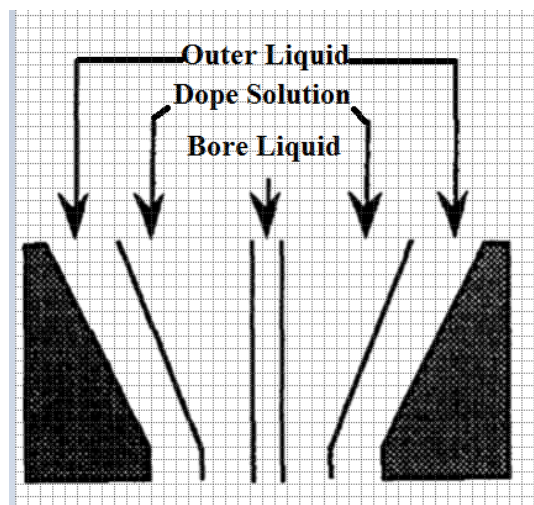


Figure 3.6 : Schematic view of triple spinneret (Wienk et al., 1993).

3.4 Treatment & Post-treatment of Hollow Fiber Membranes

Hollow fibers taken from take-up roll was properly categorized and put into PHILOS membrane flushing system (South Korea) (Figure 3.7). At 40°C hollow fiber membranes was flushed for 12 hours to remove solvent within membranes. After that half of fabricated membranes were put into distilled water and the other half were put into 4000ppm sodium

hypochloride (NaOCl) solution for post treatment for 2 days. Then all membranes were put into 10% / 90 % glycerol / water solution for 12 hours to prevent pore collapse.



Figure 3.7 : Membrane flushing system.

3.5 Preparation of Hollow Fiber Test Modules

After all kinds of treatments, dead end flow HF modules were prepared. Glue taken from PHILOS Company (South Korea) was used for this purpose. HF membranes were cut between 20 to 30cm. Then with a syringe, glue was injected into modules. Modules were waited around 12 – 15 hours for drying (Figure 3.8). Finally all modules were put into distilled water for both preservation and testing.



Figure 3.8 : Prepared test modules.

3.6 Membrane Characterization

3.6.1 Filtration experiments

For filtration experiments pressure driven filtration cell taken from Sterlitech Corporation (USA) was used after some modification (Figure 3.9a-b). Specifications of the filtration cell obtained from company can be seen on Table 3.1.

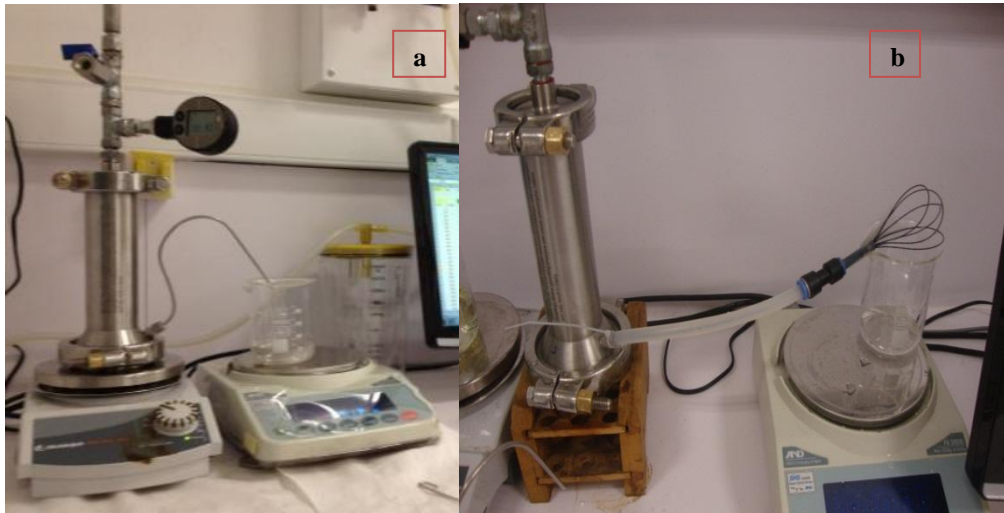


Figure 3.9 : (a) normal setup, (b) modified sterlitech setup for hollow fiber membrane.

Table 3.1 : Filtration Cell Specifications.

Volume of cell	300 mL
Maximum pressure	69 bar
Maximum temprature	121 °C

3.6.1.1 Permeability test

Before permeability tests, compaction test with distilled water were done for 30 min to remove just in case if there was any solvent or unreacted polymer remainings. After compaction at 3 different pressure flux measurements were done again with distilled water and datas were transferred to an excel file. Flux was calculated according to the equation below throughout the experiments **(3.1)**.

$$J = \frac{V}{A.T} \quad (3.1)$$

where;

J : Flux (L/m².hr),

V : Volume of permeation (liter),

A : Area (m²),

T : time (hour)

On excel file pressure and flux graph was drawn. Slope of the graph gives permeability of a HF module.

3.6.2 Fouling experiments

Rejection performance of the membranes were conducted at room temperature by using bovine serum albumin (BSA)(100ppm) aqueous solution. BSA rejection datas were collected from the permeation and feed solutions. Concentrations of BSA solutions were determined by Hach Lange DR500 UV Spectrophotometer (Figure 3.10). Flux values were calculated according to equation (3.1) and BSA rejection was calculated from the equation (3.2) below:

$$R = \left(1 - \frac{C_p}{C_f}\right) \times 100\% \quad (3.2)$$

where,

R= rejection (%),

C_p= permeate concentration (wt%)

C_f= feed concentration (wt%)

Besides Flux recovery ratio (FFR%), total fouling ratio (R_t), reversible fouling ratio (R_r), irreversible fouling ratio (R_{ir}) was calculated according to the equation (3.3), (3.4), (3.5), (3.6), (3.7) given below (Vatanpour et al., 2011);

$$FFR(\%) = \frac{J_{w,2}}{J_{w,1}} \times 100 \quad (3.3)$$

$$R_t = \left(1 - \frac{J_p}{J_{w,1}}\right) \times 100 \quad (3.4)$$

$$R_r = \left(\frac{J_{w,2} - J_p}{J_{w,1}}\right) \times 100 \quad (3.5)$$

$$R_{ir} = \left(\frac{J_{w,1} - J_{w,2}}{J_{w,1}}\right) \times 100 \quad (3.6)$$

$$R_t = R_r + R_{ir} \quad (3.7)$$

where

$J_{w,2}$: water flux of cleaned membranes,

$J_{w,1}$: water flux

J_p : flux for protein solution

R_t : Total fouling ratio (%)

R_r : Reversible fouling ratio (%)

R_{ir} : irreversible fouling ratio (%)



Figure 3.10 : Spectrophotometer used for BSA absorbance.

3.6.3 Membrane dope characterization

Viscosity of dopes were found using AND vibro viscosimeter SV-10 (UK) (Figure 3.11). 30ml of dope solution was used to determine viscosity value and before each use, calibration was done with distilled water at 25°C. Each experiments were done at room temperature.

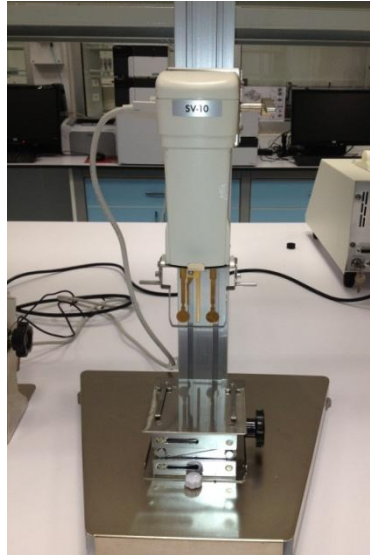


Figure 3.11 : Viscosimeter.

3.6.4 Contact angle

To be able to talk about how hydrophobic or hydrophilic a membrane is contact angle measurements were conducted using Attension T200 Theta (Figure 3.12). Between 2 μ l and 5 μ l distilled water was dropped onto dry membrane surface in air. Datas were collected from 3 different point.

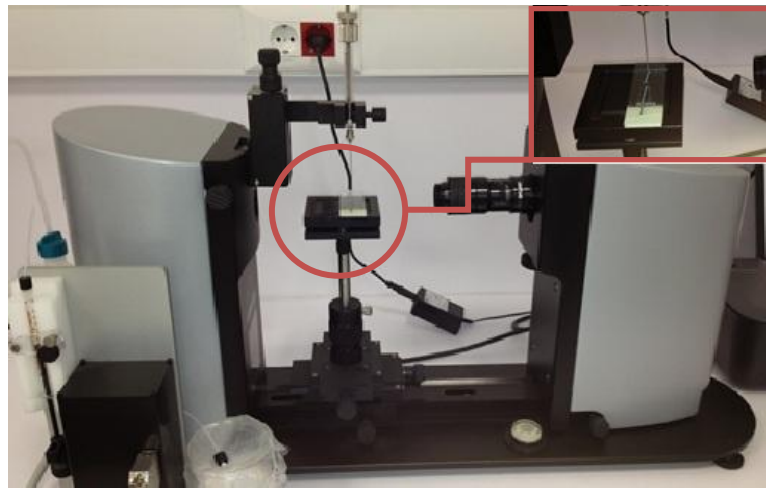


Figure 3.12 : Contact angle measurement setup.

3.6.5 Stereo microscopy

After spinning to observe the structure of hollow fiber membranes, stereo microscope (Figure 3.13) images were taken. A bunch of membrane were cut and inserted in a metal piece.



Figure 3.13 : Stereo Microscope.

3.6.6 Mechanical stability

For mechanical testing of hollow fibers SII DMS 6100 Exstar was used (Figure 3.14). Hollow fiber membrane was installed between grips and fastened. Membrane should be inserted carefully to minimizing of stretching of membrane. For each sample 3 measurements were done and average was used to avoid miscalculations. Cross sectional area of membrane was calculated by using a cross sectional thickness measurer. Data were taken in every 3 seconds and total load was 5000N in each step increment was 250N.

Tensile strength, percentage elongation at break and Young's modulus were calculated directly from the program that is used by equipment according to equations (3.8), (3.9), (3.10) given below (Rugbani, 2009);

$$\text{Tensile Strength} = \frac{F}{A_0} \quad (3.8)$$

$$\text{Elongation} = \frac{\Delta L}{L_0} \quad (3.9)$$

$$\text{Young's Modulus (E)} = \frac{\text{tensile strength}}{\text{tensile strain}} \quad (3.10)$$

where

F : force applied to the sample (N)

A₀ : cross sectional area of sample before elongation



Figure 3.14 : Mechanical stability testing equipment.

ΔL : the displacement at maximum load (mm)

L_0 : length of sample at starting point

3.6.7 Scanning electron microscopy (SEM)

Morphology of hollow fiber membranes was characterized by FEI Quanta FEG 200 SEM (Figure 3.15a). Membranes were prepared by inserting them into liquid nitrogen and cut. Then it was coated about 3-4nm with Palladium and Gold (Pd-Au) by using Quorum SC7620 ion sputtering equipment (Figure 3.15b).

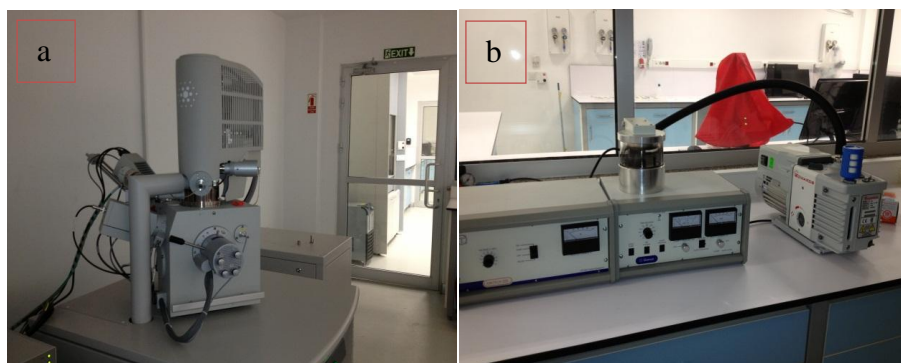


Figure 3.15 : (a) SEM setup, (b) ion sputtering setup.

3.6.8 Porosity measurements

Porosity (ϵ %) of the membranes was found using gravimetric method. Equation (3.11) was used to calculate overall porosity (Vatanpour et al., 2012) given below:

$$\epsilon = \frac{(w_1 - w_2)}{\rho \times A \times l} \quad (3.11)$$

where;

w_1 : weight of the wet membrane (g)

w_2 : weight of the dry membrane (g)

ρ : water density (0.998g/cm^3)

A : membrane effective area (m^2)

L : membrane thickness (m)

3.6.9 Zeta potential of membranes

Streaming potential measurements were made using the Anton PAAR SurPASS Electrokinetic Analyzer (Figure 3.16). Multiple pH range was used (3-10).

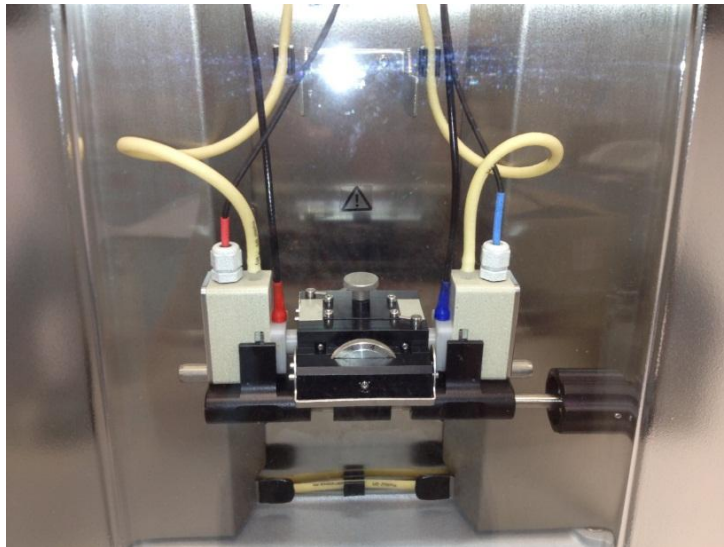


Figure 3.16 : Electrokinetic analyzer cell.

3.6.10 Fourier transformation infrared spectroscopy (FTIR)

Surface functionalization of membranes were characterized by using Perkin Elmer Spectrum 100 FTIR Spectrophotometer (Figure 3.17). Before measuring hollow fiber membranes, a background spectrum was conducted to decrease instrumental and atmospheric contributions to a minimum level.

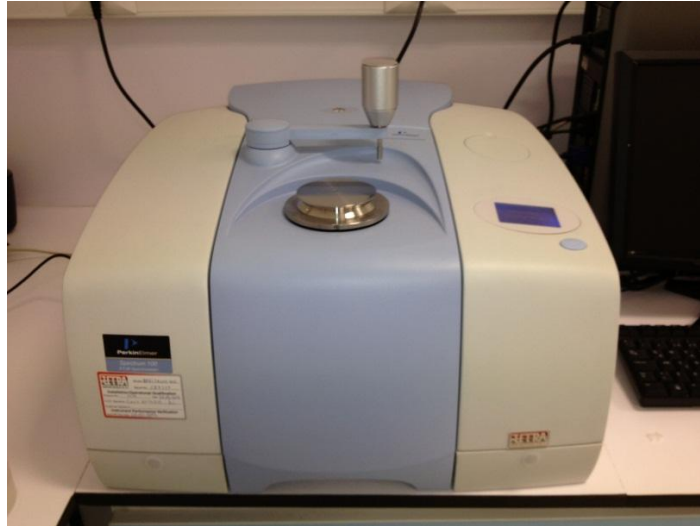


Figure 3.17 : FTIR spectrophotometer.

3.6.11 Growth of *Escherichia Coli* (*E.Coli*) on hollow fiber membranes

Antibacterial activity of CNT incorporated into membranes were assessed by using Gram negative bacteria *E.Coli*. 0.1ml *E.Coli* culture is diluted in 1 liter of water. Dead End filtration membrane modules were used to vacuum *E.Coli* solution for 10 min. Then modules were cut and inserted on agar medium (Figure 3.18) and incubated at 37°C for 1 day. Growth of bacteria was visually determined.

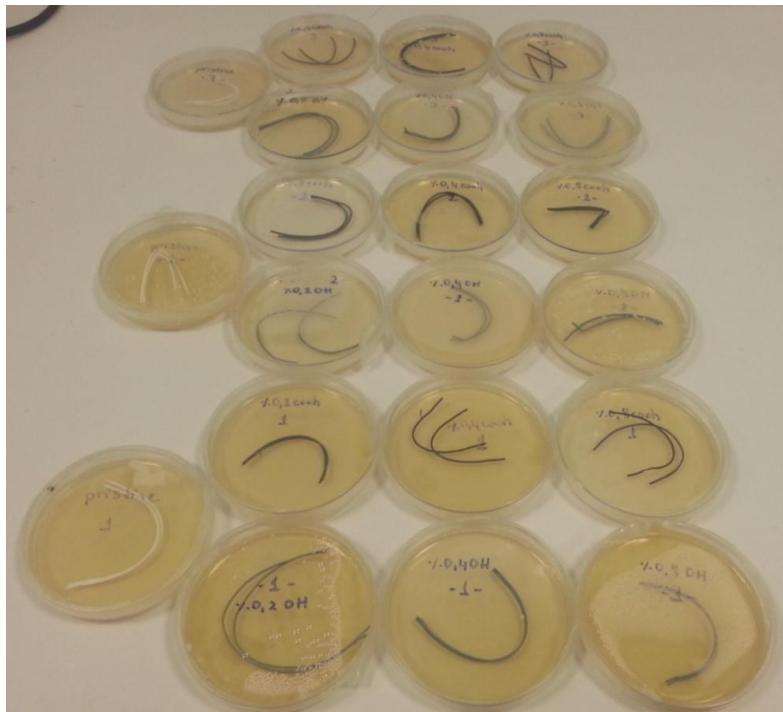


Figure 3.18 : Insertion of modules on agar medium for growth of *E.Coli*.

4. RESULTS & DISCUSSIONS

4.1 Deciding Dope Solution Recipe

Before spinning hollow fiber membranes with MWCNTs, trials had been done to find appropriate recipe. In Table 4.1, all trials can be seen.

Table 4.1 : Spinning solution composition trials to optimize hollow fiber spinning process.

Spinning solution number	Compositions									
	Dope solution						Bore Liquid		Outer liquid	
	PES (wt%)	PVP K90 (wt%)	PVP K30 (wt%)	Solvent DMF (wt%)	LiCl (wt%)	Water (wt%)	Solvent DMF (wt%)	Water (wt%)	Solvent DMF (wt%)	Water (wt%)
Trial-1	18	7	-	75	-	-	70	30	70	30
Trial-2	18	2	5	75	-	-	70	30	70	30
Trial-3	18	5	2	75	-	-	70	30	70	30
Trial-4	18	-	7	75	-	-	70	30	70	30
Trial-5	18	5	-	75	-	2	70	30	70	30
Trial-6	18	2	3	75	-	2	70	30	70	30
Trial-7	18	-	5	75	-	2	70	30	70	30
Trial-8	20	2	5	73	-	-	70	30	70	30
Trial-9	20	-	7	73	-	-	70	30	70	30
Trial-10	20	2	3	73	-	2	70	30	70	30
Trial-11	20	2	5	72	1	-	70	30	70	30

In each trials, some spinning parameter were changed such as dope flow rate, bore and outer flow rate; air gap; coagulation bath temperatures etc. According to the results, composition of Trial-8 was chosen as the recipe. In other recipes, some problems occurred like surface was not smooth, membranes had pinhole structures, mechanical stabilities were very low for UF. After that -COOH and -OH functionalized MWCNTs were added to dope solution in different concentrations. In Table 4.2, dope solution matrix of the experiments can be seen.

Table 4.2 : Spinning solution of chosen composition.

Spinning solution number	Compositions									
	Dope solution						Bore Liquid		Outer liquid	
	PES (wt%)	PVP K90 (wt%)	PVP K30 (wt%)	Solvent DMF (wt%)	MWCN T-COOH (wt%)	MWC NT-OH (wt%)	Solvent (wt%)	Water (wt%)	Solvent DMF %	Water (wt%)
Dope-1	20	2	5	73	-	-	70	30	70	30
Dope-2	20	2	5	72.8	0.2	-	70	30	70	30
Dope-3	20	2	5	72.6	0.4	-	70	30	70	30
Dope-4	20	2	5	72.2	0.8	-	70	30	70	30
Dope-5	20	2	5	72.8	-	0.2	70	30	70	30
Dope-6	20	2	5	72.6	-	0.4	70	30	70	30
Dope-7	20	2	5	72.2	-	0.8	70	30	70	30

From this point different kind of nomenclature will be used. Dope-1, dope-2, dope-3, dope-4, dope-5, dope-6, dope-7 will be defined and used as pristine, 0.2 COOH, 0.4 COOH, 0.8 COOH, 0.2 OH, 0.4 OH, 0.8 OH respectively.

4.2 Spinning Conditions

Hollow fiber membrane fabrication was done using phase inversion method. As already explained in literature part, spinning conditions can be fatal for fabrication. To see how membrane performance was affected, air gap, godet roll velocity were changed. Table 4.3 shows spinning conditions used throughout the experiments. Throughout the thesis “1” represents spinning #1, “2” represents spinning #2, “3” represents spinning #3. So, if pristine-1 is seen somewhere, this means that membrane fabricated from dope-1 and spinning parameters of spinning #1 was used.

Table 4.3 : Spinning parameters.

Parameters	Spinning #1	Spinning #2	Spinning #3
Dope solution velocity (ml/min)	4.62	4.62	4.62
Bore liquid velocity (ml/min)	4.5	4.5	4.5
Outer liquid Velocity (ml/min)	4.5	4.5	4.5
Take- up speed (m)	8,4	4,2	4,2
Air gap (cm)	15	15	0
Coagulation bath temperature (°C)	50	50	50

4.3 Effect of Viscosity

Differences in viscosity of dope solutions according to change in concentrations and functionalities of MWCNT type can be seen in Figure 4.1.

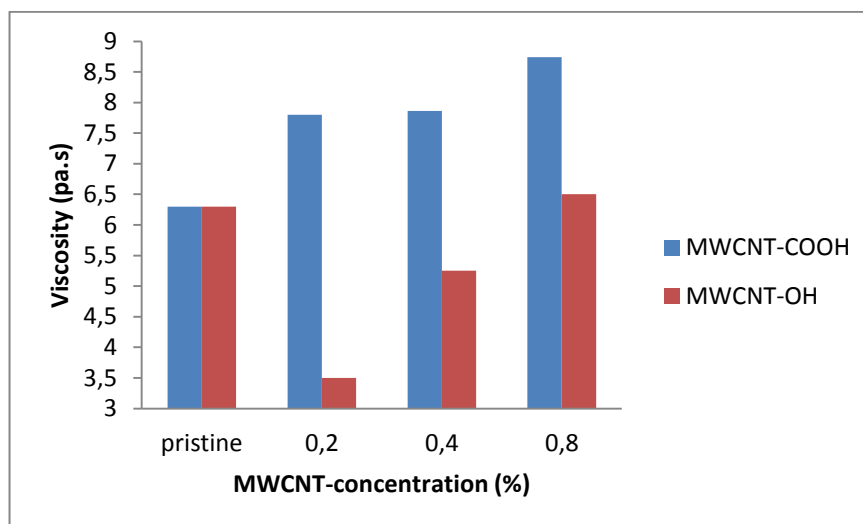


Figure 4.1 : Dope viscosity change vs. concentration.

Viscosity affects rheological properties, therefore main logic of phase inversion process was affected by viscosity changes because exchange of solvent and non-solvent rate was changed by viscosity. As shown in Figure 4.1, adding MWCNT-COOH particles in solution was increased dope viscosity whereas adding MWCNT-OH was decreased dope viscosity first and then increased. This might be due to bonding mechanism of MWCNT-OH and MWCNT-COOH to PES. One made viscosity decreased and the other lead to increment. According to Saljoughi et al. (2010), Ohya et al. (2009) viscosity results in delayed demixing in phase inversion so structure of fabricated membranes changes which is going to be seen in ongoing parts.

4.4 Morphology of the Membranes

In Figure 4.2, Figure 4.3 and Figure 4.5 cross section stereo microscope images of post treated membranes and in Appendix in Figure A.1-3 cross section of having no post treatment membranes can be seen.

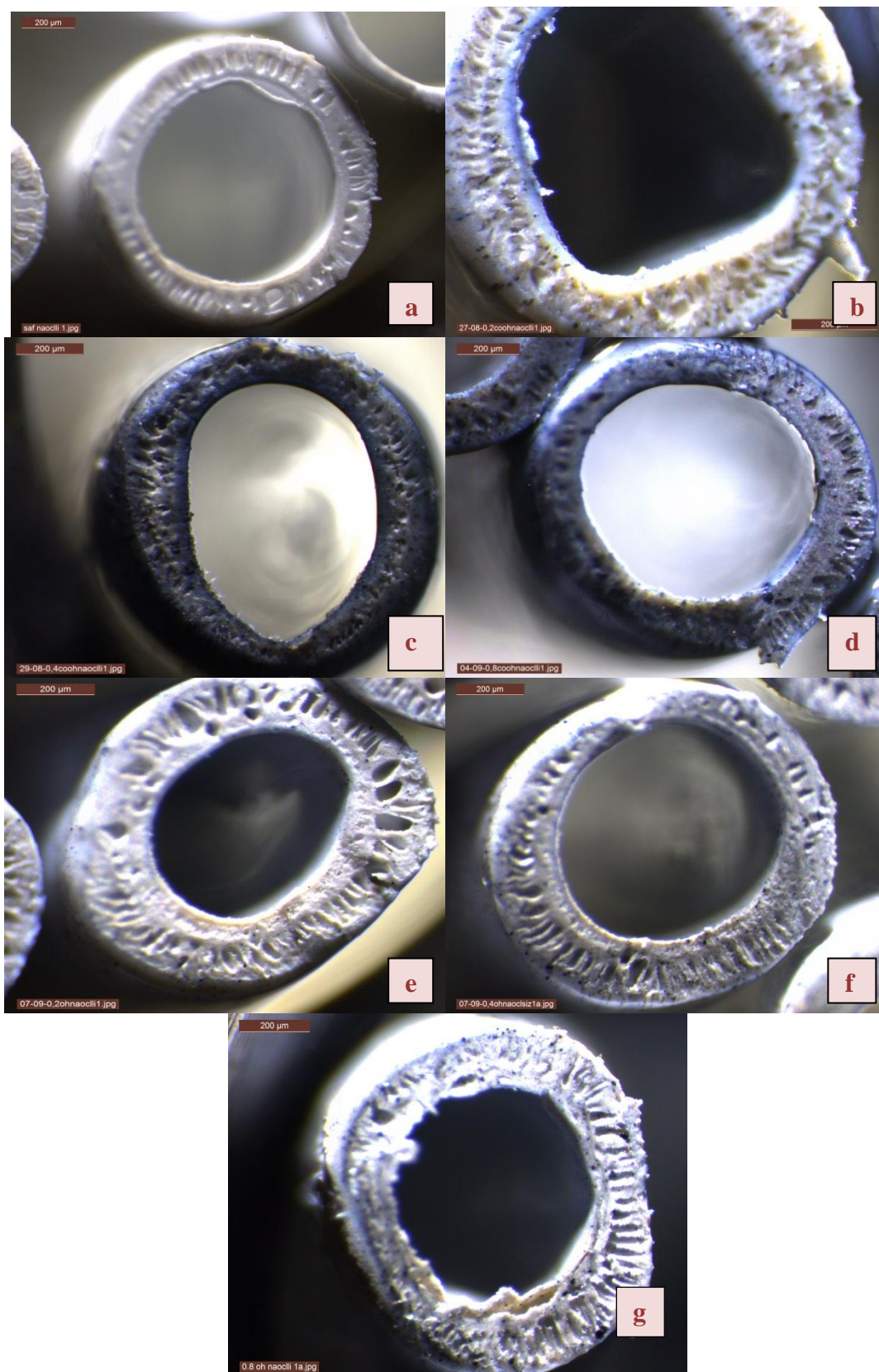


Figure 4.2 : Cross section stereo microscope pictures of #1 membranes. a) pristine 1, b) 0.2COOH 1, c) 0.4COOH 1, d) 0.8COOH 1, e) 0.2OH 1, f) 0.4OH 1, g) 0.8OH 1.



Figure 4.3 : Cross section stereo microscope pictures of #2 membranes. a) pristine 2, b) 0.2COOH 2, c) 0.4COOH 2, d) 0.8COOH 2, e) 0.2OH 2, f) 0.4OH 2, g) 0.8OH 2.

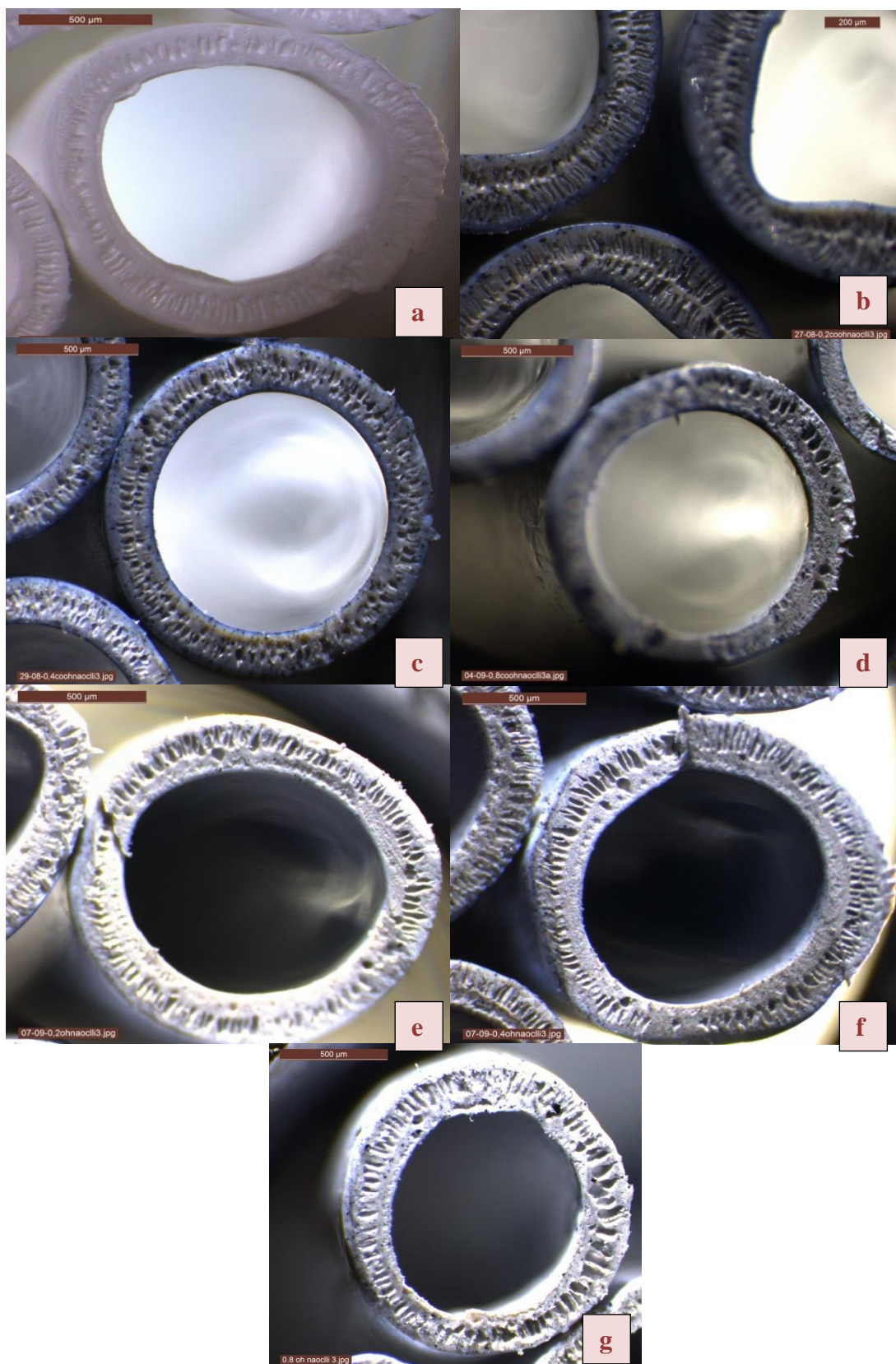


Figure 4.4 : Cross section stereo microscope pictures of #3 membranes. a) pristine 3, b) 0.2COOH 3, c) 0.4COOH 3, d) 0.8COOH 3, e) 0.2OH 3, f) 0.4OH 3, g) 0.8OH 3.

From stereo microscope images, it can be seen that, as MWCNT concentration increased, membranes color became darker. Membranes generally had a circular structure and an even distribution of effective membrane areas. General structure of HF membranes between sponge like and finger like. However details can not be observed through stereo microscope images, just a general idea can be obtained by using stereo microscopy, more detailed view of the membranes can be seen through their SEM images. In Figure 4.5, Figure 4.6, Figure 4.7 cross sectional views of the post treated hollow fiber membranes of #1, #2, #3, in Figure 4.8, Figure 4.9, Figure 4.10 detailed cross sectional views of the post treated membranes of #1, #2, #3 can be seen respectively and SEM images of cross sectional and detailed cross sectional views of membranes without post treatment of membranes #1, #2 and #3 can be found in Appendix A in Figure A.4-9 respectively. Also in Figure 4.11, MWCNT can be seen in the membrane matrix.

According to the cross sectional images of both “with post treatment” and “without post treatment” membranes, there were slight or no differences can be seen visible. For spinning #1, both outer and inner layers had spongelike structure for all membranes, whereas middle part had finger-like structure. An increase in concentration of MWCNTs increased sponge-like structure of the inner part. Finger-like structure were narrow in MWCNT-COOH membranes while finger-like structure became wider (like macrovoids) when MWCNT-OH used.

Spinning #2, showed the same trend like in spinning #1. However, it can be said that, sponge-like structure of the membranes were generally lower than the spinning #1. Pristine and 0.8 % MWCNT-OH membranes didn't have a proper circular structure and macrovoid formation was observed more than the other ones.

For spinning #3, sponge-like structure can be observed inner part of the membranes. Middle part of the membranes generally had narrow finger-like structures.

Membrane morphology is affected from air gap, coagulation bath temperature, dope viscosity, addition of nanoparticles or additives, bore liquid, outer liquid or coagulation bath temperatures. According Chou and Yang (2005), an increase in air gap means more time spent before membranes goes into coagulation bath.

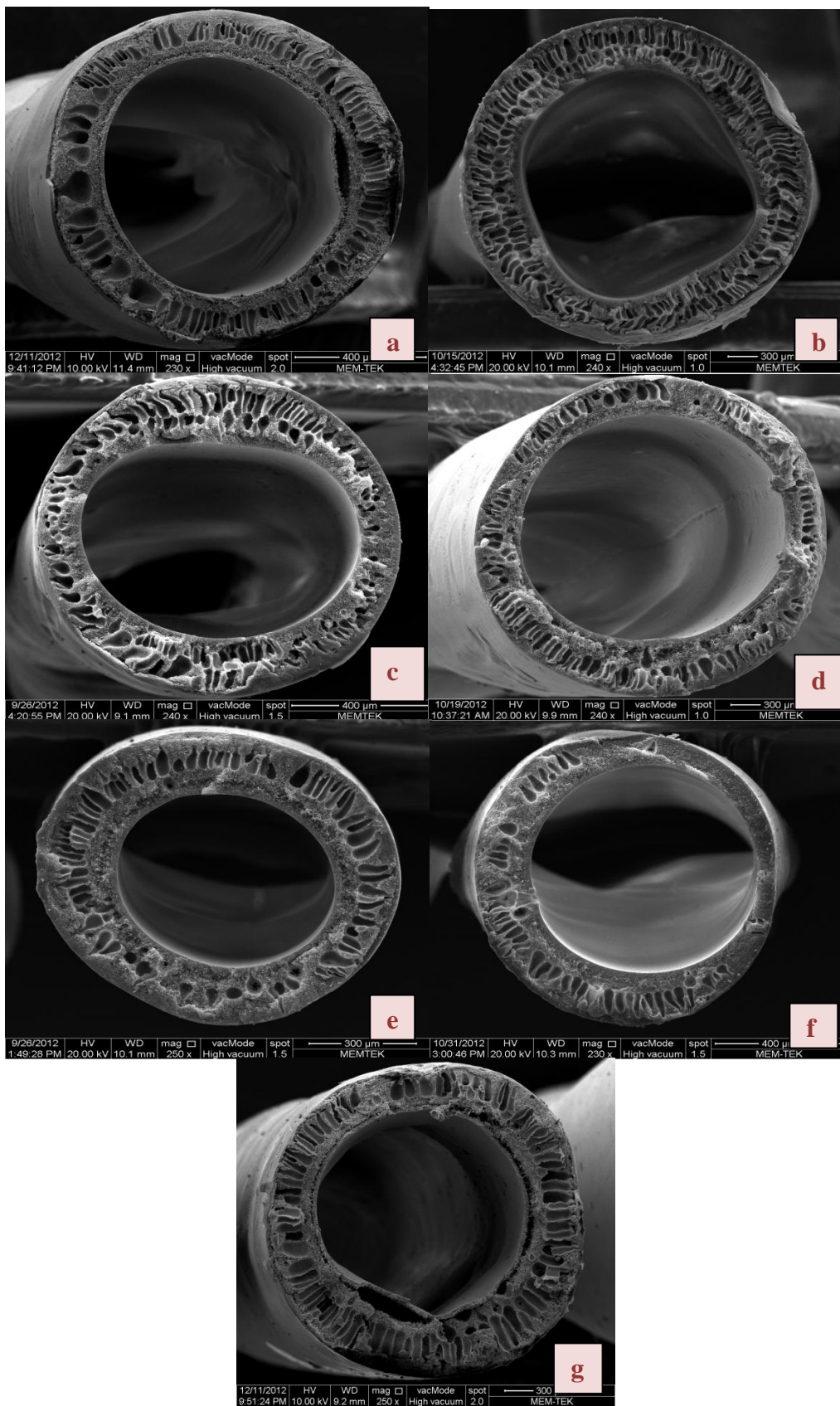


Figure 4.5 : Cross sectional view of #1 membranes. a) Pristine 1, b) 0.2COOH 1, c) 0.4COOH 1, d) 0.8COOH 1, e) 0.2OH 1, f) 0.4OH 1, g) 0.8OH 1.

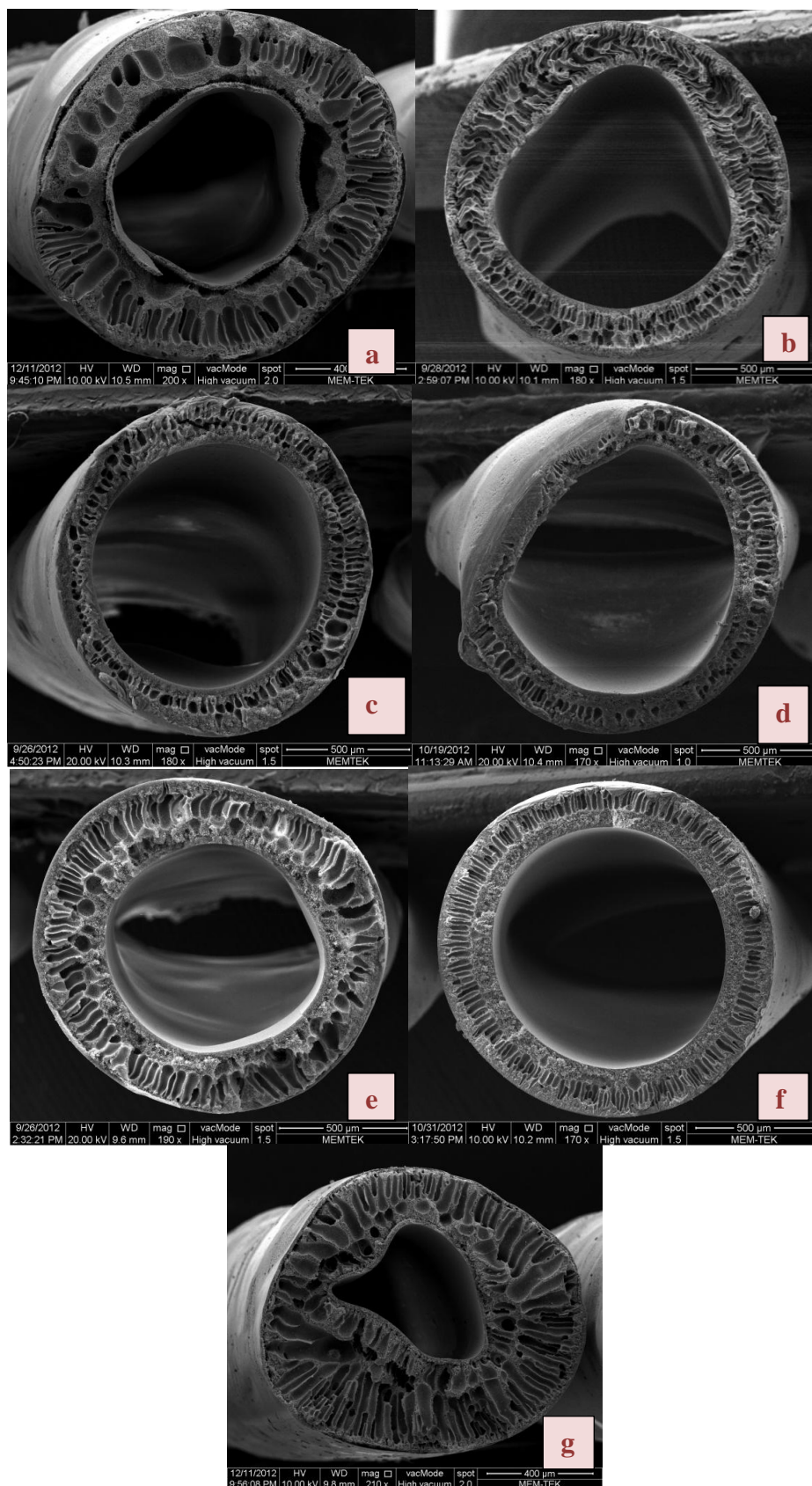


Figure 4.6 : Cross sectional view of #2 membranes. a) Pristine 2, b) 0.2COOH 2, c)0.4COOH 2, d) 0.8COOH 2, e) 0.2OH 2, f) 0.4OH 2, g) 0.8OH 2.

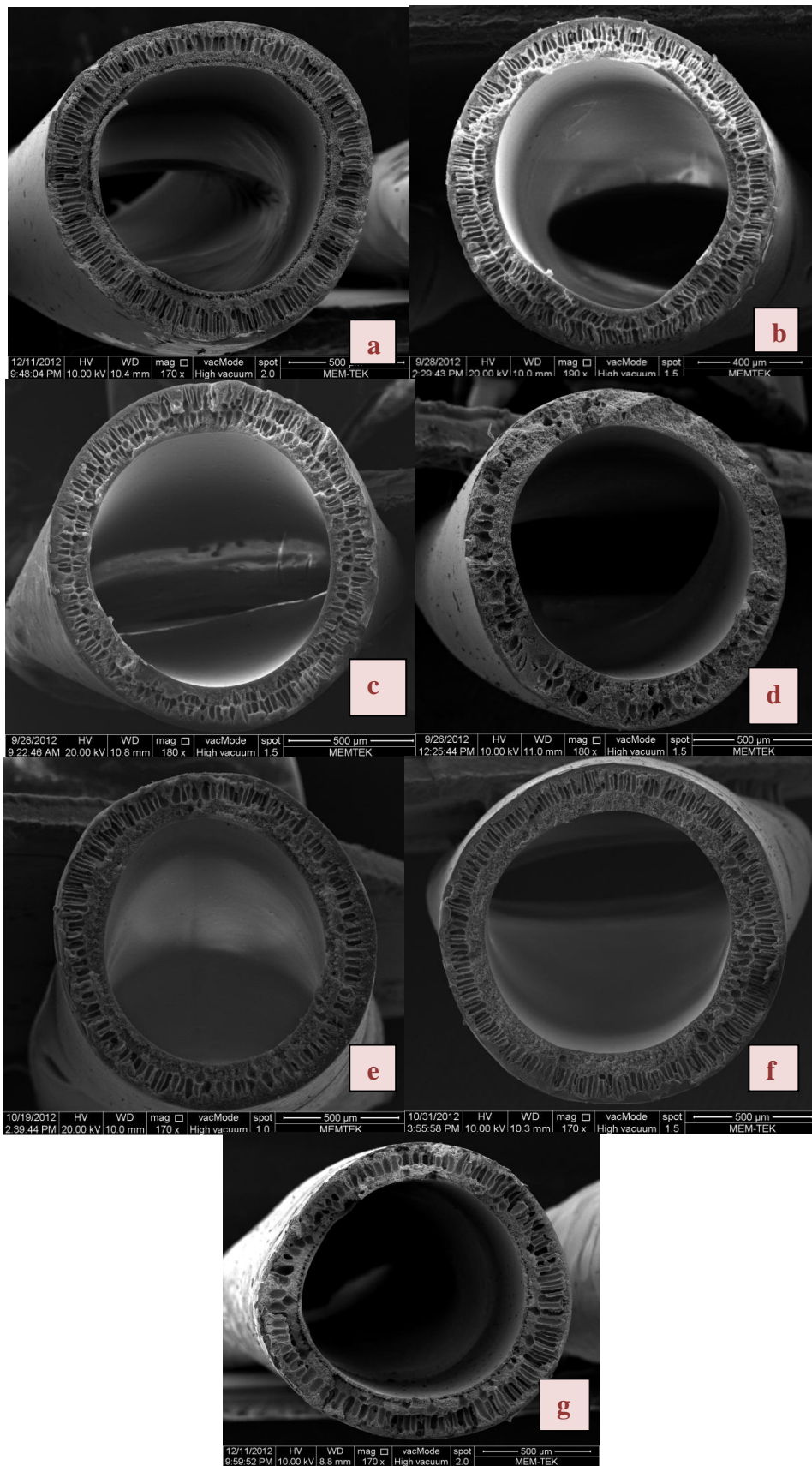


Figure 4.7 : Cross sectional view of #3 membranes. a) Pristine 3, b) 0.2COOH 3, c)0.4COOH 3, d) 0.8COOH 3, e) 0.2OH 3, f) 0.4OH 3, g) 0.8OH 3.

If humidity is higher, then more moisture goes into membrane matrix which promotes the formation polymer lean phase. When air gap increases, molecular orientation increases which leads to denser skin layers. Xu et al. (2008), found that when coagulation bath temperature increases sponge like structure is promoted, also exchange rate between solvent and non-solvent increases in a certain air gap. Ohya et al. (2009), Loh et al. (2011), and Wongchitphimon et al. (2011) observed that as viscosity increases macrovoid formation suppressed and sponge-like structure is promoted due to delayed coagulation rates. Qui et al (2009) observed that addition of MWCNT decreased macrovoid formation. Saljoughi et al (2010) found that additive has dual effects on membrane morphology. If viscosity is increased due to additives then macrovoid formation is restrained. However if thermodynamical instability mechanism take control of membrane morphology then macrovoid formation is expected. SEM images of fabricated membranes were in accordance with the findings mentioned above. Having 15 cm air gap (spinning #1 and #2) and higher coagulation bath temperature (50°C), and higher amount of solvent in both bore and outer liquid delayed coagulation rate, so these membranes had denser skin layers and sponge like structures on both sides. When MWCNT-COOH used, due to their higher viscosities less macrovoid formation were observed. At 0 air gap (spinning #3), instantaneous demixing occurred. This explains why these membranes had thinner sponge-like layer than the other ones. Also, instantaneous mixing on outer layer led to formation of macrovoids or finger-like structure near outer surface farther than inner layer.

Table 4.4 shows outer and inner diameters of fabricated membranes. As can be seen, increasing take-up speed of membranes in spinning #1, decreased membrane diameter both from outside and inside. However there had discordant trend since addition of both functional MWCNTs showed indefinite changes over membrane diameter. Take-up speed was main parameter affects diameter of membranes.

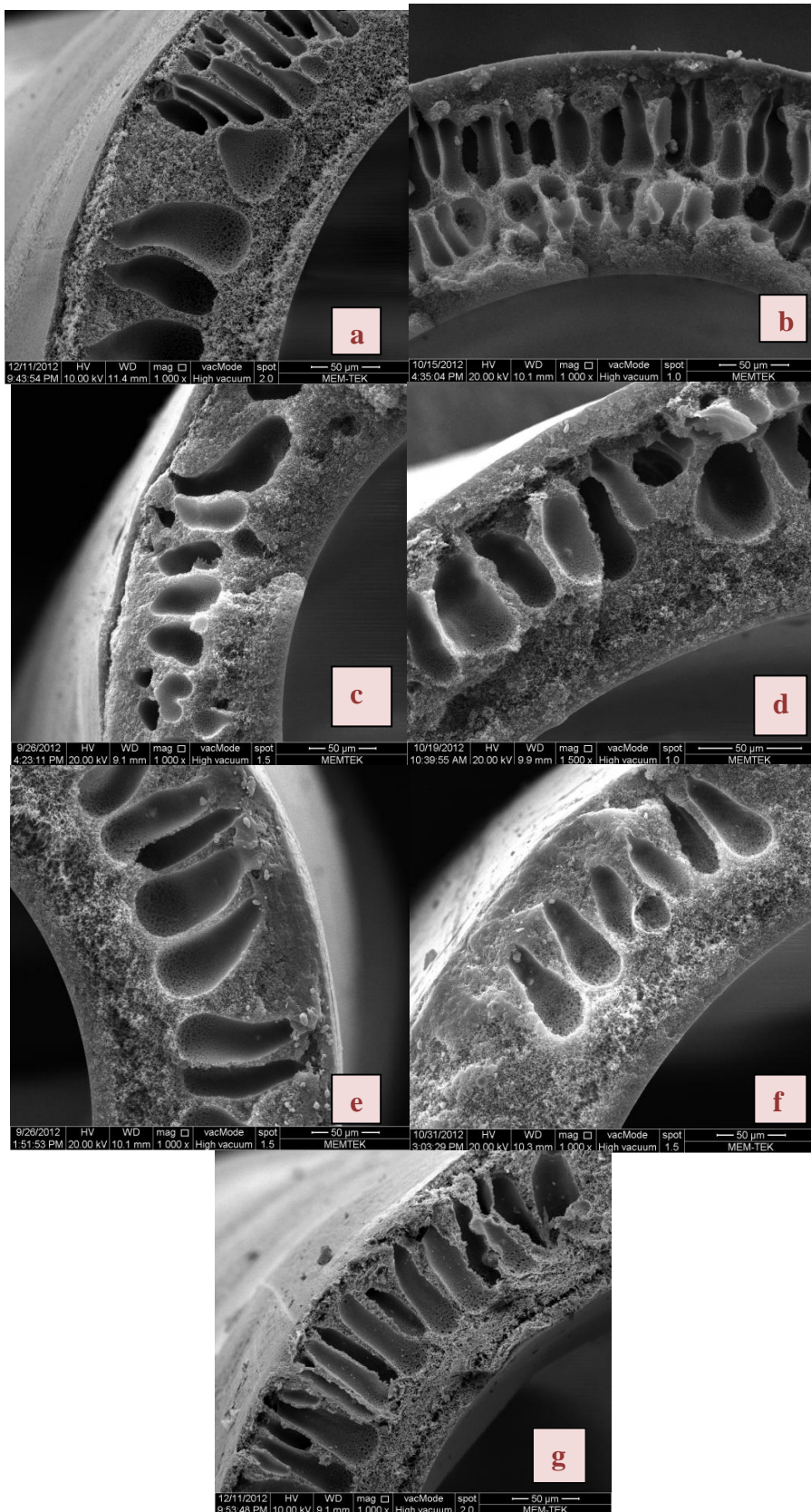


Figure 4.8 : Detailed cross sectional view of #1 membranes. a) Pristine 1, b) 0.2COOH 1, c) 0.4COOH 1, d) 0.8COOH 1, e) 0.2OH 1, f) 0.4OH 1, g) 0.8OH 1.

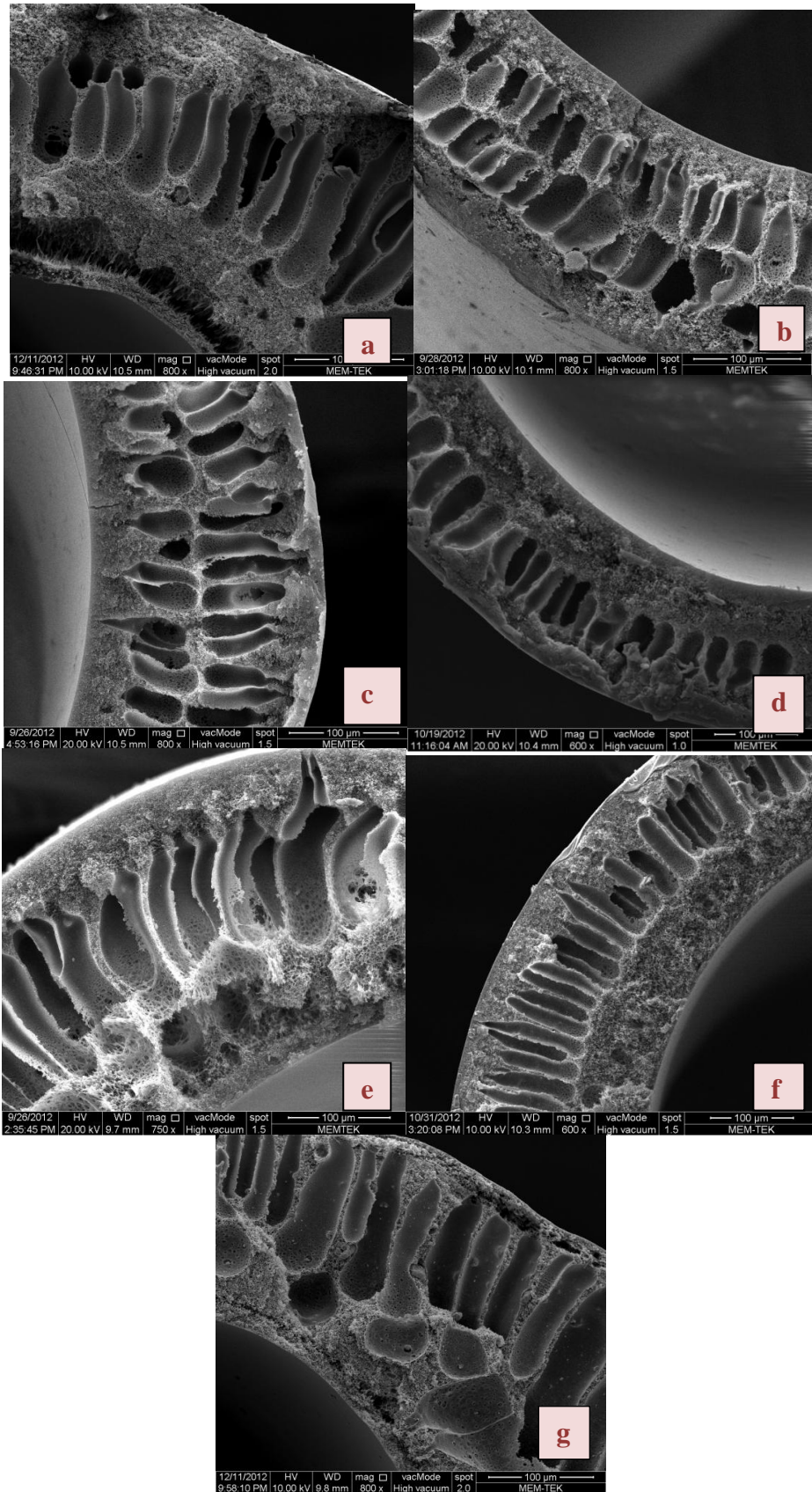


Figure 4.9 : Detailed cross sectional view of #2 membranes. a) Pristine 2, b) 0.2COOH 2, c) 0.4COOH 2, d) 0.8COOH 2, e) 0.2OH 2, f) 0.4OH 2, g) 0.8OH 2.

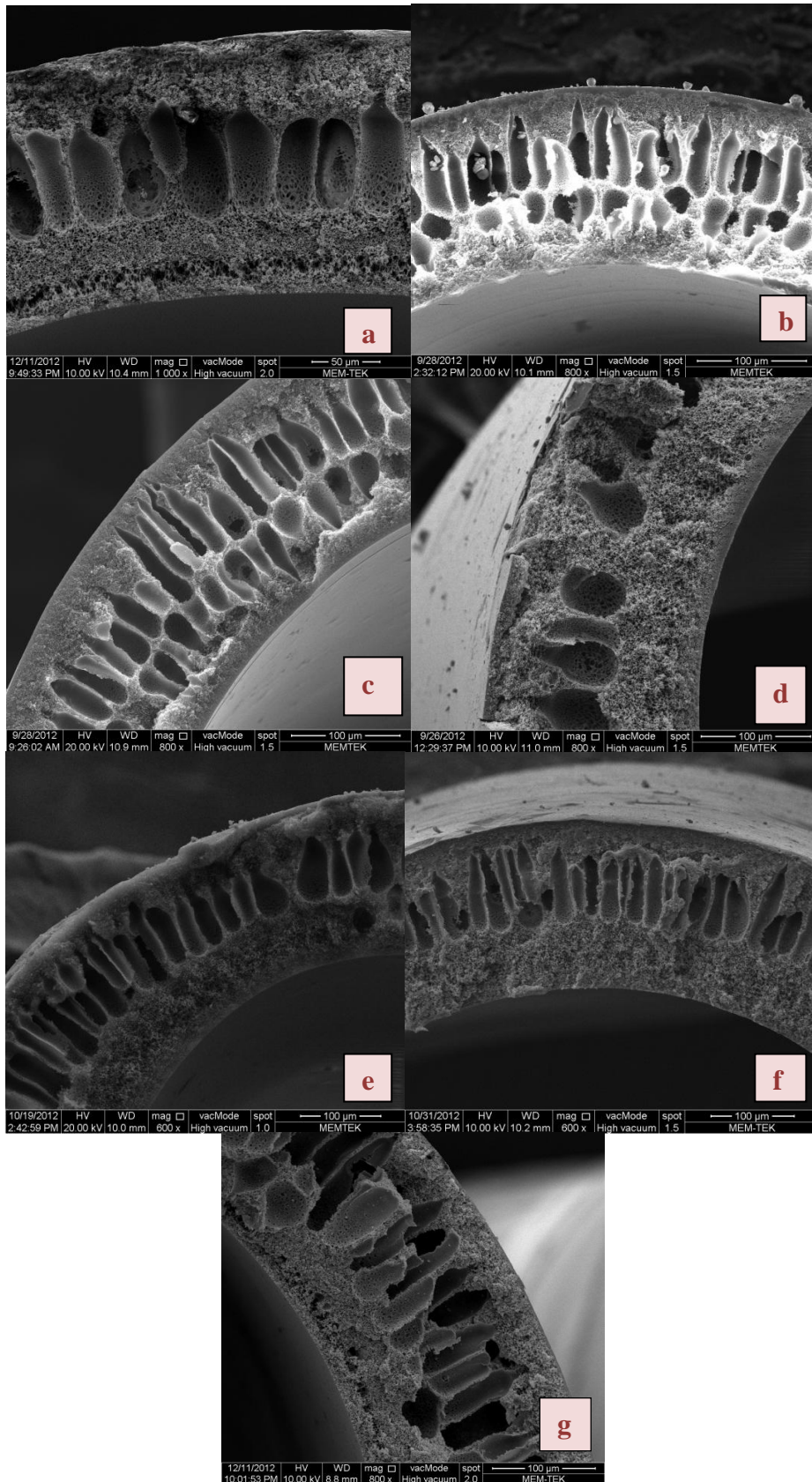


Figure 4.10 : Detailed cross sectional view of #3 membranes. a) Pristine 3, b) 0.2COOH 3, c) 0.4COOH 3, d) 0.8COOH 3, e) 0.2OH 3, f) 0.4OH 3, g) 0.8OH 3.

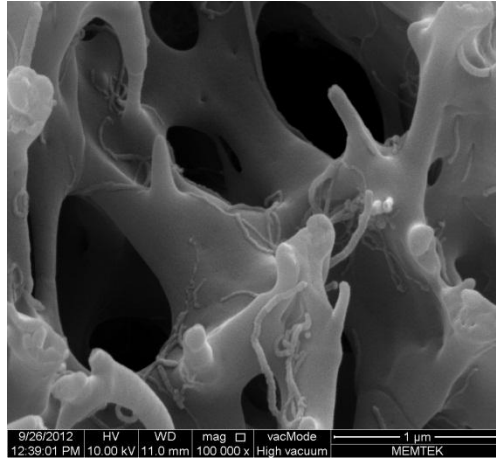


Figure 4.11 : MWCNT in membrane matrix (0.8 % MWCNT-COOH).

Table 4.4 : Outer and inner diameters of fabricated membranes.

Module #	Outer diameter (OD) (mm)	Inner diameter (ID) (mm)	Module #	OD (mm)	ID (mm)	Module #	OD (mm)	ID (mm)
Pristine 1	1,131	0,763	Pristine 2	1,078	0,552	Pristine 3	1,525	1,071
0.2 COOH 1	1,047	0,731	0.2 COOH 2	1,349	0,853	0.2 COOH 3	1,281	0,907
0.4 COOH 1	1,038	0,703	0.4 COOH 2	1,339	0,959	0.4 COOH 3	1,409	1,036
0.8 COOH 1	1,064	0,779	0.8 COOH 2	1,433	1,089	0.8 COOH 3	1,367	0,994
0.2OH 1	0,953	0,558	0.2OH 2	1,294	0,768	0.2OH 3	1,436	0,978
0.4OH 1	1,019	0,720	0.4OH 2	1,414	0,998	0.4OH 3	1,455	1,025
0.8OH 1	0,980	0,540	0.8OH 2	1,493	0,974	0.8OH 3	1,396	0,844

Outer surface images of post treated membranes of #1, #2, #3 and of without post treatment membranes of #1, #2, #3 taken by SEM can be seen through Figure 4.12, Figure 4.13, Figure 4.14 and in Appendix in Figure A.10, Figure A.11, Figure A.12, respectively.

In Figure 4.12, pristine membrane had open porous structure. As MWCNT-COOH added into membrane matrix, outer surfaces of membranes became smooth, having dense skin layer. However when concentration MWCNT-COOH increased outer surface became rougher. As MWCNT-OH added into membrane matrix, micro-porous structure was observed. When concentration increased, this micro-porous structure converted into open-porous structure. Effect of leaching of PVP can be visibly seen in these membranes. In Figure A.10, membranes without post-treatment can be seen. Herein pristine membrane had again porous structure but dimensions of it was blazingly became smaller. Since MWCNT-COOH membranes affected from

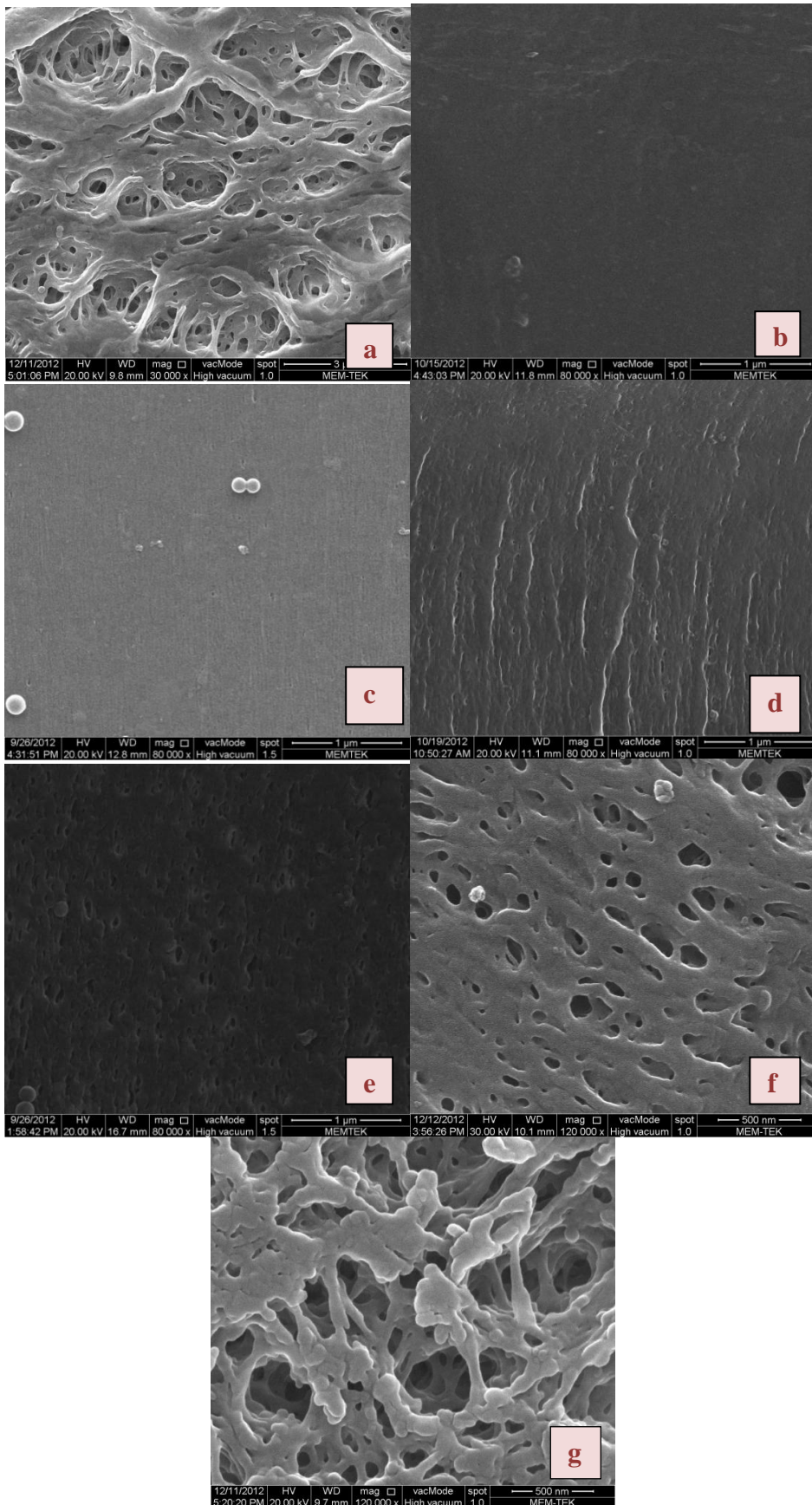


Figure 4.12 : Outer surface images of #1 membranes. a) Pristine 1, b) 0.2COOH 1, c) 0.4COOH 1, d) 0.8COOH 1, e) 0.2OH 1, f) 0.4OH 1, g) 0.8OH 1.

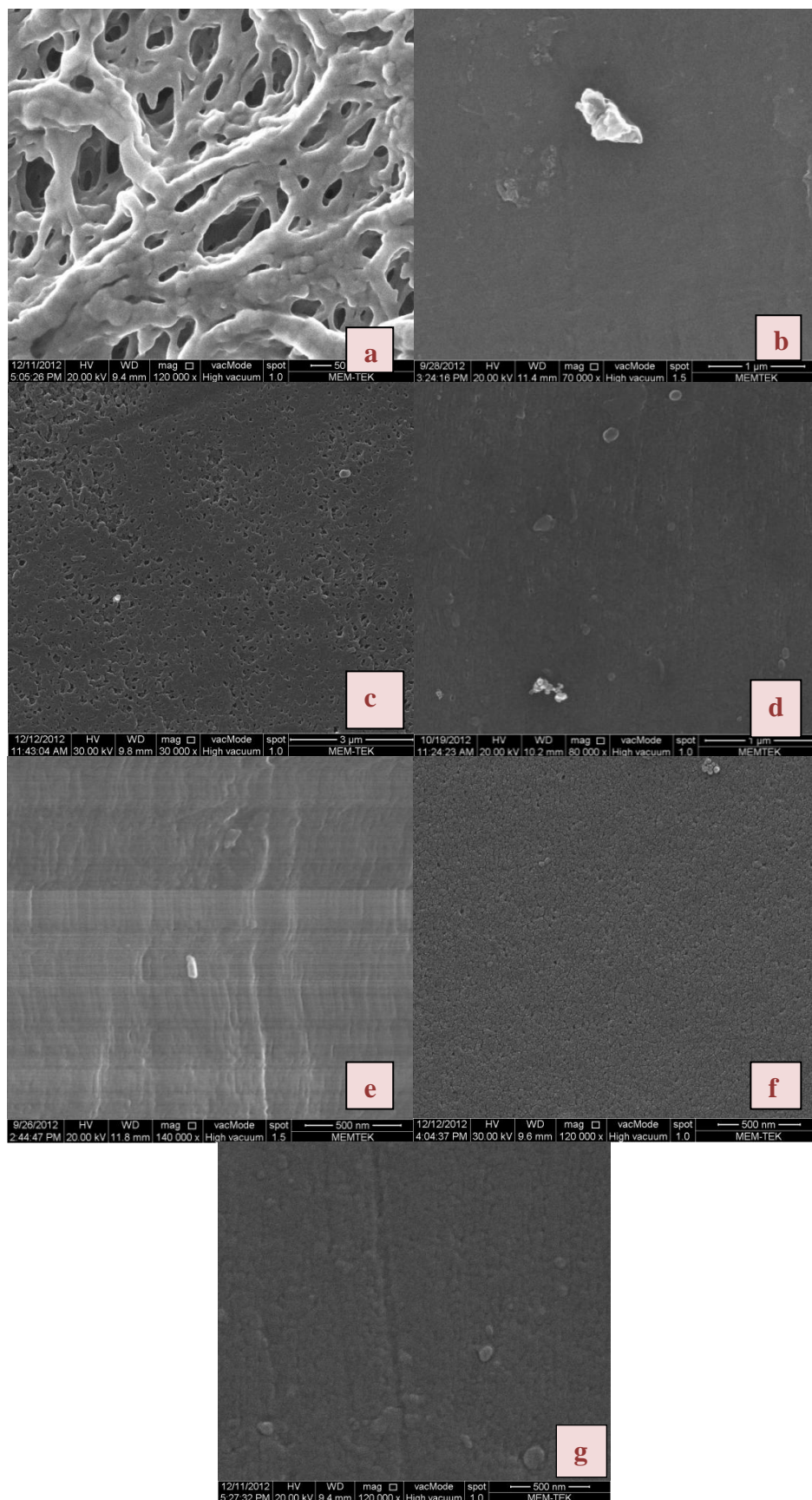


Figure 4.13 : Outer surface images of #2 membranes. a) Pristine 2, b) 0.2COOH 2, c) 0.4COOH 2, d) 0.8COOH 2, e) 0.2OH 2, f) 0.4OH 2, g) 0.8OH 2.

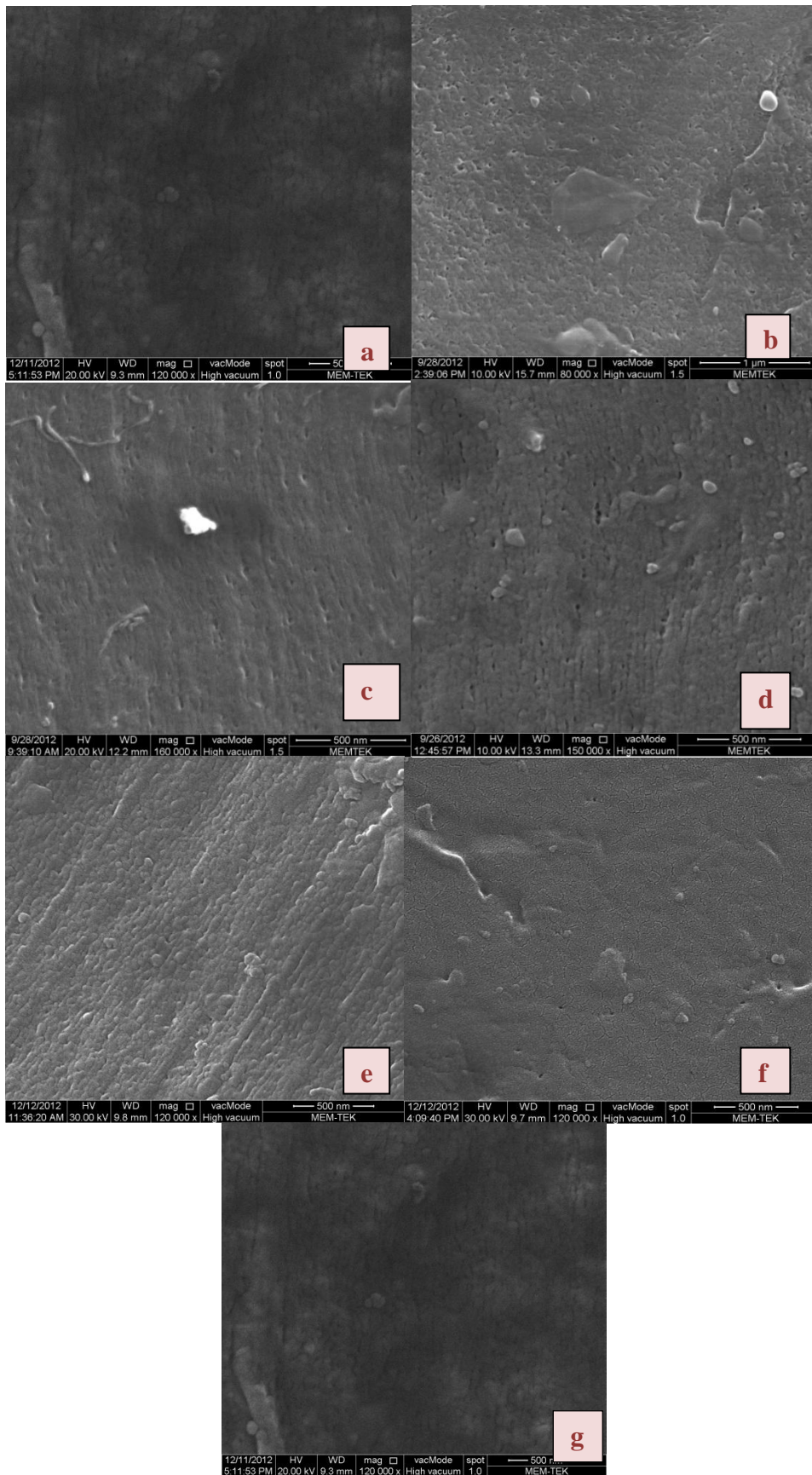


Figure 4.14 : Outer surface images of #3 membranes. a) Pristine 3, b) 0.2COOH 3, c) 0.4COOH 3, d) 0.8COOH 3, e) 0.2OH 3, f) 0.4OH 3, g) 0.8OH 3.

delayed demixing more than MWCNT-OH due to their high viscosities, they had thicker sponge-like structure. This can be seen in outer surfaces of the membranes. MWCNT-COOH had thicker sponge-like underneath outer surface than MWCNT-OH membranes. Due to that underneath of the outer surface of MWCNT-OH membranes we can see finger-like structures.

According to Figure 4.13, membranes had dense outer surfaces except pristine membrane. As concentration of MWCNT-COOH increased, there was no or a slight change occurred on outer surfaces of the membranes. As concentration of MWCNT-OH increased, non-porous structure became a little bit porous. In Figure A.11, membranes showed similar outer surface structures.

Effect of instantaneous demixing process can be seen in Figure 4.14 and Figure A.12. Because of 0 cm air gap, outer surfaces of all membranes whether they were post treated or not had dense outer surfaces.

Chou and Yang (2005) observed that as take up speed of membranes increased, membranes were stretched because of that more porous structure obtained. In spinning #1, this effect can be seen visibly. Outer surfaces of these membranes (post-treated or not) had more porous structures over spinning #2 and spinning #3. As the concentration of both functional MWCNTs increased, surface became rougher which was in accordance with the observation of Qui et al. (2009). Air gap and take-up speed affect outer surfaces more than cross sections of the membranes. In 0 cm air gap, Chen et al. (2010) observed denser outer surfaces due to instantaneous mixing. Effect of this can be observed in the membranes in spinning #3. Membranes in spinning #2 and #3 had more porous structure, one of the reasons of that was high solvent concentration in outer liquid. According to Li and He (2007), higher solvent concentrations cause more porous structure, also air gap promotes occurrence of polymer lean phase underneath top layer due to either high solvent concentration in outer liquid or lower viscosity values which is why MWCNT-OH membranes in spinning #1 had more porous structure than MWCNT-COOH membranes.

4.5 Permeability of Hollow Fiber Membranes

Just to see how the post-treatment affects permeation value, permeabilities of hollow fibers both without post-treatment and with post-treatment were calculated. Results

are presented in Figure 4.15, 4.16, 4.17. According to Wienk (1993), presence of PVP in membrane matrix cause very low flux due to swelling of porous structure and hypochloride treatment is used to increase permeability of UF membranes. It can be concluded that post-treatment increased permeability, because NaOCl broke longer molecular chains of PVP, due to this PVP was washed from membrane matrix. Besides an increase in concentration and also an increase in molecular weight of the PVP was led to increasement in permeability too. So all remaining experiment were done with the post-treated membranes.

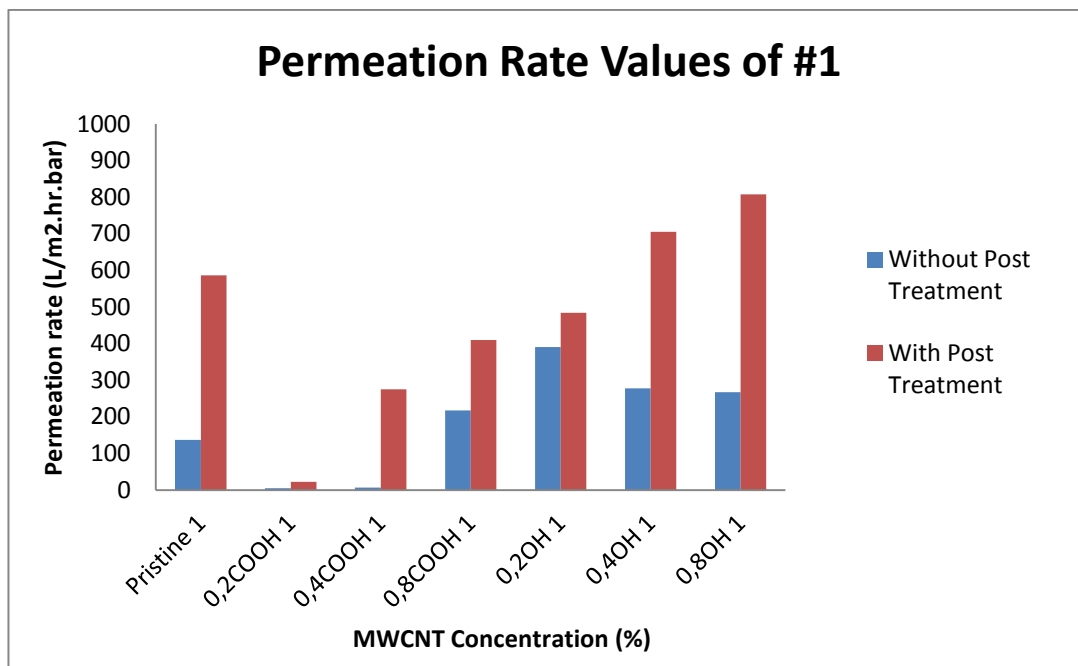


Figure 4.15 : Permeation rate values for spinning condition 1 (Air gap: 15cm, take-up speed : 8.4m).

It can be seen that through Figure 4.15 as MWCNT-COOH content increased, first permability decreased and after some point it increased again whereas as MWCNT-OH content increased, there was a slight decrease in permeability and after that permeability increased as MWCNT-OH concentration increased. The highest permeability result were 808 L/m².hr.bar which belonged to 0.8 % MWCNT-OH and the lowest permeability result were belonged to 0.2 % MWCNT-COOH as 22.4 L/m².hr.bar.

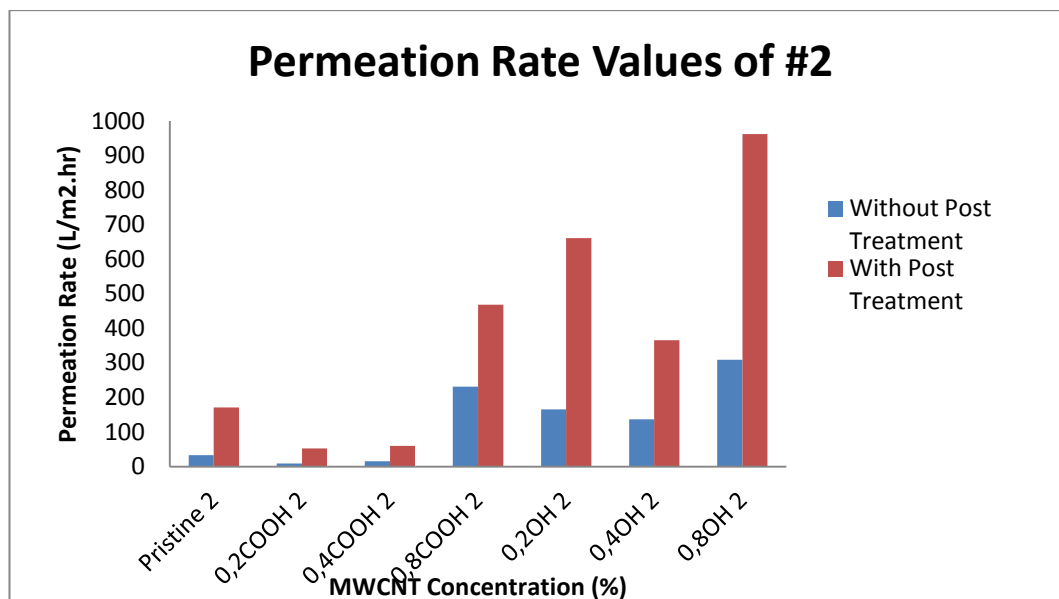


Figure 4.16 : Permeation rate values of spinning condition 2 (Air gap: 15cm, take-up speed : 4.2m).

Fabricated membranes through spinning #2, had permeability values were seen in Figure 4.16. Addition of MWCNT-COOH decreased permeability of membranes up to a point and then increased permeability over pristine membranes. However when MWCNT-OH was used, permeability values were always higher than pristine membranes. Increasing MWCNT-OH concentration, changed permeability values discordantly. The highest permeability was 962 L/m².hr.bar at 0.8 % MWCNT-OH while the lowest permeability were 52,3 L/m².hr.bar at 0.2 % MWCNT-COOH.

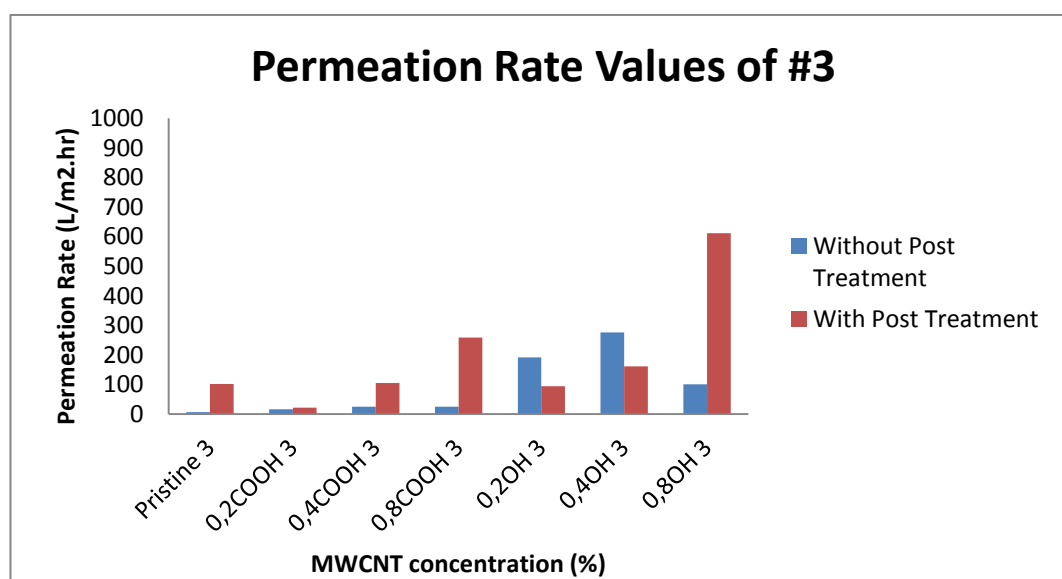


Figure 4.17 : Permeation rate values of spinning condition 3 (Air gap: 0cm, take-up speed : 4.2m).

According to Figure 4.17, permeation rates for both functional MWCNT membranes had the same trend. As concentration of MWCNT increased, a slight decrease occurred in membranes but further increase led to increment in permeation rates over pristine membranes. The highest permeation rate were obtained at again 0.8 % MWCNT-OH concentration as 611,4 L/m².hr.bar while the lowest permeation rate were obtained at 0.2 % MWCNT-COOH as 21,2 L/m².hr.bar.

In spinning condition #1 and #2, air gap was 15cm. If the time spent in air gap is longer, then nucleation and growth of polymer lean phase promotes and these lead to larger pores (Wienk et al., 1995). Besides when solvent concentration is higher in outer liquid, this leads to more open structures (Li and He, 2007), so an increase in permeability is waited. Because of that permeation rates of spinning #1 and #2 were higher than spinning #3. Surface roughness parameter can affect this property due to increment of MWCNT concentration made membranes more rough can be observed in SEM images however there is no atomic force microscopy (AFM) results exist for this parameter. Although MWCNT-OH dope viscosities were lower than pristine dope viscosity, permeation rates were increased as concentration of MWCNT-OH increased. The reason for that can be the more finger-like structure of MWCNT-OH membranes and more open porous outer structures of membranes. Also take-up speed affects permeability of the membranes according to Chou and Yang (2005). Take-up speed was 2 times higher in spinning #1 than spinning #2 and #3. It can be seen that permeation rates were higher in spinning #1 than spinning #2 and #3.

4.6 FTIR Spectra

FTIR spectra was used to identify functional groups on membrane. FTIR spectra results was shown in Figure 4.18 altogether. At 1578cm⁻¹ and 1486cm⁻¹ absorption bands for PES was observed. This transmittance value was interpreted as C-H aromatic bond (Bolong et al., 2008). Peaks around 1660cm⁻¹ belonged to amide C=O stretch in COOH group (Bolong et al, 2008; Li et al., 2005). Peaks around 1324cm⁻¹ and 1150cm⁻¹ was belonged to asymmetric and symmetric (SO₂) sulphone groups in PES (Ismail et al., 2006). O-H bond give peaks around 3200-3500cm⁻¹ (Li et al., 2005). Therefore 3348cm⁻¹ belonged to O-H bonds.

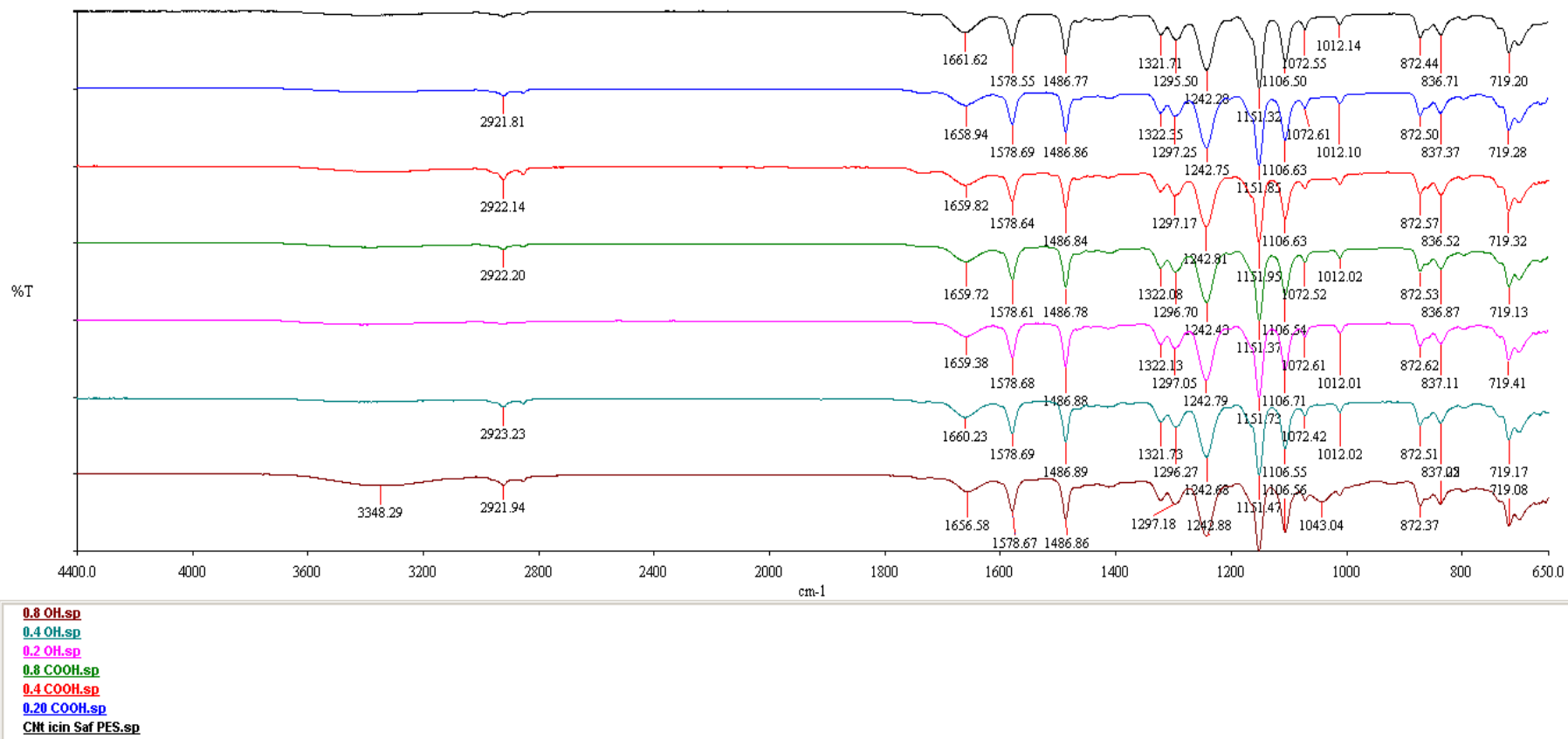


Figure 4.18 : FTIR spectra of all dopes.

4.7 Contact Angle Results

Contact angle results were given in Figure 4.19, Figure 4.20, Figure 4.21.

Contact angle measurement showed how hydrophilic the spun membranes were. As can be seen in Figures 4.19-4.21, membranes have not processed with post treatment (blue bars) were more hydrophilic than post treated ones (red bars). It was because of there were still hydrophilic PVP in the pores of membranes. However, when post treatment was applied, NaOCl broke the structure of PVP and molecular chains of PVP became smaller (Wienk, 1995), so they can washed up from membrane. Therefore, membrane hydrophilicity decreased but flux showed an increasing trend. This phenomena can be explained by adding functionalized hydrophilic MWCNTs to solution, and also washing of PVP increased pore sizes of the membranes.

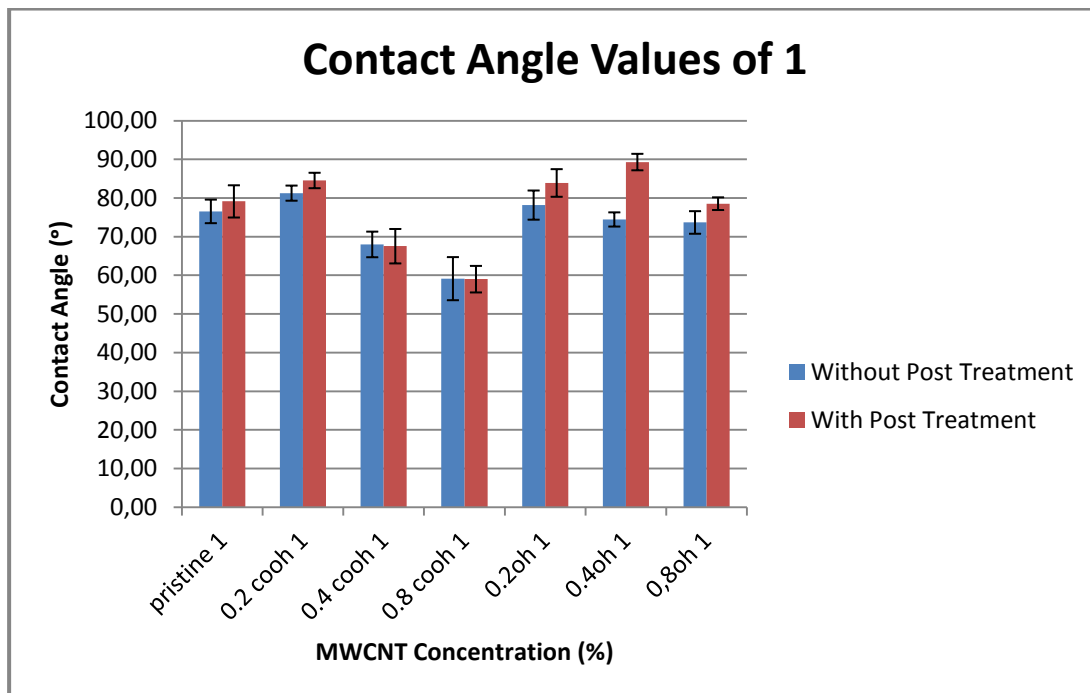


Figure 4.19 : Contact angle results of spinning #1 (Air gap: 15cm, take-up speed : 8.4m).

In Figure 4.19, when MWCNT-COOH concentration increased, hydrophilicity of membranes were first decreased, then increased. The best hydrophilicity result obtained at 0.8% MWCNT-COOH as $59^{\circ} \pm 3.4^{\circ}$. When MWCNT-OH membranes was controlled, it can be seen that hydrophilicity of membranes were decreased over pristine membranes.

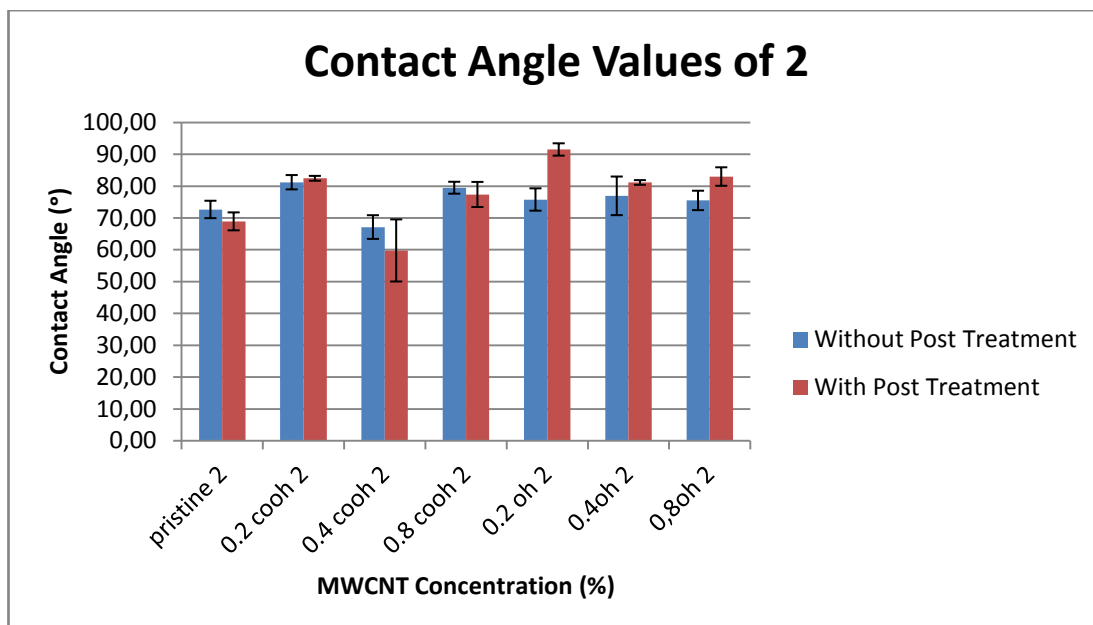


Figure 4.20 : Contact angle results of spinning #2 (Air gap: 15cm, take-up speed : 4.2m).

In Figure 4.20, for both functional MWCNTs, contact angle results were higher than pristine membranes except 0.4% MWCNT-COOH ($59.8^{\circ} \pm 9,8^{\circ}$). It seems contact angle results was not dependent on MWCNTs concentrations due to their discordant trend.

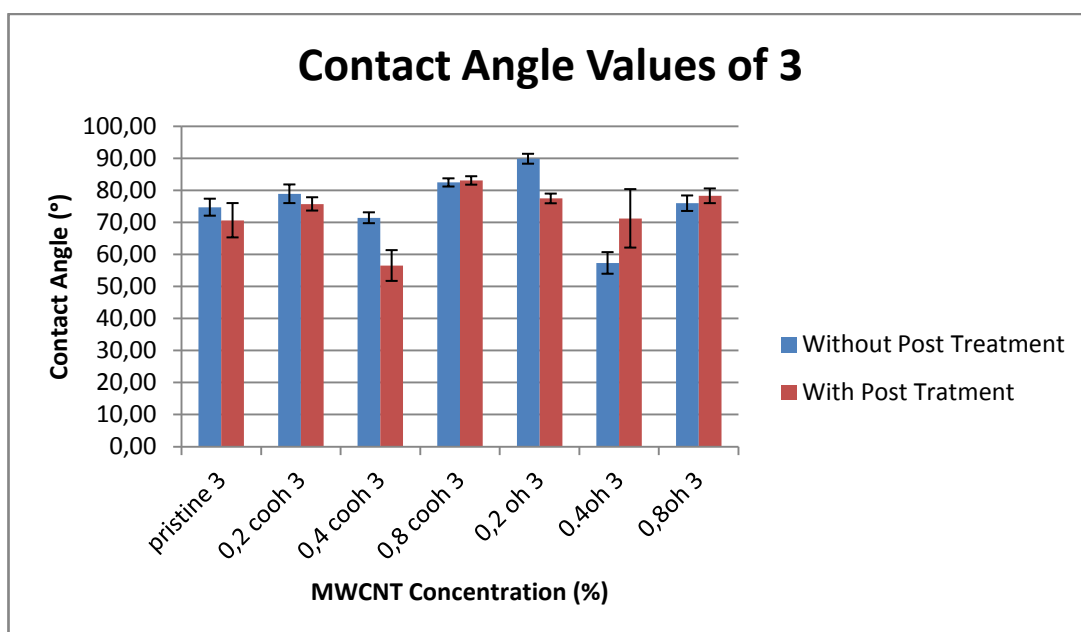


Figure 4.21 : Contact angle results of spinning #3 (Air gap: 0cm, take-up speed : 4.2m).

According to Figure 4.21, contact angle results of pristine and MWCNT membranes were close to each other. The best hydrophilicity was obtained at 0.4% MWCNT-

COOH concentration. As MWCNT content increased hydrophilicity of membranes first increased and then decreased after it was increased again.

4.8 Porosity of Membranes

Porosity values can be seen in Figure 4.22, Figure 4.23, Figure 4.24. Herein given results showed overall porosity. The results showed low porosity values in the range of 12-69% which can be attributed to relatively high polymer concentration and sponge-like structure of membranes.

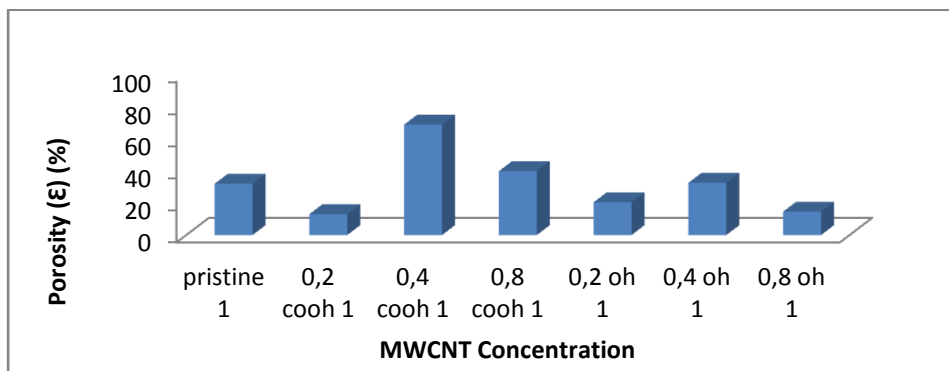


Figure 4.22 : Porosity values of spinning #1 (Air gap: 15cm, take-up speed : 8.4m).

Overall porosity values of MWCNT-COOH membranes were higher than pristine and MWCNT-OH membranes. As concentration increased, first porosity decreased which explained permeability decrease also at 0.2 % MWCNT-COOH, then increasing concentration increased overall porosity again up to a value, increasing concentration decreased porosity value. However MWCNT-OH membranes in any concentration had lower porosities than pristine membrane. And trend acted like the same with MWCNT-COOH concentration trend.

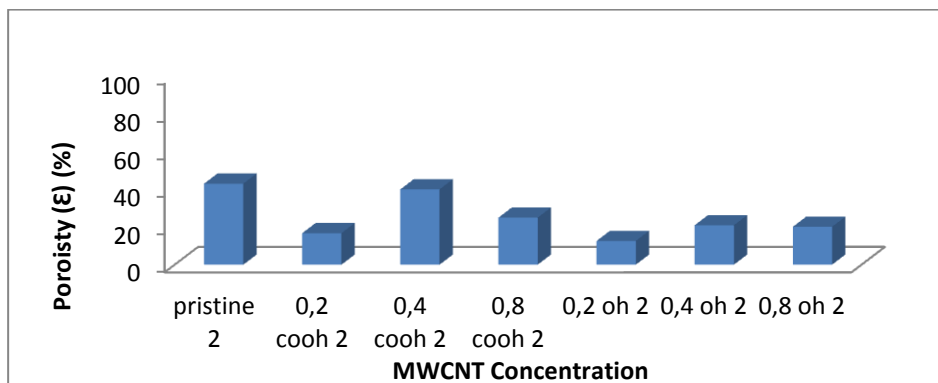


Figure 4.23 : Porosity values of spinning #2 (Air gap: 15cm, take-up speed : 4.2m).

General porosity percentages in Figure 4.23 were higher than first spinning condition which was shown in Figure 4.22. Overall porosity of pristine membrane, 49%, was higher than MWCNTs. As MWCNT-COOH concentration increased 0.2 %, 0.4 %, 0.8 %, overall porosity was decreased, increased and decreased respectively, showed discordant trend. However in MWCNT-OH membranes, increasing concentration decreased porosity but further increment in concentration increased porosity values slightly. In all MWCNT-OH cases, overall porosity values were lower than pristine membranes.

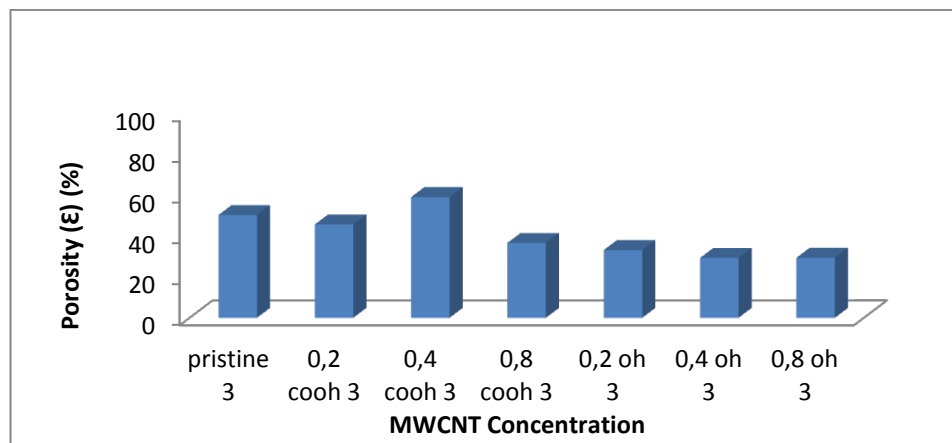


Figure 4.24 : Porosity values of spinning #3 (Air gap: 0cm, take-up speed : 4.2m).

In Figure 4.24, it can be seen that overall porosity values were higher than other spinning conditions yet addition of MWCNTs into membranes decreased their overall porosities when it was compared to pristine membrane (50.3%) except 0.4 % MWCNT-COOH (59,1%).

Porosity values generally is affected by take-up speed, viscosity etc. According to Ohya et al (2009), when viscosity is lower, coagulation composition is reached in a short time and these leads to low degree of nucleation and growth. This means lower porosity. Our results showed the same trend for this explanation. Addition of MWCNT-COOH lead to higher viscosity values whereas MWCNT-OH decreased viscosity values. Therefore, lower overall porosity values of MWCNT-OH membranes can be linked to lower viscosity values which resulted in lower degree of nucleation of growth. Chou and Yang (2005), was found that increasing take-up speed, porosity was decreased due to higher compact structures. Spinning #1 had higher take-up speed than the other ones, in this study. And it can be concluded that

porosity values of #1 when all dopes took into account was lower than #2 and #3 and reason for that was the compaction in the structure. The best overall porosities were obtained at 0.4 % MWCNT-COOH in all spinning conditions.

4.9 Surface Charge of Fabricated Membranes

Zeta potential values for each membranes between pH 3-10 can be seen in Figure 4.25-31. Electrical characteristics of a membrane surface can be explained by electrokinetic properties of a membrane which is expressed in zeta potential. By measuring zeta potential in a wide pH range, surface charge of membranes can be found and also selection of proper membranes can be done logically for treatment of water or wastewater according to desired environment. Electrokinetic properties of membrane surface and foulants expressed as in zeta potential show the interaction of both organic and inorganic colloidal substances with membrane surfaces (Amoudi and Lovitt, 2007), so basically gives an idea about fouling.

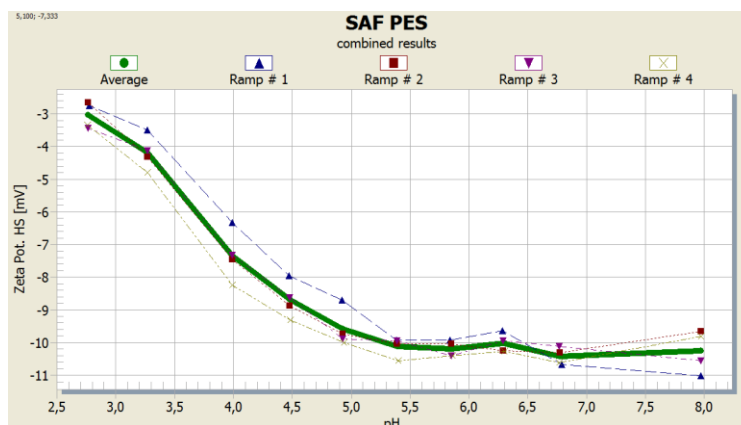


Figure 4.25 : Zeta potential values of pristine membranes in mV.

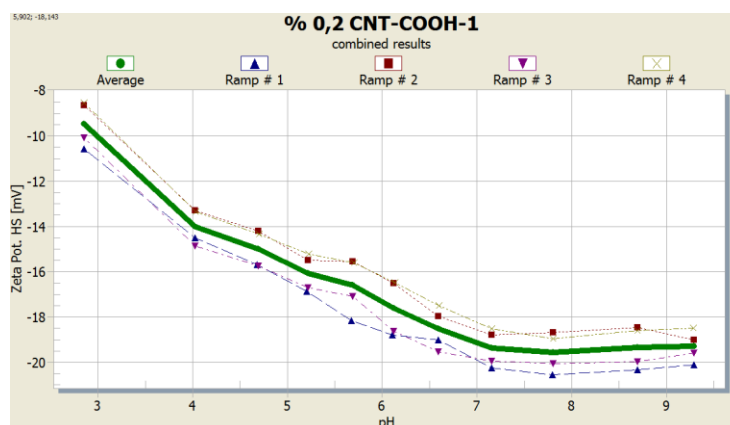


Figure 4.26 : Zeta potential values of 0.2 % MWCNT-COOH membranes in mV.

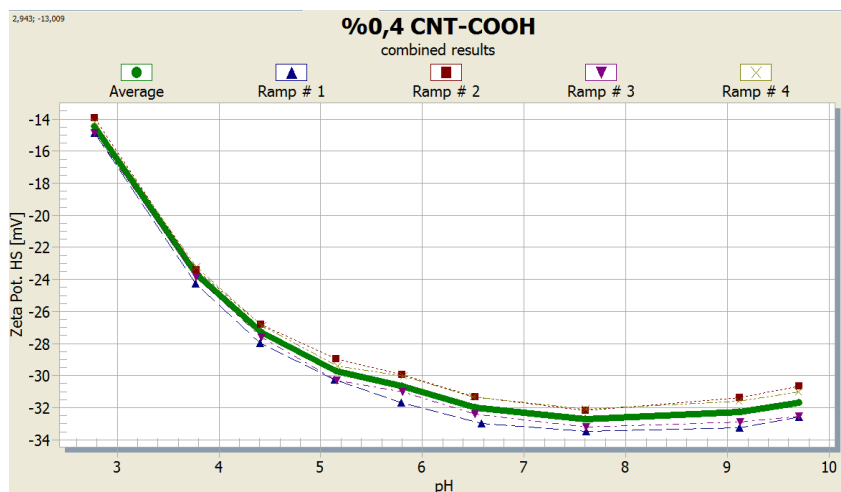


Figure 4.27 : Zeta potential values of 0.4 % MWCNT-COOH membranes in mV.

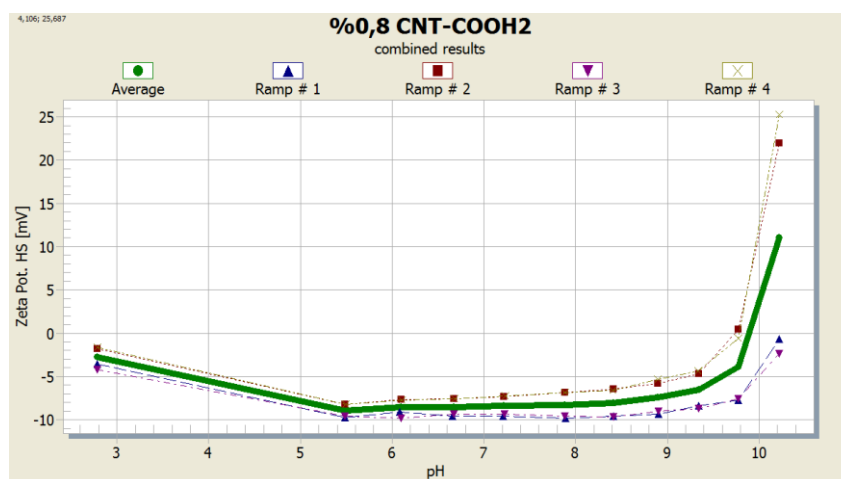


Figure 4.28 : Zeta potential values of 0.8 % MWCNT-COOH membranes in mV.

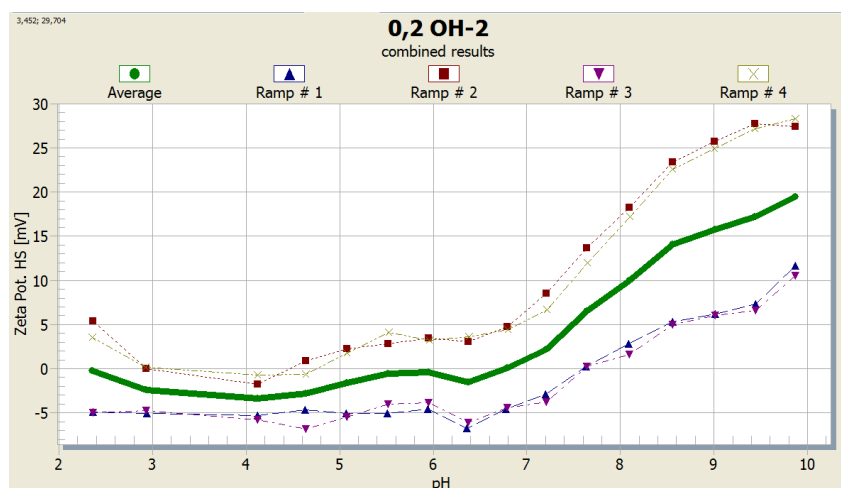


Figure 4.29 : Zeta potential values of 0.2 % MWCNT-OH membranes in mV.

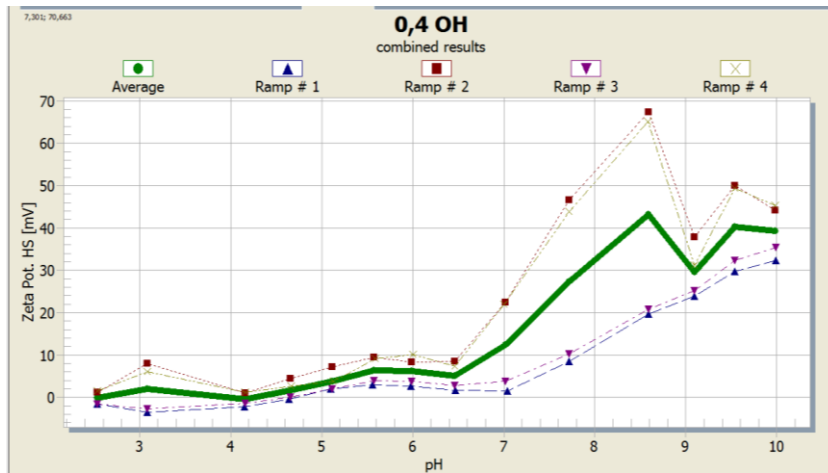


Figure 4.30 : Zeta potential values of 0.4 % MWCNT-OH membranes in mV.

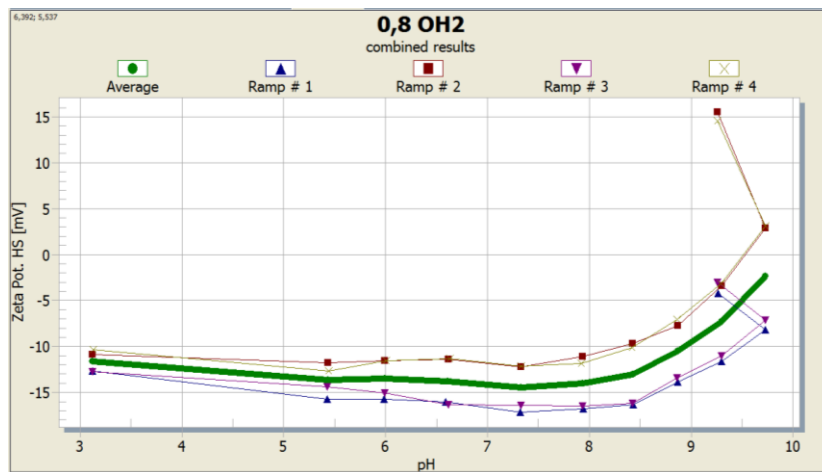


Figure 4.31 : Zeta potential values of 0.8 % MWCNT-OH membranes in mV.

All spinning conditions were combined and thought as they were one, so zeta potential values were found just for different dope concentrations. Fouling caused by protein solution (BSA) which has a pH of 6.8-7 was important for spun membranes. BSA protein is negatively charged at pH 6.8-7. So, if spun membranes had higher negativities in this pH range, lower fouling rates were expected. Zeta potential results for MWCNT-COOH membranes were negative at pH 6.8-7 whereas zeta potentials of MWCNT-OH membranes were near zero at these pH values. Results will be discussed in the ongoing part.

4.10 Fouling of Membranes

Water flux recovery (FR%), Total fouling (Rt), reversible fouling (Rr), irreversible fouling (Rir) ratios, and BSA rejection ratios can be seen in Figures 4.32-40.

Water flux recovery (FR%) means suitable membrane recycling properties after it was fouled with BSA. Higher FR percentages mean membranes have better antifouling properties.

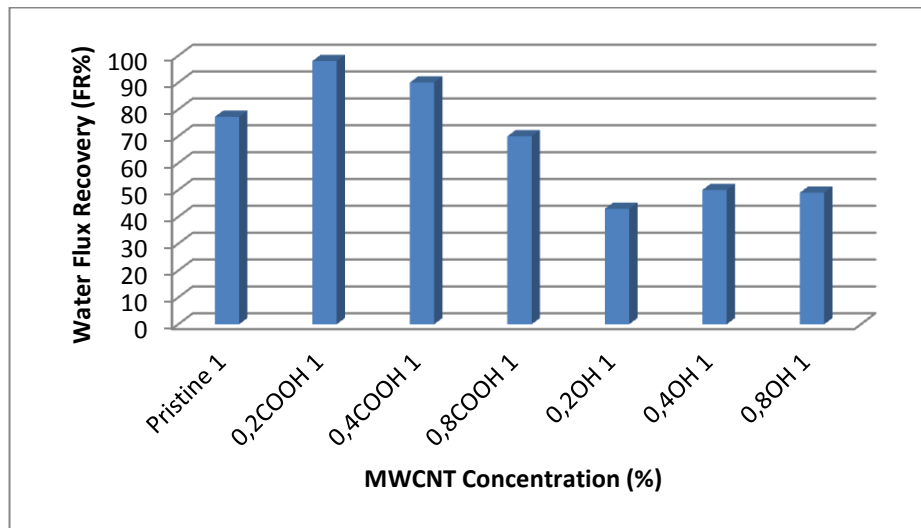


Figure 4.32 : Water flux recovery (FR%) of spinning condition #1 (Air gap: 15cm, take-up speed : 8.4m).

It can be seen that in Figure 4.32, adding carboxyl MWCNT, increased water flux recovery over pristine membranes however increasing carboxyl content decreased this ratio. Lower FR% ratio means that physical cleaning of membranes by water was not sufficient to remove foulants and some of the efficiencies of the membranes were lost. The reason for this was the increment in the adsorption of protein molecules as concentration increased. Zeta potential values and also contact angle results support these results. Surfaces of membranes have high negative values when MWCNT-COOH was used and also their hydrophilicities were higher than MWCNT-OH membranes. More negative surface charge means less adsorption of protein molecules. When hydroxyl functionalized MWCNT was used, water flux recovery ratio was decreased compared to pristine membranes and also for MWCNT-COOHs in all concentrations. Lower FR% ratio means that physical cleaning of membranes by water was not sufficient to remove foulants and showed that MWCNT-OH membranes fouled much more than MWCNT-COOH.

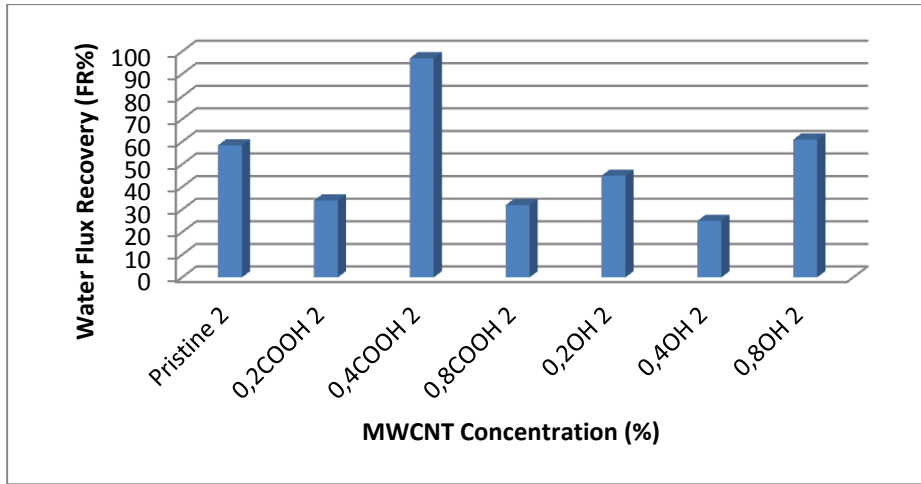


Figure 4.33 : Water flux recovery (FR%) of spinning condition 2 (Air gap: 15cm, take-up speed : 4.2m).

In spinning condition 2 when take up speed decreased, FR ratio of both functional MWCNTs decreased values under pristine membranes (60%) except 0.4 MWCNT-COOH % and 0.8 MWCNT-OH % (97 % and 61 % respectively). Water flux recovery efficiencies were decreased significant amount over pristine membranes. These results show that physical cleaning of membranes was not enough to remove foulants and a serious amount of membrane efficiency was gone. Results showed consistency with hydrophilicities and zeta potential values. Generally FR% ratio of spinning 1 was better than spinning condition 2.

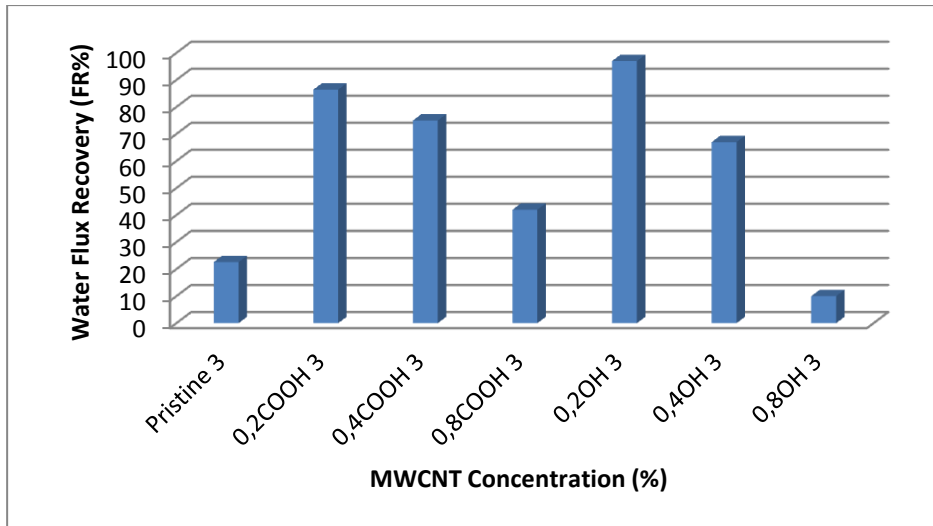


Figure 4.34 : Water flux recovery (FR%) of spinning condition 3 (Air gap: 0cm, take-up speed : 4.2m).

In Figure 4.34, both functional MWCNTs have higher FR ratios over pristine membranes except 0.8 % MWCNT-OH 3. But when concentration was increased,

flux recovery was decreased. So, it can be said that increasing the concentrations of MWCNTs lower the antifouling property of membranes. Even though this decreased FR ratios, still FR ratios of MWCNTs were higher than pristine membranes excluding 0.8% MWCNT-OH 3. Here also results were consistent with zeta potential values and hydrophilicity of membranes. It can be seen that surfaces of MWCNT-COOH membranes after protein filtration can be more efficiently cleaned. However increasing MWCNT content for both functionality decreased this cleaning efficiency.

According to Figure 4.32-34 above, the best water flux recovery results when both functionality took into account were observed in spinning condition 3 where membranes had no air gap. Then spinning condition #1 which had 15cm air gap had better FR ratios. The highest FR% ratios were obtained at 0.2 % MWCNT-COOH1, 0.2 % MWCNT-OH 3 and 0.4 % MWCNT-COOH 2 as 98%, 97%, 97% respectively.

Membrane fouling consists of two types of fouling which are reversible and irreversible fouling. Reversible fouling mainly is caused by reversible protein adsorption whereas irreversible fouling is caused by strong adsorption of protein molecules and entrapment of protein molecules in membrane pores. Reversible fouling can be removed from membrane by hydraulic cleaning (Vatanpour et al, 2012).

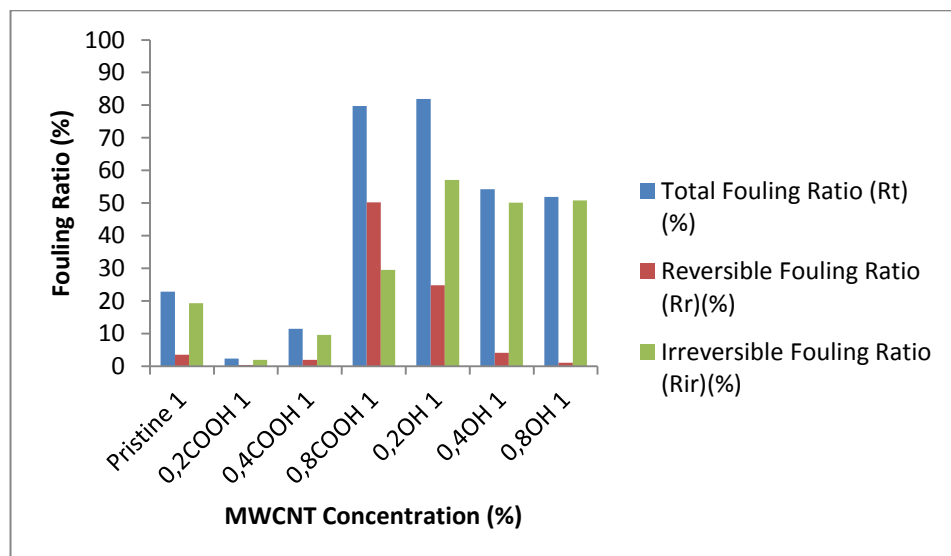


Figure 4.35 : Total fouling (Rt), reversible fouling (Rr) and irreversible fouling (Rir) ratios of spinning condition #1 (Air gap: 15cm, take-up speed : 8.4m).

In Figure 4.35, total fouling rates for MWCNT-COOHs first decreased but as concentration increased, a sharp increase was observed. However for MWCNT-OH membranes, total fouling rates were higher than pristine and carboxyl functionalized MWCNTs. Increasing concentration decreased Rt values slightly for MWCNT-OH. Main fouling mechanism was irreversible fouling excluding 0.8 % MWCNT-COOH.

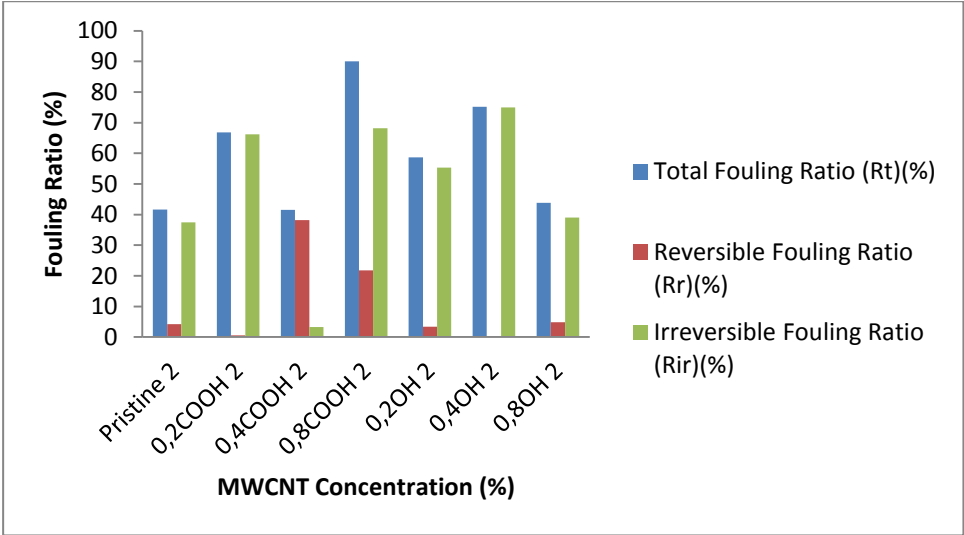


Figure 4.36 : Total fouling (Rt), reversible fouling (Rr) and irreversible fouling (Rir) ratios of spinning condition #2 (Air gap: 15cm, take-up speed : 4.2m).

For spinning condition 2, all functional MWCNTs’ total fouling ratios were higher than pristine membranes and showed discordant trend. Excluding 0.4 % MWCNT-

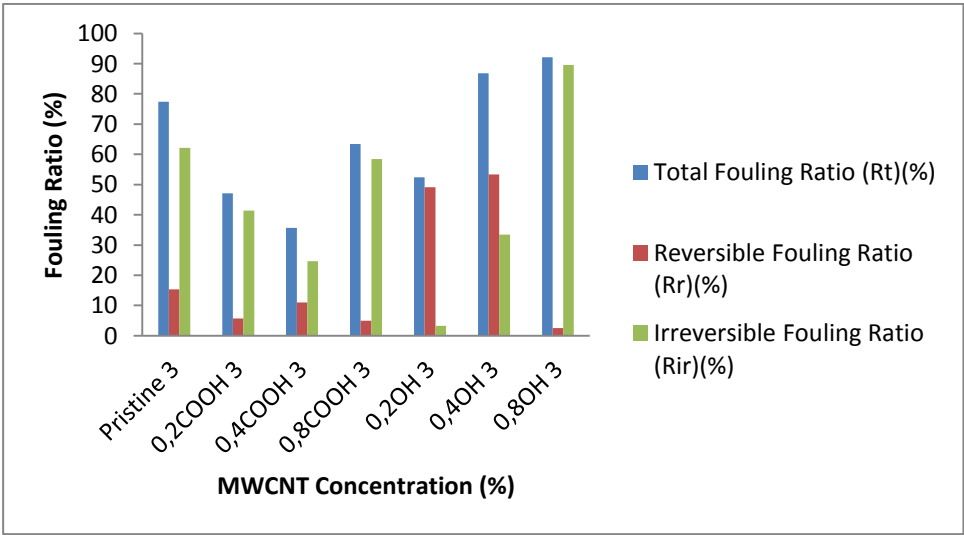


Figure 4.37 : Total fouling (Rt), reversible fouling (Rr) and irreversible fouling (Rir) ratios of spinning condition #3 (Air gap: 0cm, take-up speed : 4.2m).

COOH, all functional MWCNTs' main fouling mechanism were irreversible fouling. When air gap was 0 cm, increasing MWCNT-COOH concentration decreased fouling ratio up to some point and further increment of concentration increased fouling however still total fouling rate of MWCNT-COOH membranes were better than pristine membranes. When MWCNT-OH took into consideration, it can be observed that, increasing concentration first decreased fouling rate then increased fouling rate. Main fouling mechanism for MWCNT-COOH membranes were irreversible whereas for MWCNT-OH membranes, it was reversible fouling.

It is thought that parameters like hydrophilicity, surface roughness, pore size and surface charge affect fouling mechanisms of membranes (Vatanpour et al, 2012). Hollow fiber membranes fabricated for this study, overwhelmingly had irreversible fouling mechanism. Higher fouling rates of MWCNT-OH membranes can be explained due to contact angle results of MWCNT-OH which had higher hydrophobicities. And it can be said that generally if flux of a membrane was higher, then fouling of that membrane was more probable. Membranes having the best antifouling properties were 0.2 % MWCNT-COOH 1, 0.4 % MWCNT-COOH 1 and 0.4 % MWCNT-COOH 2 having 2,3 %, 11,5 % and 41,5 % total fouling ratio, respectively.

BSA adsorped onto membranes surface and also into membrane pore structure and caused membrane fouling.

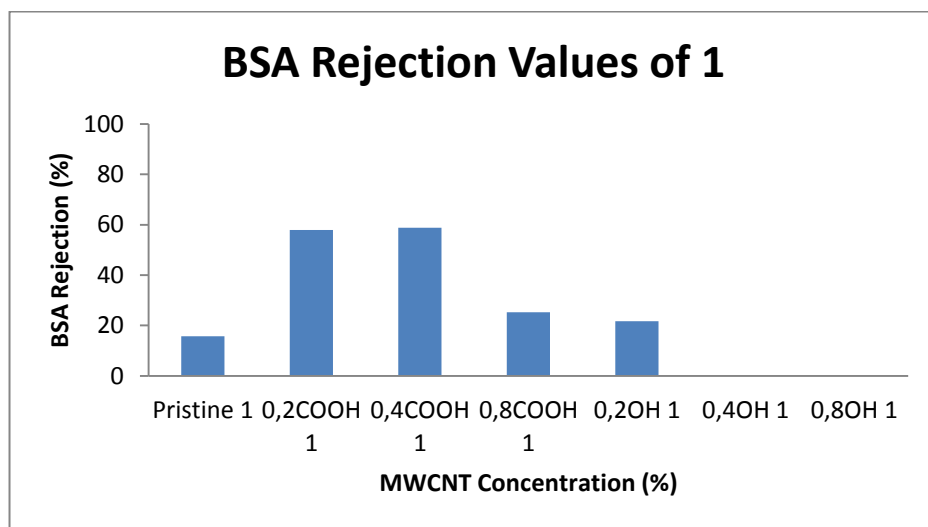


Figure 4.38 : BSA rejection of spinning #1 (Air gap: 15cm, take-up speed : 8.4m).

According to the Figure 4.38, BSA rejections first increased and decreased as the concentration increased in both functionality. However MWCNT-OH membranes were worse than MWCNT-COOH.

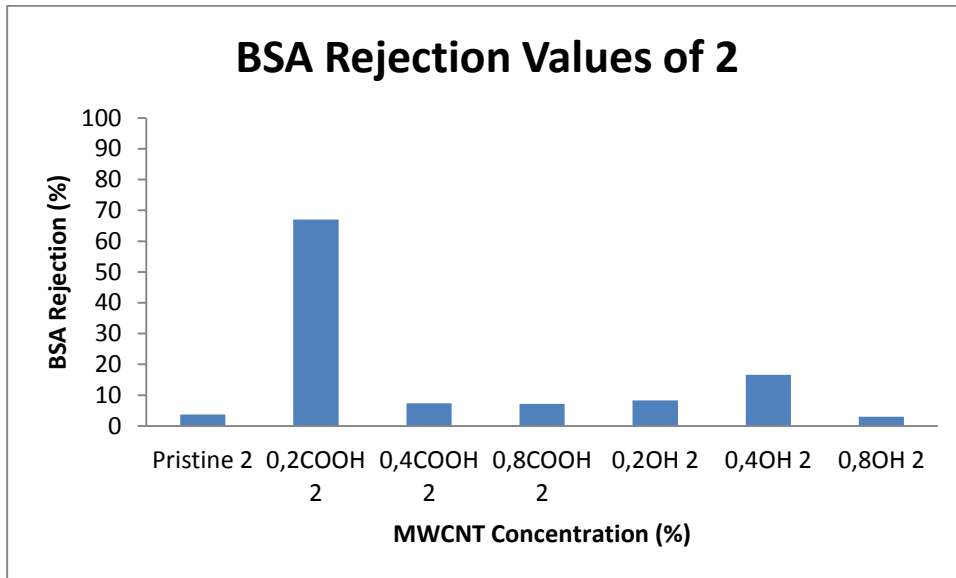


Figure 4.39 : BSA rejection of spinning #2 (Air gap: 15cm, take-up speed : 4.2m).

For spinning #2, (Figure 4.39), the best BSA rejection observed in 0.2 % MWCNT-COOH concentration, 67%. General trend for this spinning condition was lower BSA rejections.

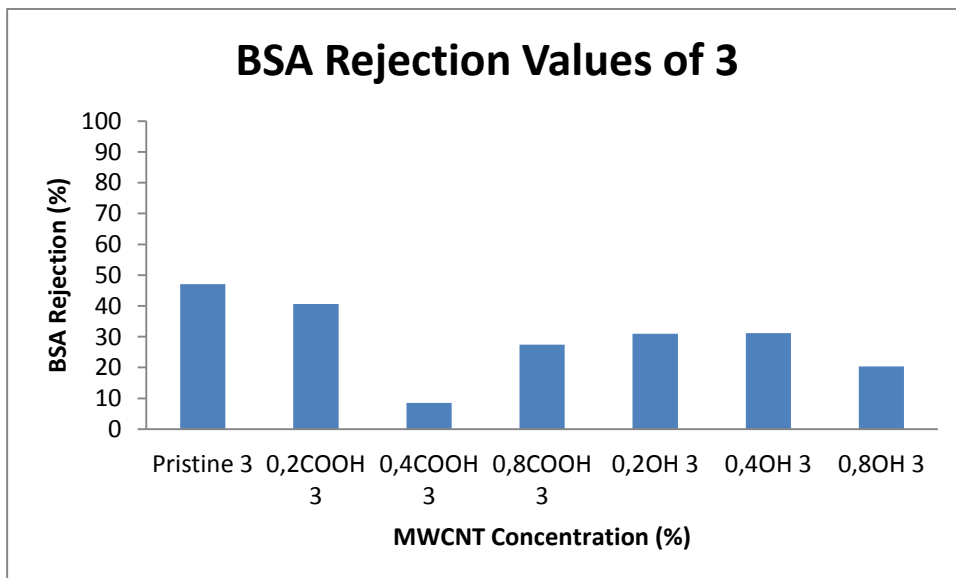


Figure 4.40 : BSA rejection of spinning #3 (Air gap: 0cm, take-up speed : 4.2m).

In Figure 4.40, the best results belonged to pristine membranes. Addition of MWCNTs caused a decrease in BSA rejections.

Lower rejection expected when flux is higher. Adding higher PVP with high Mw values, increased the flux of fabricated membranes but, decreased rejection properties of the membranes. BSA rejection rate were in accordance with permeability values obtained. According to the results given above, the best BSA rejection obtained at 15cm air gap and lower take-up velocity and at 0.2 % MWCNT-COOH concentration as 69% and the worst BSA rejections were observed at 15cm air gap and higher take-up speed and at 0.4 % and 0.8 % MWCNT-OH concentration as 0.3 % and 0.2 % respectively.

4.11 Mechanical Properties of the Membranes

With the addition of different MWCNTs concentration and functionality, how mechanical properties (elongation at break and young's modulus) were changed was observed. Young's modulus values can be seen in Figure 4.41, Figure 4.42, Figure 4.43.

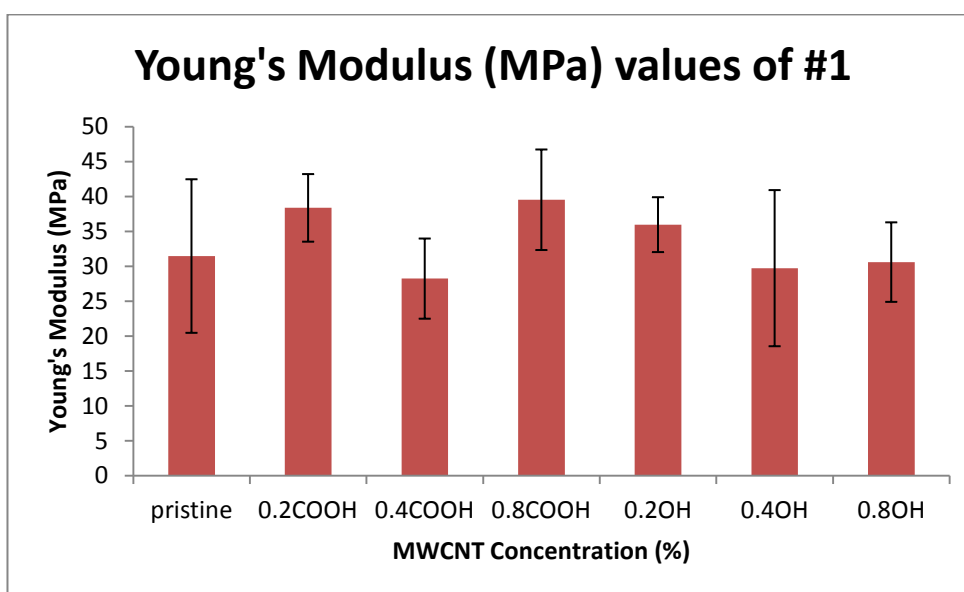


Figure 4.41 : Young's modulus values (MPa) of membranes of spinning #1 (Air gap: 15cm, take-up speed : 8.4m).

It can be said that addition of MWCNT-COOHs into membrane matrix increased mechanical strength of membranes except 0.4 % MWCNT-COOH 1. However adding MWCNT-OHs into membrane matrix decreased young's modulus of

membranes except 0.2 % MWCNT-OH 1. Chung et al (1998), conclude that low viscosity solutions tend to form looser structures (looser outer skins). In Figure 4.12, it can be observed that outer surfaces of MWCNT-OHs membrane had looser structures. These loose structure can be reason for the decrease in young's modulus values. The best young's modulus value observed at 0.8 % MWCNT-COOH 1 as 39,5MPa.

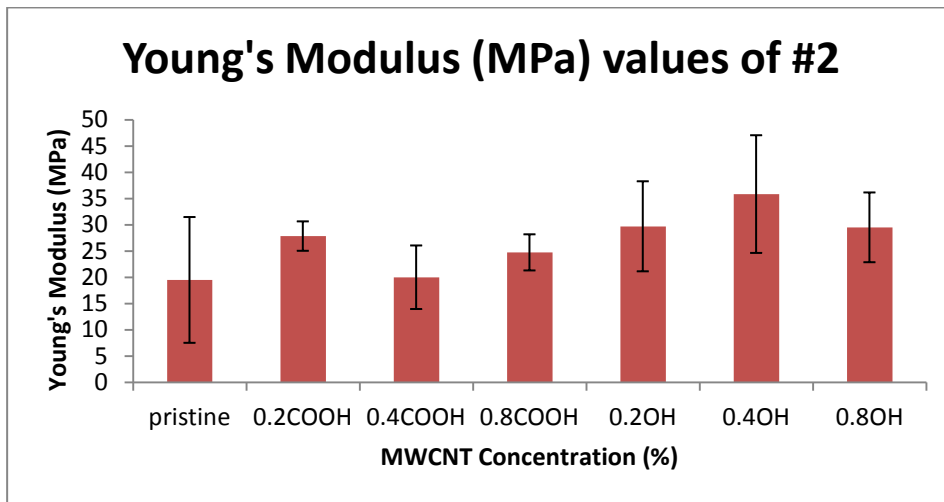


Figure 4.42 : Young's modulus values (MPa) of membranes of spinning #2 (Air gap: 15cm, take-up speed : 4.2m).

According to Figure 4.42, all young's modulus values of MWCNT membranes were higher than pristine membranes. The best results was obtained at 0.4 % MWCNT-OH 2 as 35,8MPa. Increasing MWCNT concentration for both functionality, changed young's modulus values discordantly.

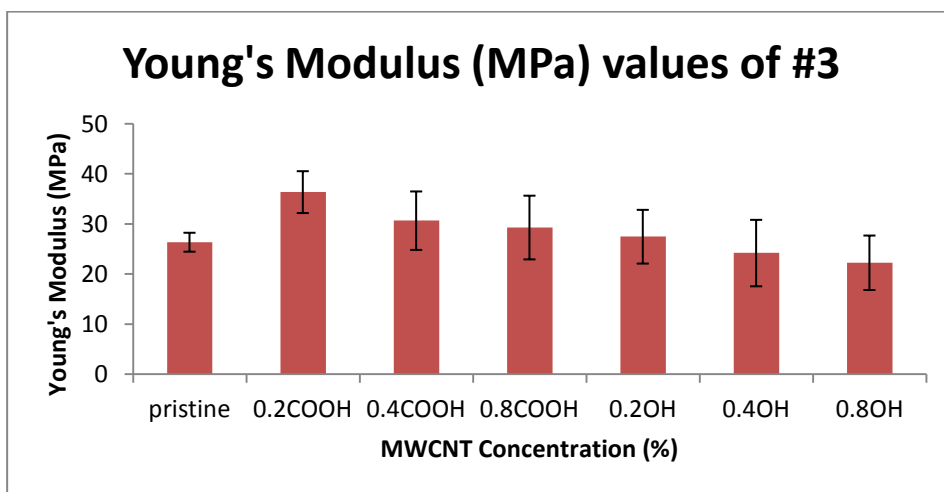


Figure 4.43 : Young's modulus values (MPa) of membranes of spinning #3 (Air gap: 0cm, take-up speed : 4.2m).

In Figure 4.43, addition of MWCNT-COOH increased young's modulus values and addition of MWCNT-OH decreased young's modulus values over pristine membranes (26,4 MPa) except 0.2 % MWCNT-OH 3 (27,5MPa).

Chou and Yang (2005) found that increasing take-up speed increased mechanical properties of membranes due to stretching and rearranging of molecular chain into more ordered state. Spinning condition 1 held at higher take-up speed than the others and mechanical properties of this set was higher than the spinning 2 and spinning 3. The best young's modulus values were got at 0.8 % MWCNT-COOH 1, 0.2 % MWCNT-COOH 1 and 0.2 % MWCNT-COOH 3 as 39,5MPa, 38,4MPa and 36,4MPa respectively.

Elongation at break values can be examined in Table 4.5.

Table 4.5 : Elongation at break percentages of fabricated membranes.

Module #	Elongation at break (%)	Module #	Elongation at break (%)	Module #	Elongation at break (%)
Pristine 1	5,01±0,9	Pristine 2	9,87±4,1	Pristine 3	5,96±0,8
0.2 COOH 1	6,38±0,8	0.2 COOH 2	7,43±1,7	0.2 COOH 3	4,37±0,2
0.4 COOH 1	8,35±0,7	0.4 COOH 2	10,57±3,3	0.4 COOH 3	7,77±0,7
0.8 COOH 1	5,18±0,4	0.8 COOH 2	5,51±0,1	0.8 COOH 3	5,89±1,0
0.2OH 1	4,74±0,7	0.2OH 2	6,65±0,9	0.2OH 3	4,51±0,6
0.4OH 1	6,16±0,6	0.4OH 2	5,62±2,3	0.4OH 3	7,33±1,8
0.8OH 1	6,66±1,6	0.8OH 2	6,59±1,2	0.8OH 3	8,27±2,3

Lower elongation values mean lower flexibilities. According to this, spinning condition 1, adding MWCNTs to membrane matrix increased flexibility of the membranes except 0.2 % MWCNT-OH and increasing of concentration of MWCNTs changed elongation at break percentages discordantly. For spinning 2 all MWCNT membranes were low elongation at break percentages over pristine membrane except 0.4 % MWCNT-COOH. For spinning 3, only 0.2 % MWCNT-COOH and MWCNT-OH had lower flexibility than pristine membrane.

4.12 Growth of E.Coli on Hollow Fiber Membranes

Antibacterial activity of functionalized MWCNT membranes were observed visually by using *E.Coli*. Experiment results were shown (Figure 4.44) that both all

membranes fabricated from all dopes can not be able to inhibit the growth of *E.Coli*. Growth of bacteria on membranes showed that both functionalized MWCNTs have not an antibacterial activity. These results showed resemblances to the findings of Zodrow (2009).

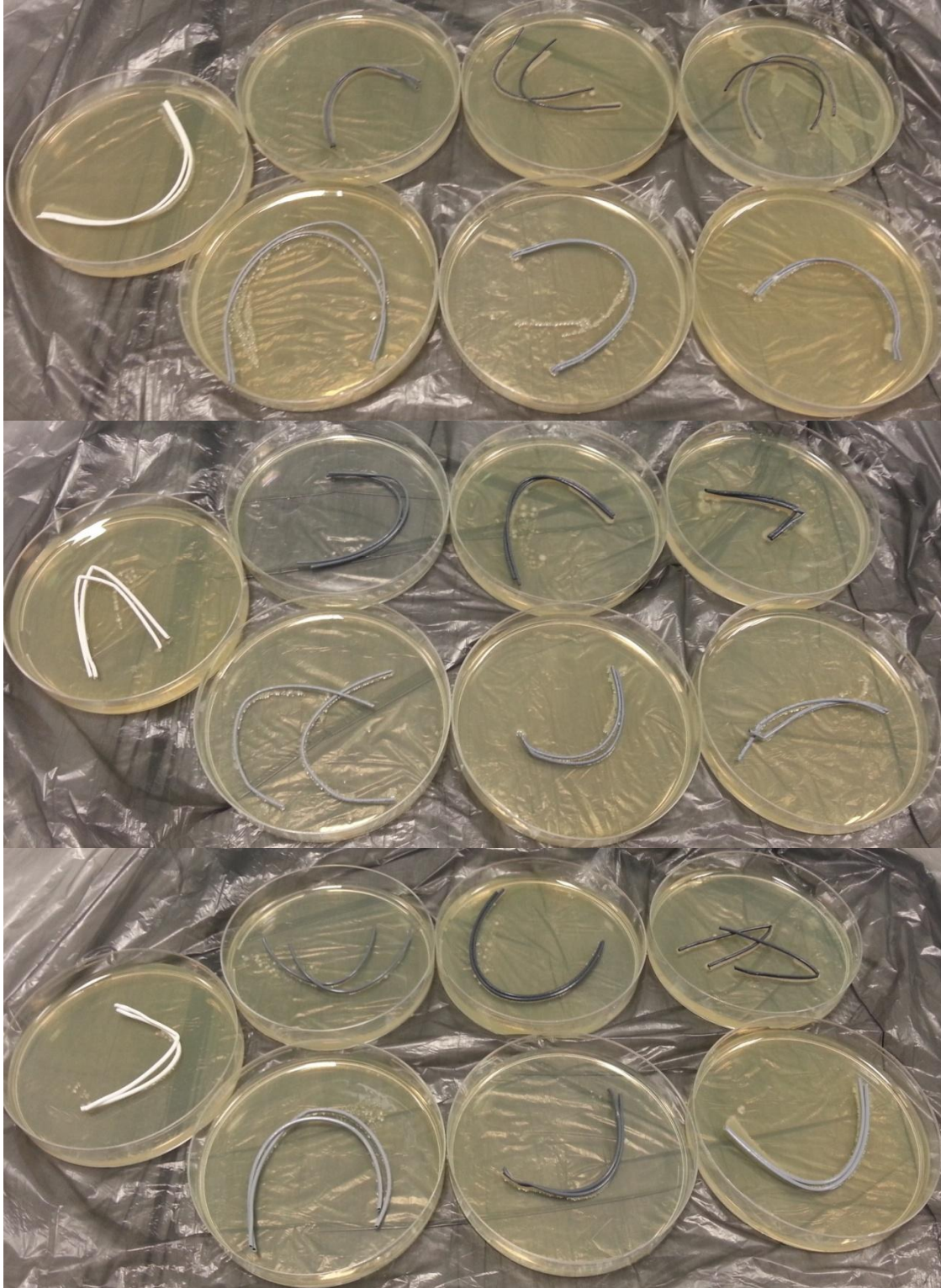


Figure 4.44 : Growth of *E.Coli* on hollow fiber membranes on agar medium.

5. CONCLUSIONS AND RECOMMENDATIONS

Hollow fiber membranes were fabricated through phase inversion method for obtaining high permeabilities, low fouling ratios, high BSA rejections, high mechanical stability values, high porosities. To reach the aim mentioned above, first pristine membrane recipe was optimized. After that effects of different MWCNTs were investigated with different characterization methods.

Optimized pristine recipe included %20 PES, % 5 PVP K30, %2 PVP K90 and %73 DMF. Totally 6 different dopes were spun with MWCNTs with this recipe. 0.2 %, 0.4 % and 0.8 % MWCNT-COOH and the same weight amount of MWCNT-OHs were spun respectively. Also effects of different spinning parameters were investigated since hollow fiber membrane fabrication is affected by so many parameters. For this purpose in each dope solution 3 different membranes were spun. In first spinning 15 cm air gap and 8.4m take-up speed was used. In spinning 2, air gap was kept as the same with first one but take-up speed was decreased to half. In spinning 3, 0 cm air gap was used and take-up speed was kept as the same with 2.

From SEM and stereo microscope images, it was seen that generally membranes had proper circular structure and cross sections had both sponge-like and finger-like structure as expected. Effects of different spinning parameters were clearly seen in cross sections, outer layers and also diameters of membranes.

It was thought that post treatment will be beneficial to membrane performance. So, permeation rates of both post treated and non treated membranes were measured. According to the permeation results, it was decided that in the ongoing parts only characterization of post treated membranes will be done except contact angle measurements. The best permeation rate was obtained at 0.8 % MWCNT-OH as 962,14 L/m².hr.bar when air gap:15cm and take-up speed:4.2m and the worst permeation rate was obtained at 0.2 % MWCNT-COOH as 21,17 L/m².hr.bar when air gap:15cm and take-up speed:8.4m. MWCNT addition generally changed

permeation rates. Increasing their concentration led to some decrease but further increasing of concentration generally increased permeation rates.

According to contact angle results effect of leaching of PVP with post treatment was observed. Post treated membranes had higher contact angle results. However increasing the concentration of both MWCNTs decreased contact angle results and hydrophilicity in the big picture. The best contact angle result was $56.5^\circ \pm 4.8^\circ$ obtained at 0.4 % MWCNT-COOH when air gap:0cm and take-up speed:4.2m and the worst was $91.5^\circ \pm 1.9^\circ$ belonged to 0.2 % MWCNT-OH when air gap:15cm and take-up speed:4.2m. Contact angle results affected fouling mechanisms of the membranes. The overall porosity values were also found. The highest porosity was observed at 0.4 % MWCNT-COOH when air gap:15cm and take-up speed:8.4m as 69 % whereas the least porosity observed at 0.2 % MWCNT-OH when air gap:15cm and take-up speed:4.2m as 12,5 %.

For fouling of the membranes water flux recovery, total fouling which was composed of irreversible and reversible fouling rates, and BSA rejection values were calculated. The best efficient membrane for flux recovery after protein flux was 0.2 % MWCNT-COOH when air gap:15cm and take-up speed:8.4m as 98 % and least efficient one was 0.8 % MWCNT-OH when air gap:0cm and take-up speed:4.2m as 10 %. Spinning parameters affected FR%, and also an increment in the concentration of MWCNTs decreased the FR ratio. In regard to R_r and R_{ir} percentages total fouling mechanism of the membranes were found as irreversible fouling (R_{ir}). The most fouled membranes was found as 0.8 % MWCNT-OH when air gap:0cm and take-up speed:4.2m as 92,1 % and the least fouled membrane was found as 0.2 % MWCNT-COOH when air gap:15cm and take-up speed:8.4m as 2,3 %. Generally fouling percentages were increased as the permeation rate increased. The best and the worst BSA rejection were obtained at 0.2 % MWCNT-COOH when air gap:15cm and take-up speed:4.2m as 67 % and 0.8 % MWCNT-OH when air gap:15cm and take-up speed:8.4m as 0.17 %.

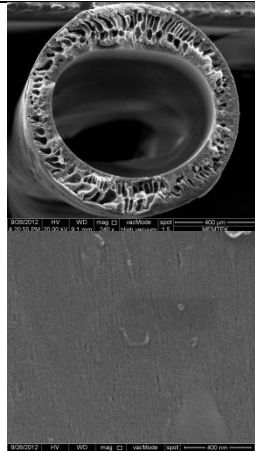
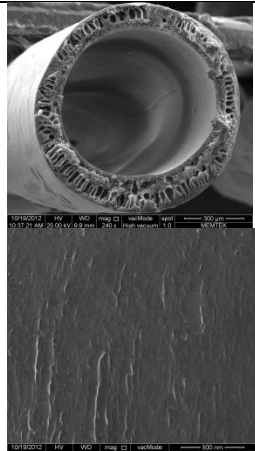
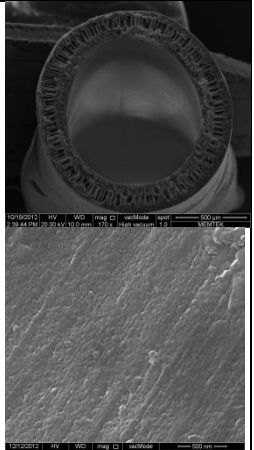
It was expected that addition of MWCNTs into membrane matrix will enhance mechanical properties of membranes. With respect to the results, addition of MWCNTs improved the mechanical properties of fabricated membranes and different spinning parameters affected this properties in a different way. The long

lasting membrane was 0.8 % MWCNT-COOH when air gap:15cm and take-up speed:8.4m having 40 MPa \pm 7.2 MPa young's modulus value whereas the weakest membrane was pristine when air gap:15cm and take-up speed:4.2m having 19 MPa \pm 10MPa young's modulus value. Regarding elongation at break percentages the most flexible membrane was 0.4 % MWCNT-COOH when air gap:15cm and take-up speed:4.2m as 10,6 % \pm 3.3 % elongation and the least flexible one was 0.2 % MWCNT-COOH when air gap:0cm and take-up speed:4.2m as 4,37 % \pm 0,2% elongation.

Antibacterial activity of the membranes were also investigated however it was found that MWCNTs showed no antibacterial activity.

When considering all results, 3 different membranes were chosen as optimized membranes which include all desired properties together. In Table 5.1, optimized membranes and their properties can be seen.

Table 5.1 : Membranes were chosen as the best optimized membranes considering all dope solutions and spinning parameters and their properties.

Chosen Membranes		0.4% MWCNT-COOH (air gap:15cm, take-up speed:8.4m)	0.8% MWCNT-COOH (air gap: 15cm, take-up speed: 8.4m)	0.2% MWCNT-OH (air gap:0cm, take-up speed:4.2m)
Permeability (L/m ² .hr.bar)		275.04	409	94
Contact angle (°)		67 \pm 4,5	59 \pm 3,4	77 \pm 1,5
Porosity (%)		69	40	33
FR %		90	70	97
BSA Rejection %		58	25	30
Rt (%)	Rr (%)	1,85	56,9	49,1
	Rir (%)	9,7	29,7	3,29
Mechanical Stability	Young's modulus (MPa)	28	40	27
	Elongation at break (%)	8,35 \pm 0,7	5,18 \pm 0,4	4,51 \pm 0,6
SEM images				

REFERENCES

- Ahmed, S.F.**, (2010). Preparation and Characterization of Hollow Fiber Nanofiltration Membranes, MSc. Thesis, *University of Technology*, Malaysia.
- Albrecht, W., Kneifel, K., Weigel, T., Hilke, R., Just, R., Schossig, M., Ebert, K., Lendlein, A.**, (2005). Preparation of highly asymmetric hollow fiber membranes from polyetherimide by a modified dry-wet phase inversion technique using a triple spinneret, *Journal of membrane science*, 262, 69-80.
- Amoudi, A.A., Lovitt, R.W.**, (2007). Fouling strategies and the cleaning system of NF membranes and factors affecting cleaning efficiency, *Journal of membrane science*, 303, 4-28.
- Aroon, M.F., Ismail, A.F., Montezar-Rahmati, M.M., Matsuuara, T.**, (2010). Effect of Raw Multi-Wall Carbon Nanotubes on Morphology and Separation Properties of Polyimide Membranes, *Separation science and technology*, 45-16, 2287-2297.
- Baker, W. R.**, (2004). Membrane Technology And Applications, 2nd edition, *John Wiley and Sons, Ltd*.
- Bolong, N., Ismail, A.F., Salim, M.R., Matsuuara, T.**, (2008). Miscibility characteristics of polyethersulfone (PES) hollow fiber membranes with charged surface modifying macromolecules (cSMM) for water separations applications, *Jurnal Teknologi*, 49, 123-132.
- Bruggen, B.V.D.**, (2012). The separation power of nanotubes in membranes: a review, *ISRN Nanotechnology*, volume 2012, 17.
- Chen, G.E., Li, F.J., Han, L.F., Xu, Z.L., Yu, L.Y.**, (2010). Preparation of microporous polyethersulfone hollow fiber membranes using non-solvent vapour induced phase separation, *Iranian polymer journal*, 19 (11), 863-873.
- Choudhary, V., Gupta, A.**, (2011). Polymer/Carbon nanotube Composites, Book Chapter 4, *Intech*, 65-90.
- Chou, W.L., Yang, M.C.**, (2005). Effect of take-up speed on physical properties and permeation performance of cellulose acetate hollow fibers, *Journal of membrane science*, 250, 259-267.
- Chung, T.S., Xu, Z.L., Lin, W.**, (1999). Fundamental Understanding of the Effect of Air-Gap Distance on the Fabrication of Hollow Fiber Membranes, *Journal of Applied Polymer Science*, 72, 379-395.
- Çelik, E., Park, H., Choi, H., Choi, H.** (2011). Carbon nanotube blended polyethersulfone membranes for fouling control in water treatment, *Water research*, 45, 274-282.
- Çulfaz, P.Z., Rolevink, E., Rijn, C., Lammertink R.G.H., Wessling, W.**, (2010). Microstructured hollow fiber membranes for ultrafiltration, *Journal of membrane science*, 347, 32-41.

- Desmukh, S.P., Li, K.,** (1998). Effect of ethanol composition in water coagulation bath on morphology of PVDF hollow fibre membranes, *Journal of membrane science*, 150, 75-85.
- Goh, P.S., Ismail, A.F., Ng, B.C.,** (2012). Carbon nanotubes for desalination: Performance evaluation and current hurdles, *Desalination*, 308, 2-14.
- Goh, P.S., Ng, B.C., Ismail, A.F., Aziz, M., Hayashi, Y.,** (2012). Pre-Treatment of Multi-walled Carbon Nanotubes for Polyetherimide Mixed Matrix Hollow Fiber Membranes, *Journal of Colloid and Interface Science*, doi: 10.1016/j.jcis.2012.07.033.
- Han, L.F., Xu, Z.L., Yu, L.Y., Wei, Y.M., Cao, Y.,** (2010). Performance of PVDF/Multinanoparticles composite hollow fibre ultrafiltration membranes, *Iranian polymer journal*, 19 (7), 553-565.
- Ismail, A.F., Mustaffar, M.I., Illias, R.M., Abdullah, M.S.,** (2006). Effect of dope extrusion rate on morphology and performance of hollow fibers membrane for ultrafiltration, *separation and purification technology*, 49, 10-19.
- Khayet, M.** (2003). The effects of air gap length on the internal and external morphology of hollow fiber membranes, *Chemical engineering science*, 58, 3091-3104.
- Kools, W.,** (1998). Membrane Formation By Phase Inversion in Multicomponent Polymer Systems Mechanisms and Morphologies, PhD thesis, *University of Twente*.
- Koros W.J., Ma, Y.H., Shimidzu, T.,** (1996). Terminology for membranes and Membrane processes, *Pure & Appl. Chem.*, Vol. 68, No. 7, pp. 1479-1489.
- Li N.N., Fane A.G., Ho W.S.W., Matsuura T.,** (2008). Advanced membrane technology and applications, *Wiley Publications*.
- Li, W., Bai, Y., Zhang, Y., Sun, M., Cheng, R., Xu, X., Chen, Y., Mo, Y.,** (2005). Effect of hydroxyl radical on the structure of multi walled carbon nanotubes, *Synthetic materials*, 155, 509-515.
- Li, X., Liu, H., Xiao, C., Ma, S., Zhao, X.,** (2012). Effect of take-up speed on polyvinylidene fluoride hollow fiber membrane in a thermally induced phase separation process, *Journal of applied polymer science*, DOI: 10.1002/app.37919.
- Li, X.M., He, T.,** (2007). Does more solvent in bore liquid create more open inner structure in hollow fiber membranes?, *Polymers for advanced technologies*, 19, 801-806.
- Liu, Z., Zhang, G., Peng, Y. Ji, S.,** (2008). The hollow fiber ultrafiltration membrane with inner skin and its application, *Desalination*, 233, 55-63
- Loh, C.H., Wang, R., Shi, L., Fane, A.G.,** (2011). Fabrication of high performance polyethersulfone UF hollow fiber membranes using Pluronic block copolymers as pore forming additives, *Journal of membrane science*, 380, 111-123.
- Machado, P.S.T., Habert, A.C., Borges, C.P.,** (1999). Membrane formation mechanism based on precipitation kinetics and membrane morphology : flat and hollow fiber polysulfone membranes, *Journal of membrane science*, 155, 171-183.

- Merkel, T.C., Freeman B.D., Spontak R.J., He, Z., Pinnau I., Meakin, P., Hill, A.J.,** (2002). Ultrapermeable, reverse-selective nanocomposite membranes, *Science* 296, 519.
- Ng, L.Y., Mohammad, A.W., Leo, C.P., Hilal, N.,** (2010). Polymeric membranes incorporated with metal/metal oxide nanoparticles: A comprehensive review, *Desalination*, doi: 10.1016/j.desal.2010.11.033.
- Ohya, H., Shiki, S., Kawakami, H.,** (2009). Fabrication study of polysulfone hollow fiber microfiltration membranes: optimal dope viscosity for nucleation and growth, *Journal of membrane science*, 326, 293-302.
- Pabby, A.K., Sastre, A.M.,** (2008). Hollow fiber membrane-based separation technology: Performance and design, Book Chapter 4, *Taylor & Francis Group, LLC*, page 92-135
- Peng, N., Widjojo, N., Sukitpaneenit, P., Teoh, M.M., Limscomp, G.G., Chung, T.S., Lai, J.Y.,** (2012). Evolution of polymeric hollow fibers as sustainable technologies: Past, present and future, *Progress in polymer science*, 37, 1401-1424.
- Qin, J., Chung, T.S.,** (1999). Effect of dope flow rate on the morphology, separation performance, thermal and mechanical properties of ultrafiltration hollow fiber membranes, *Journal of Membrane Science*, 157, 35-51.
- Razmjou, A., Resosudarmo, A., Holmes, R.L., Li, H.,** (2011). The effect of modified TiO₂ nanoparticles on the polyethersulfone ultrafiltration hollow fiber membranes, *Desalination*, 287, 271-280.
- Rugbani, A.,** (2009). Investigating The Influence of Fabrication Parameters on the Diameter and Mechanical Properties of Polysulfone Ultrafiltration Hollow-Fibre Membranes, MSc. Thesis, *University of Stellenbosch*.
- Saljoughi, E., Amirilargani, M., Mohammadi, T.,** (2010). Effect of PEG additive and coagulation bath temperature on the morphology, permeability and thermal/chemical stability of asymmetric CA membranes, *Desalination*, 262, 72-78.
- Singh, R.,** (2006). Hybrid Membrane Systems for Water Purification: Technology, Systems Design and Operations, *Elsevier*.
- Spitalsky, Z., Tasis, D., Papagelis, K., Galiotis, C.,** (2010). Carbon nanotube-polymer composites: Chemistry, processing, mechanical and electrical properties, *Progress in polymer science*, 35, 357-401.
- Scott, K.,** (1999). Handbook of Industrial Membranes, *Elsevier*, second edition.
- Vatanpour V., Madaeni, S.S., Moradian, R., Zinadini, S., Astinchap, B.,** (2011). Fabrication and characterization of novel antifouling nanofiltration from oxidized multiwalled carbon nanotube/polyether sulfone nanocomposite, *Journal of Membrane Science*, 375, 284-294.
- Vatanpour V., Madaeni, S.S., Moradian, R., Zinadini, S., Astinchap, B.,** (2012). Novel antibiofouling nanofiltration polyethersulphone membrane fabricated from embedding TiO₂ coated multiwalled carbon nanotubes, *Separation and purification technology*, 90, 69-82.
- Wagner, J.,** (2001). Membrane Filtration Handbook Practical Tips and Hints by *Chem. Eng Second Edition, Revision 2*. page 7, 10-13.
- Wang, K.Y., Matsuura, T., Chung, T.S., Guo, W.F.** (2004). The effects of flow angle and shear rate within the spinneret on the separation

performance of polyethersulfone (PES) ultrafiltration hollow fiber membranes, *Journal of membrane science*, 240, 67-79.

- Wienk, I.M.**, (1993). Ultrafiltration Membranes from a polymer blend: hollow fiber preparation and characterization, thesis, *University of Twente*.
- Wienk, I.M., Meuleman, E.E.B., Borneman, Z., Boomgaard, T., Smolders, C.A.**, (1995). Chemical Treatment of Membranes of a Polymer Blend: Mechanism of the Reaction of Hypochlorite with Poly(vinyl pyrrolidone), *Journal of Polymer Science: Part A Polymer Chemistry*, 33, 49-54.
- Wienk, I.M., Scholtenhuis, F.H.A.O., Boomgaard, T., Smolders, C.A.**, (1995). Spinning of hollow fiber ultrafiltration membranes from a polymer blend, *Journal of membrane science*, 106, 233-243.
- Wienk, I.M., Teunis H.A., Boomgaard Th v.d., Smolders C.A.** (1993). A new spinning technique for hollow fiber ultrafiltration membranes, *Journal of Membrane Science*, 78, 93-100.
- Wongchitphimon S., Wang, R., Jiratananon, R., Shi, L., Loh, C.H.**, (2011). Effect of polyethylene glycol (PEG) as an additive on the fabrication of polyvinylidene fluoride-co-hexafluoropropylene (PVDF-HFP) asymmetric microporous hollow fiber membranes, *Journal of membrane science*, 369, 329-338.
- Xu, P.D., Lü, S.L., Zhen, W.X., Ku, B.K., Yi, X.Y.**, (2008). Effect of coagulation bath temperature on the structure and performance of polyethersulfone hollow fiber membranes by dry/wet process, *Journal of clinical rehabilitative tissue engineering research*, 12, 5381-5384.
- Xu, Z.L., Q, F.A.**, (2004). Polyethersulfone (PES) hollow fiber ultrafiltration membranes prepared by PES/non-solvent/NMP solution, *Journal of Membrane Science*, 233, 101-111.
- Zhang, X., Wen, Y., Yang, Y., Liu, L.**, (2008). Effect of Air-Gap Distance on the Formation and Characterization of Hollow Polyacrylonitrile (PAN) Nascent Fibers, *Journal of macromolecular science, part B: physics*, 47, 1039-1049.
- Zodrow, K.R.** (2009). Polysulfone ultrafiltration membranes impregnated with silver nanoparticles show improved biofouling resistance and virus removal, MSc. Thesis, *Rice University*.
- Url-1** <<http://www.nanowerk.com/spotlight/spotid=4662.php>>, date retrieved 12.10.2012
- Url-2** <<http://www.yale.edu/env/elimelech/Conc-Polarization/sld002.htm>>, date retrieved 23.10.2012
- Url-3** <<http://www.yale.edu/env/elimelech/CP1/sld003.htm>>, date retrieved 23.10.2012
- Url-4** <<http://sciencelay.com/technology/applied-science/membrane-separation/>>, date retrieved, 23.10.2012
- Url-5** <<http://www.cheresources.com/content/articles/separation-technology/hollow-fiber-membranes?pg=3>>, date retrieved 23.10.2012

- Url-6** <<http://www.biologica.eng.uminho.pt/psb/docs/textoFicha3.pdf>>, date
retrieved 23.10.2012
- Url-7** <<http://www.toyobo.co.jp/e/seihin/ro/tokucho.htm>>, date retrieved
08.12.2012
- Url-8** <<http://www.fibersource.com/f-tutor/techpag.htm>>, date retrieved
08.12.2012
- Url-9** <<https://data.epo.org/publication-server/rest/v1.0/publication-dates/20100922/patents/EP2094764NWB1/document.html>>, date
retrieved 08.12.2012
- Url-10** <http://www.tjskl.org.cn/products-search/czad2acb/polyvinylpyrrolidone_k-pz262ff89.html>, date retrieved 08.12.2012

APPENDICES

APPENDIX A: SEM and Stereo Microscope Images of Fabricated Membranes

APPENDIX A

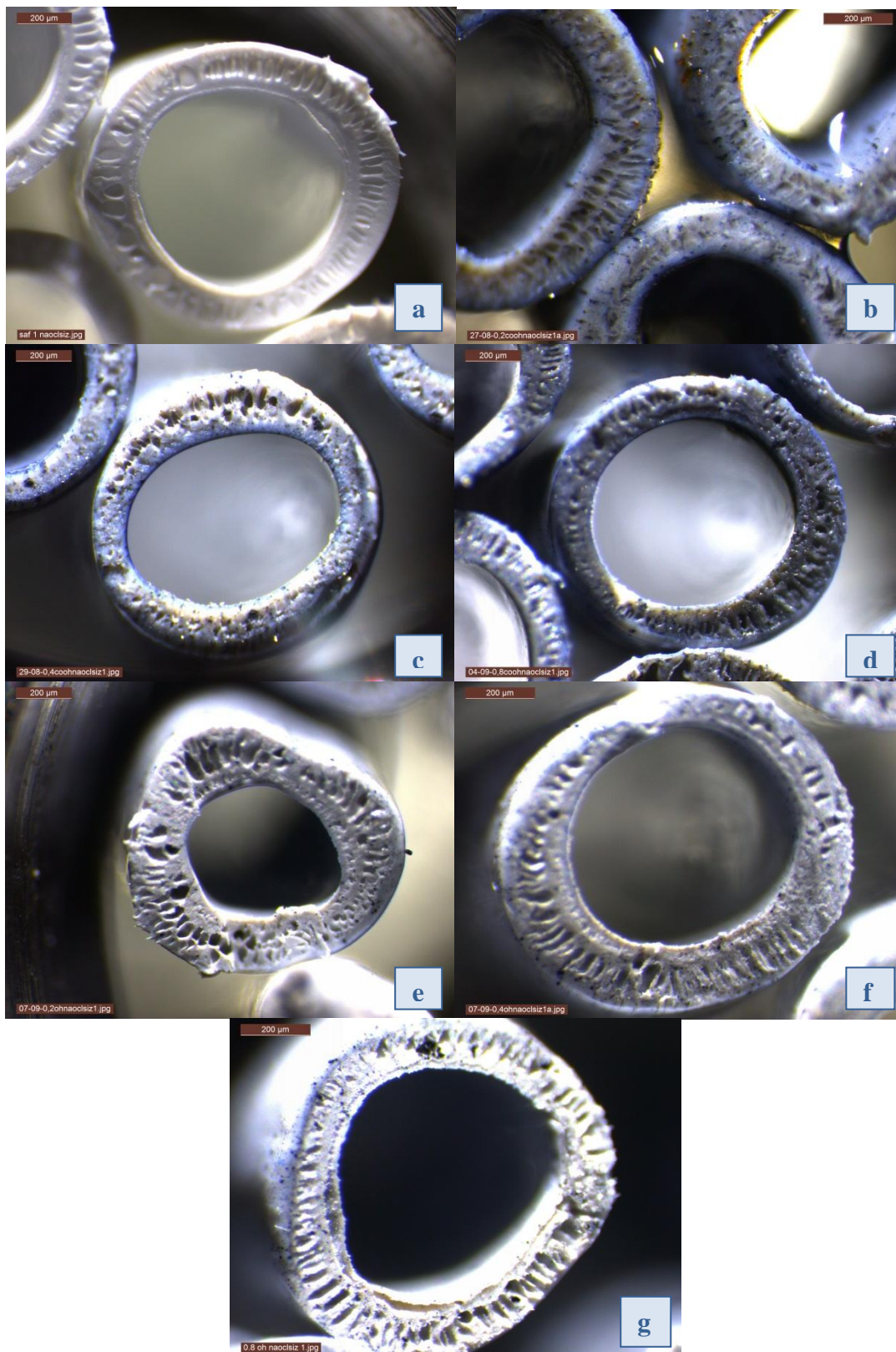


Figure A.1 : Cross section stereo microscope pictures of #1 membranes without post treatment. a) pristine 1, b) 0.2COOH 1, c) 0.4COOH 1, d) 0.8COOH 1, e) 0.2OH 1, f) 0.4OH 1, g) 0.8OH 1.

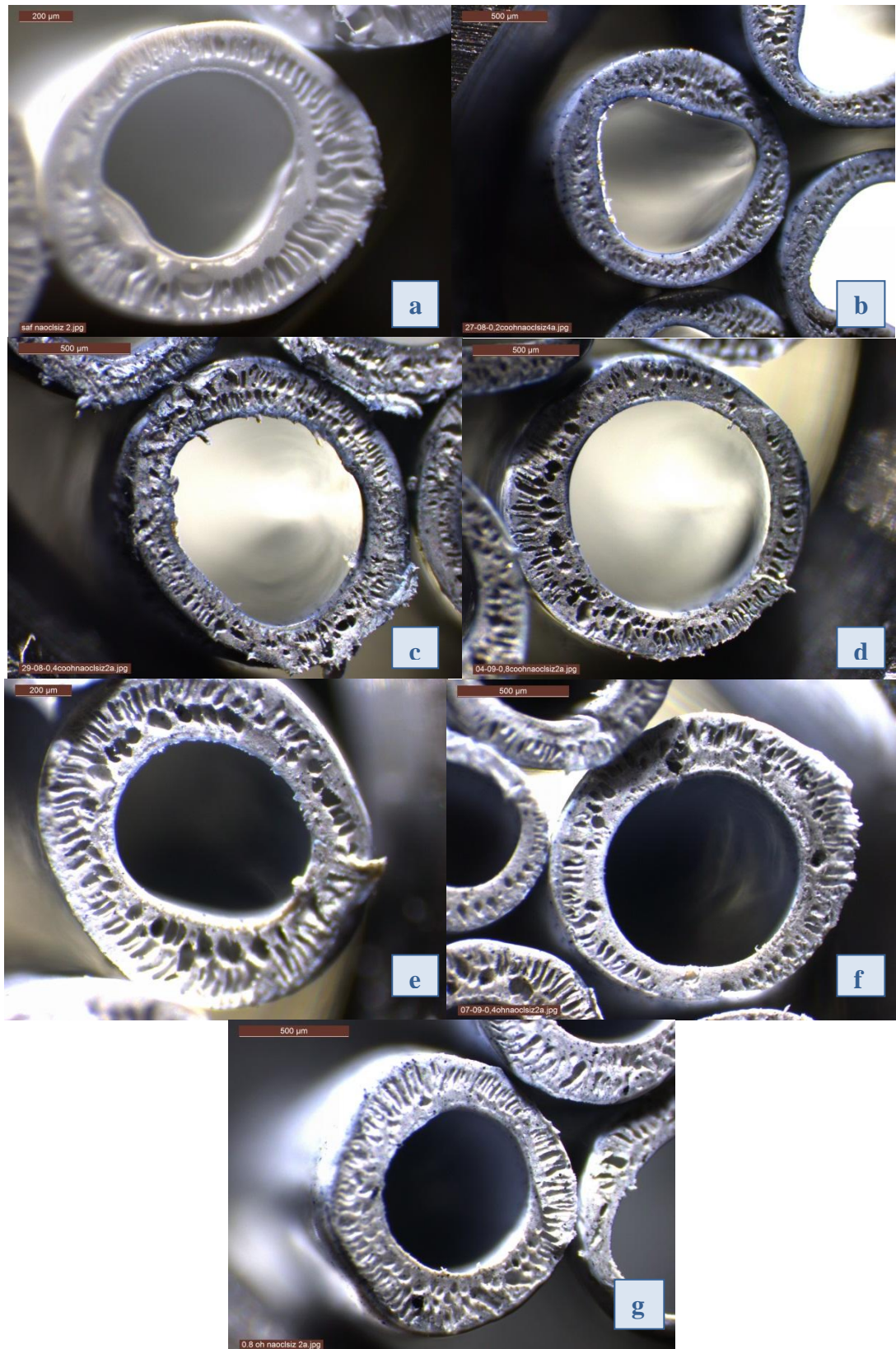


Figure A.2 : Cross section stereo microscope pictures of #2 membranes without post treatment. a) pristine 2, b) 0.2COOH 2, c) 0.4COOH 2, d) 0.8COOH 2, e) 0.2OH 2, f) 0.4OH 2, g) 0.8OH 2.

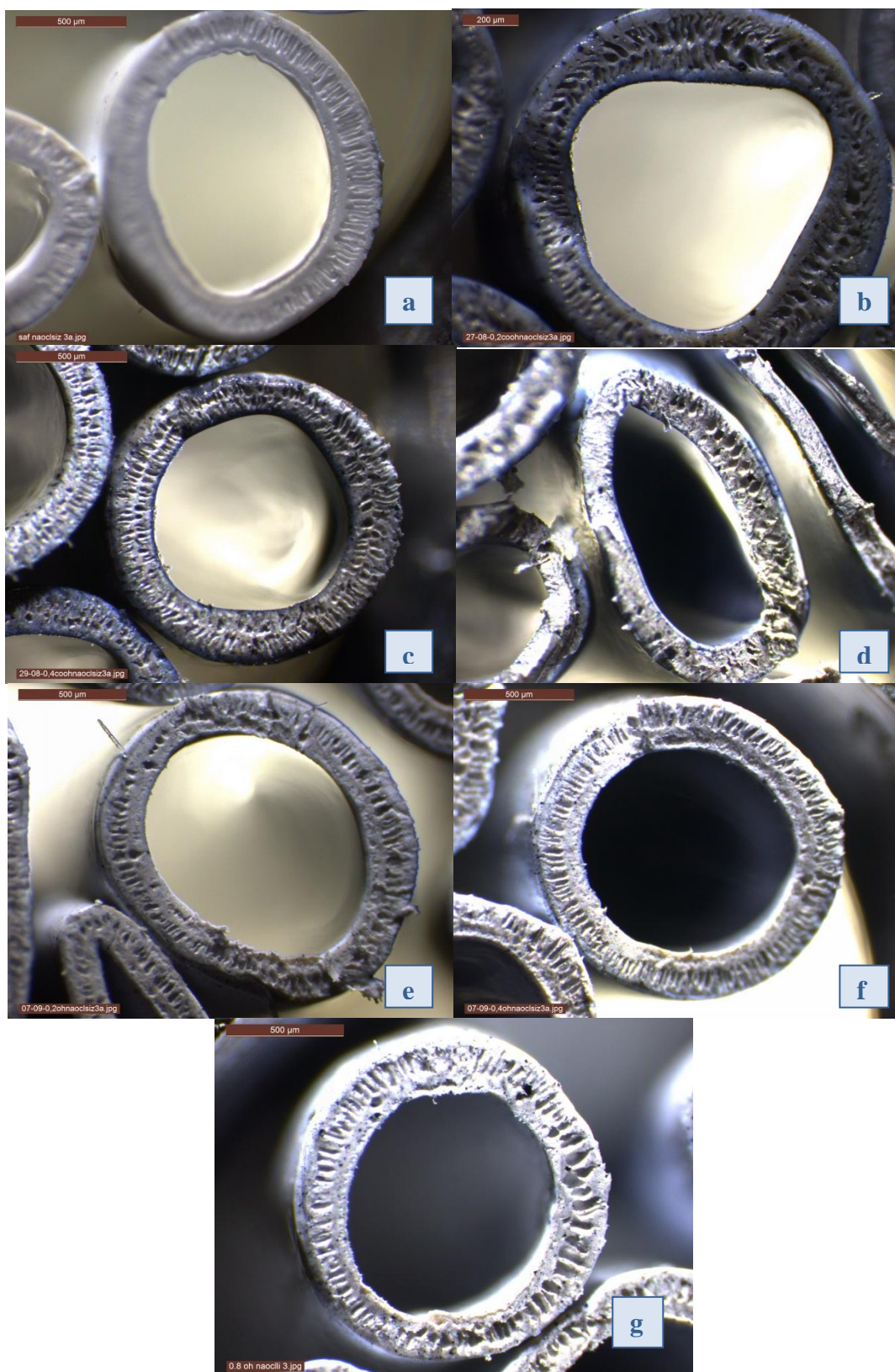


Figure A.3 : Cross section stereo microscope pictures of #3 membranes without post treatment. a) pristine 3, b) 0.2COOH 3, c) 0.4COOH 3, d) 0.8COOH 3, e) 0.2OH 3, f) 0.4OH 3, g) 0.8OH 3.



Figure A.4 : Cross sectional view of #1 membranes without post treatment. a) Pristine 1, b) 0.2COOH 1, c) 0.4COOH 1, d) 0.8COOH 1, e) 0.2OH 1, f) 0.4OH 1, g) 0.8OH 1.

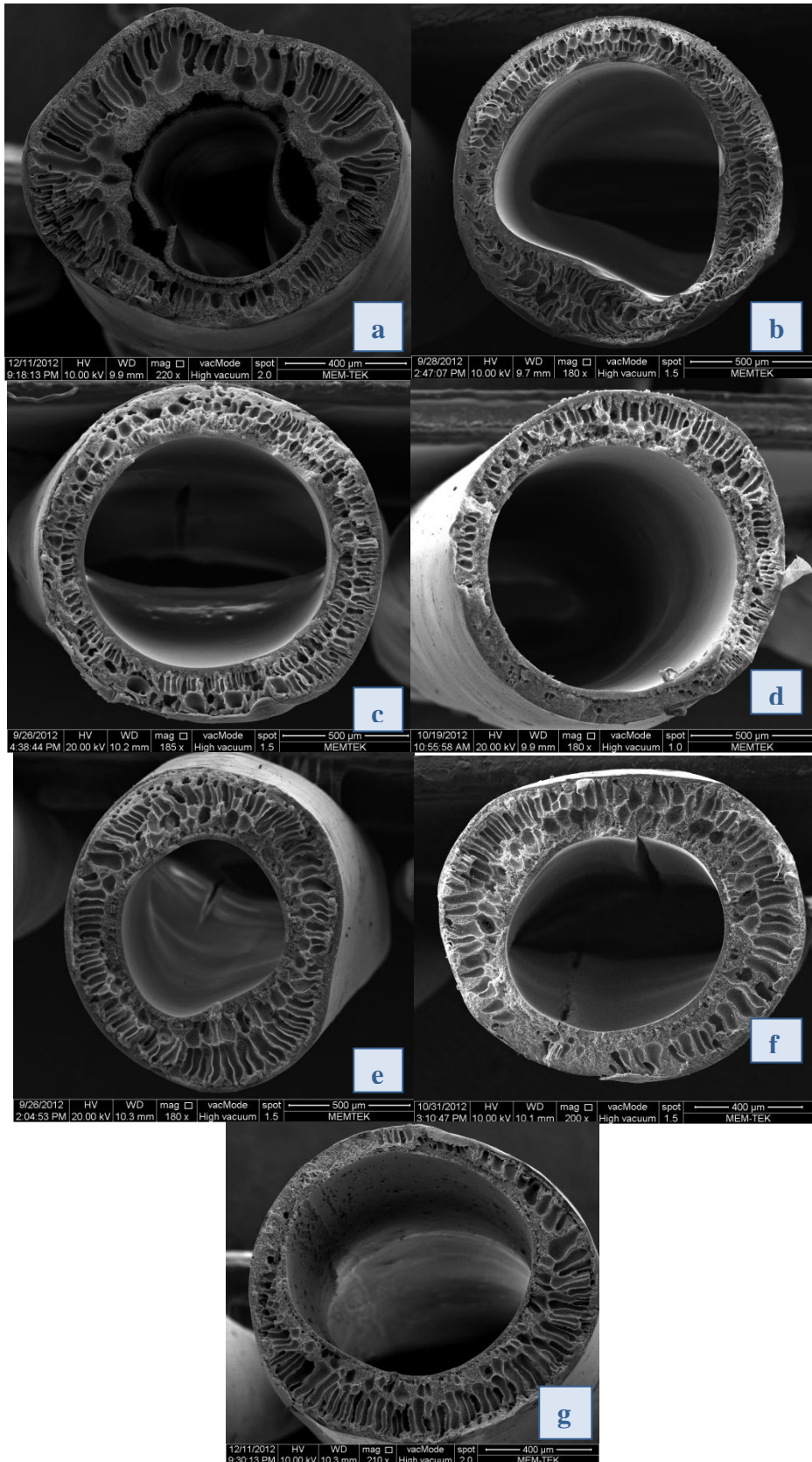


Figure A.5 : Cross sectional view of #2 membranes without post treatment. a) Pristine 2, b) 0.2COOH 2, c) 0.4COOH 2, d) 0.8COOH 2, e) 0.2OH 2, f) 0.4OH 2, g) 0.8OH 2.

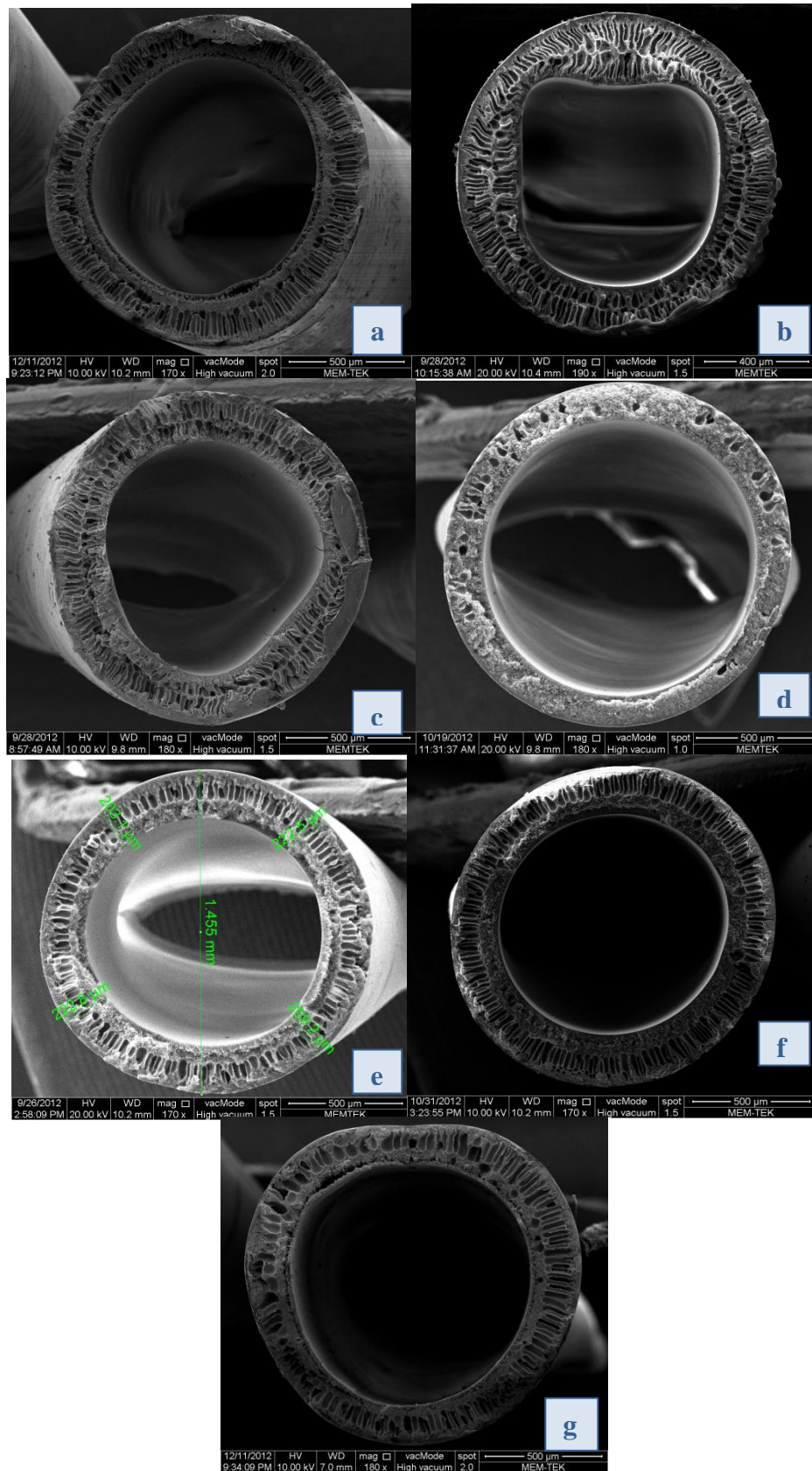


Figure A.6 : Cross sectional view of #3 membranes without post treatment. a) Pristine 3, b) 0.2COOH 3, c) 0.4COOH 3, d) 0.8COOH 3, e) 0.2OH 3, f) 0.4OH 3, g) 0.8OH 3.

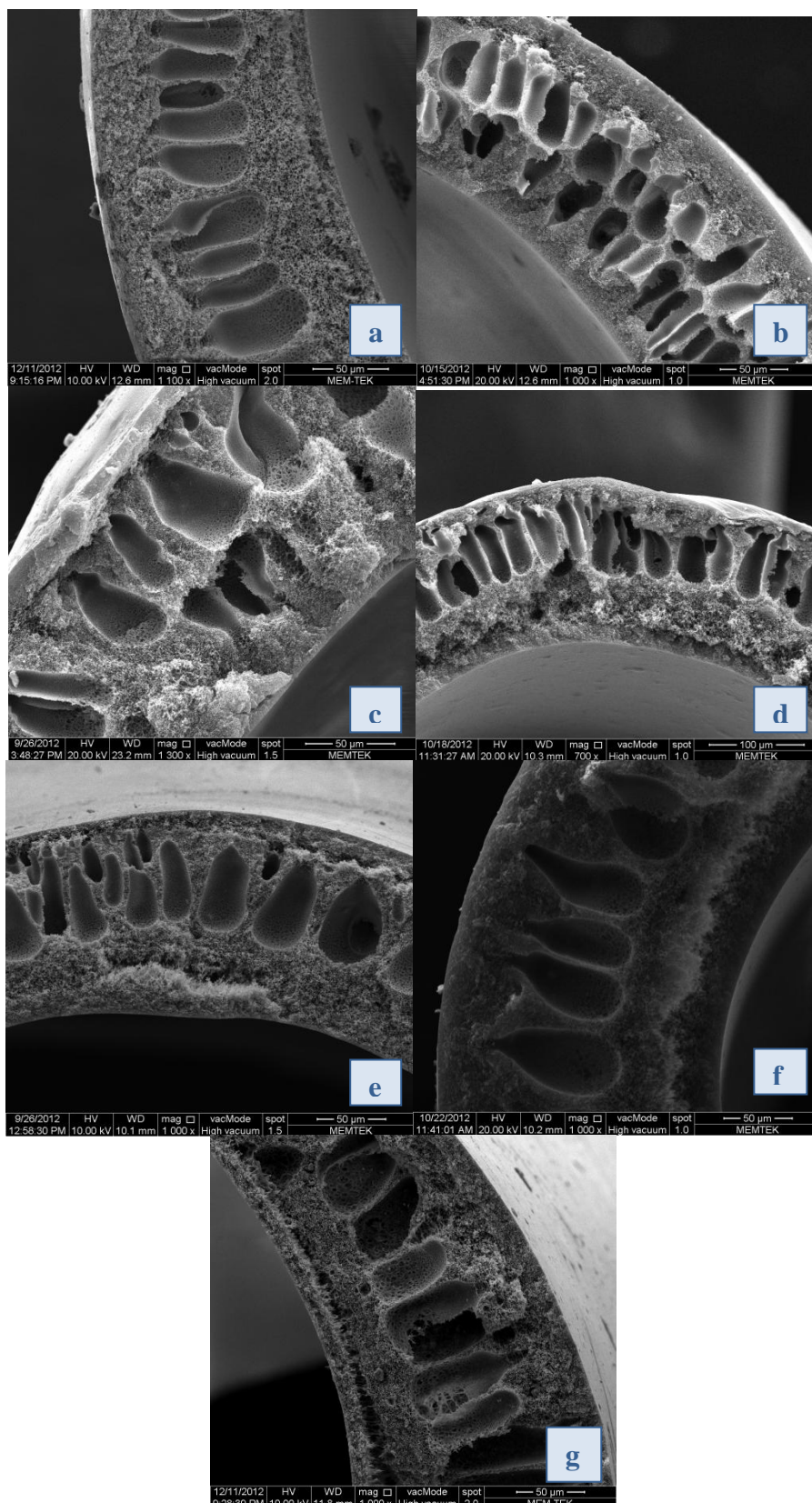


Figure A.7 : Detailed cross sectional view of #1 membranes without post treatment.
 a) Pristine 1, b) 0.2COOH 1, c) 0.4COOH 1, d) 0.8COOH 1, e) 0.2OH 1, f) 0.4OH 1, g) 0.8OH 1.

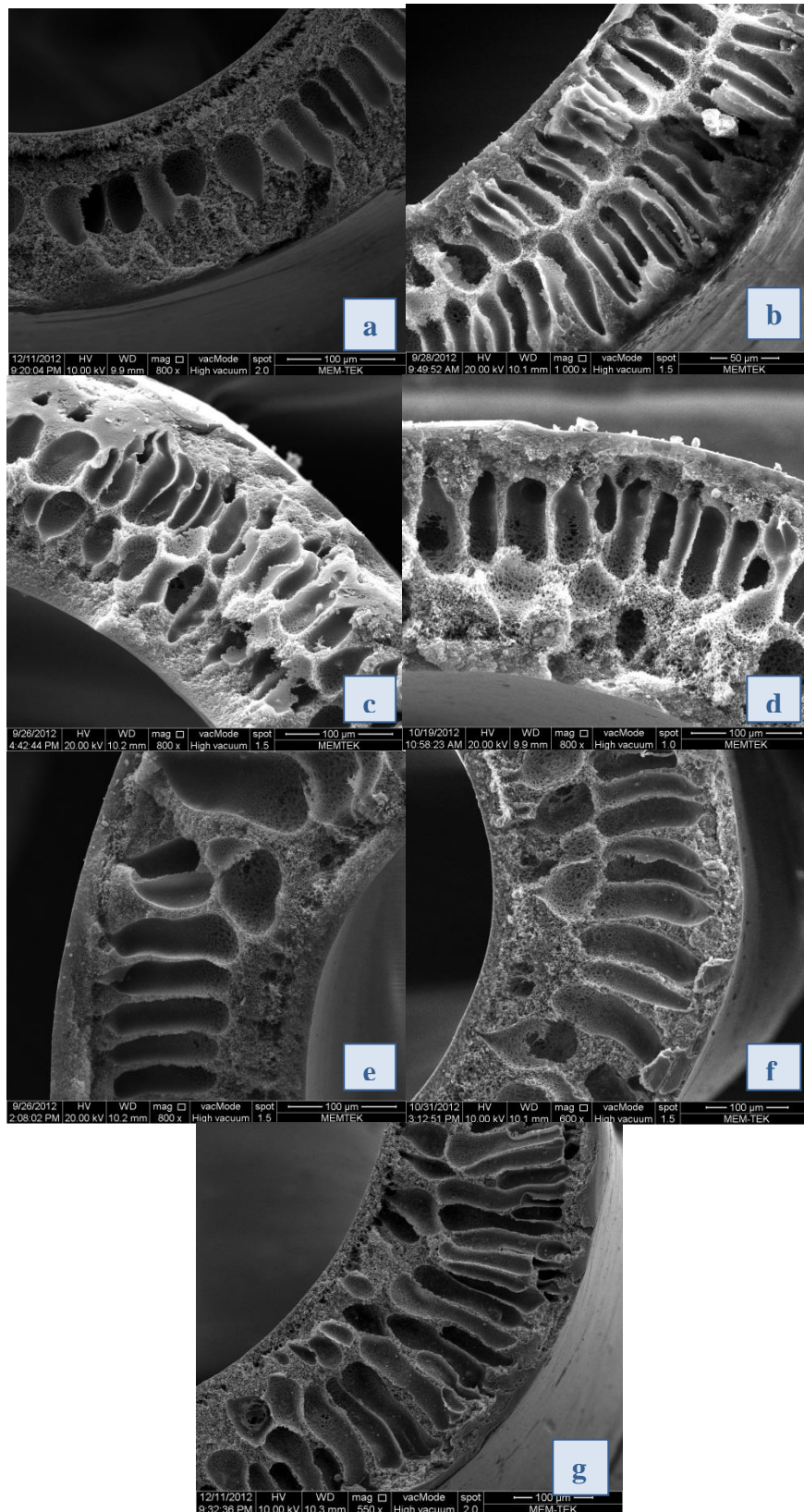


Figure A.8 : Detailed cross sectional view of #2 membranes without post treatment.
 a) Pristine 2, b) 0.2COOH 2, c) 0.4COOH 2, d) 0.8COOH 2, e) 0.2OH 2, f) 0.4OH 2, g) 0.8OH 2.

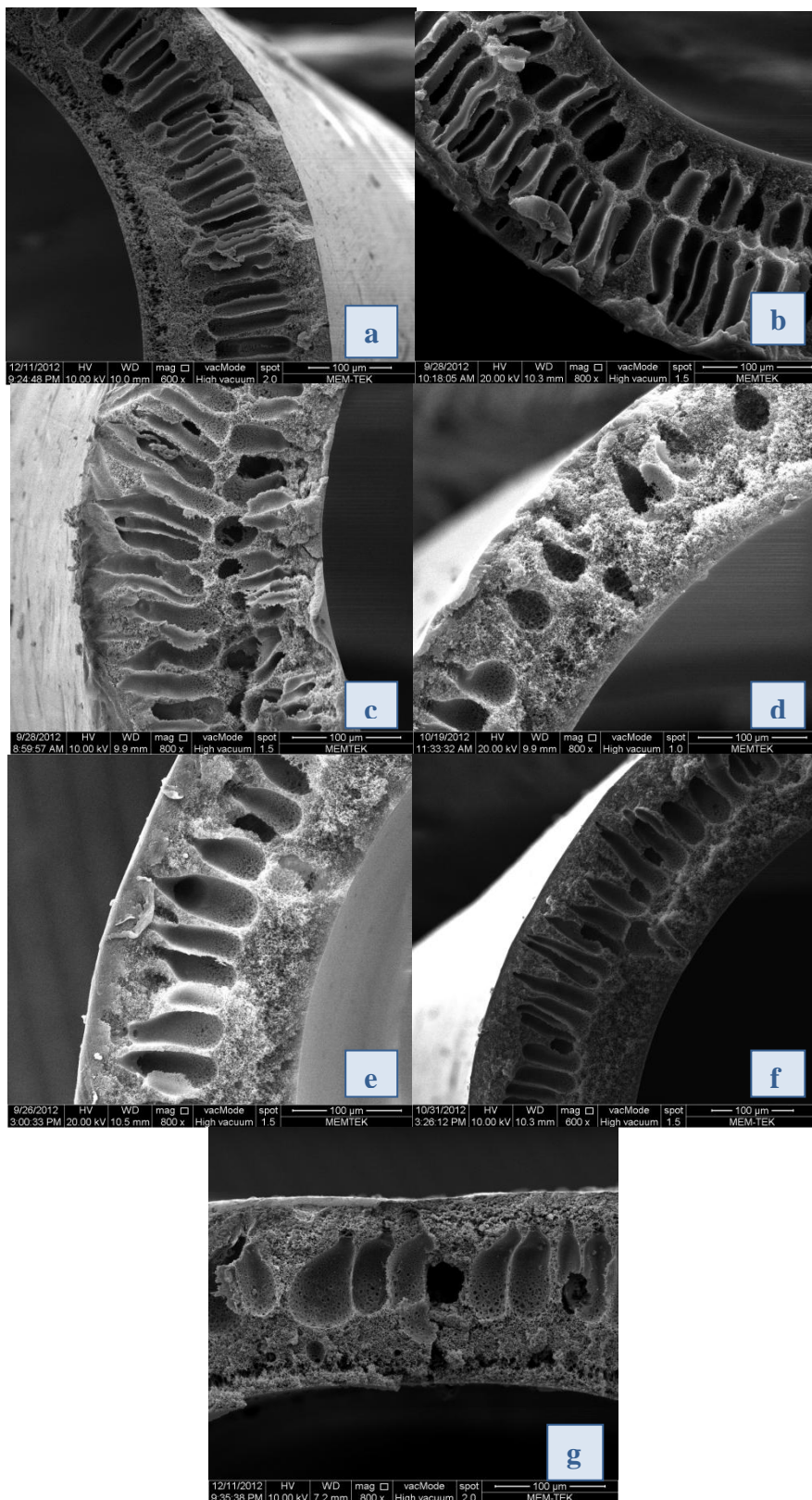


Figure A.9 : Detailed cross sectional view of #3 membranes without post treatment.
 a) Pristine 3, b) 0.2COOH 3, c) 0.4COOH 3, d) 0.8COOH 3, e) 0.2OH 3, f) 0.4OH 3, g) 0.8OH 3.

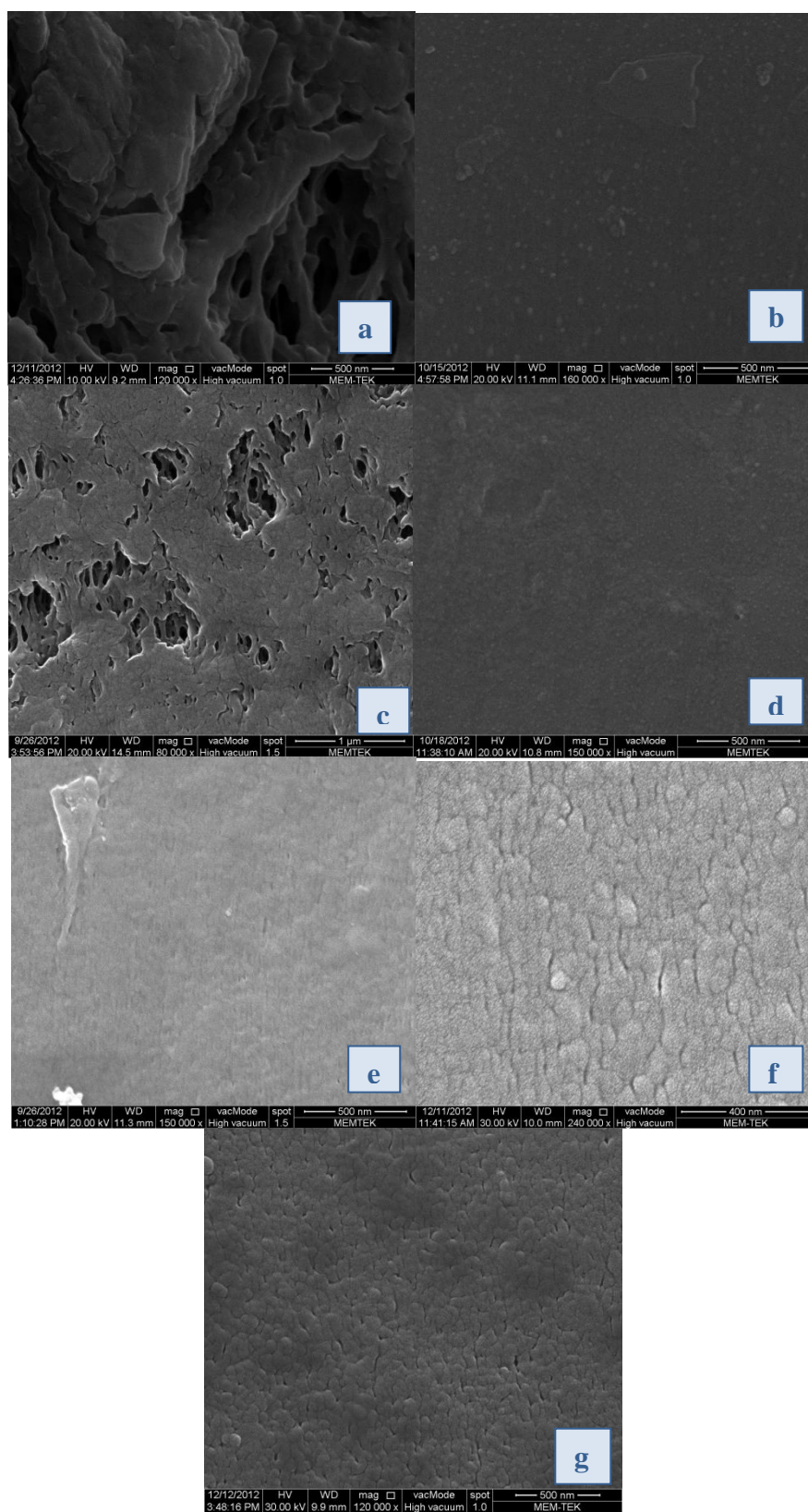


Figure A.10 : Outer surface images of #1 membranes without post treatment. a) Pristine 1, b) 0.2COOH 1, c) 0.4COOH 1, d) 0.8COOH 1, e) 0.2OH 1, f) 0.4OH 1, g) 0.8OH 1.

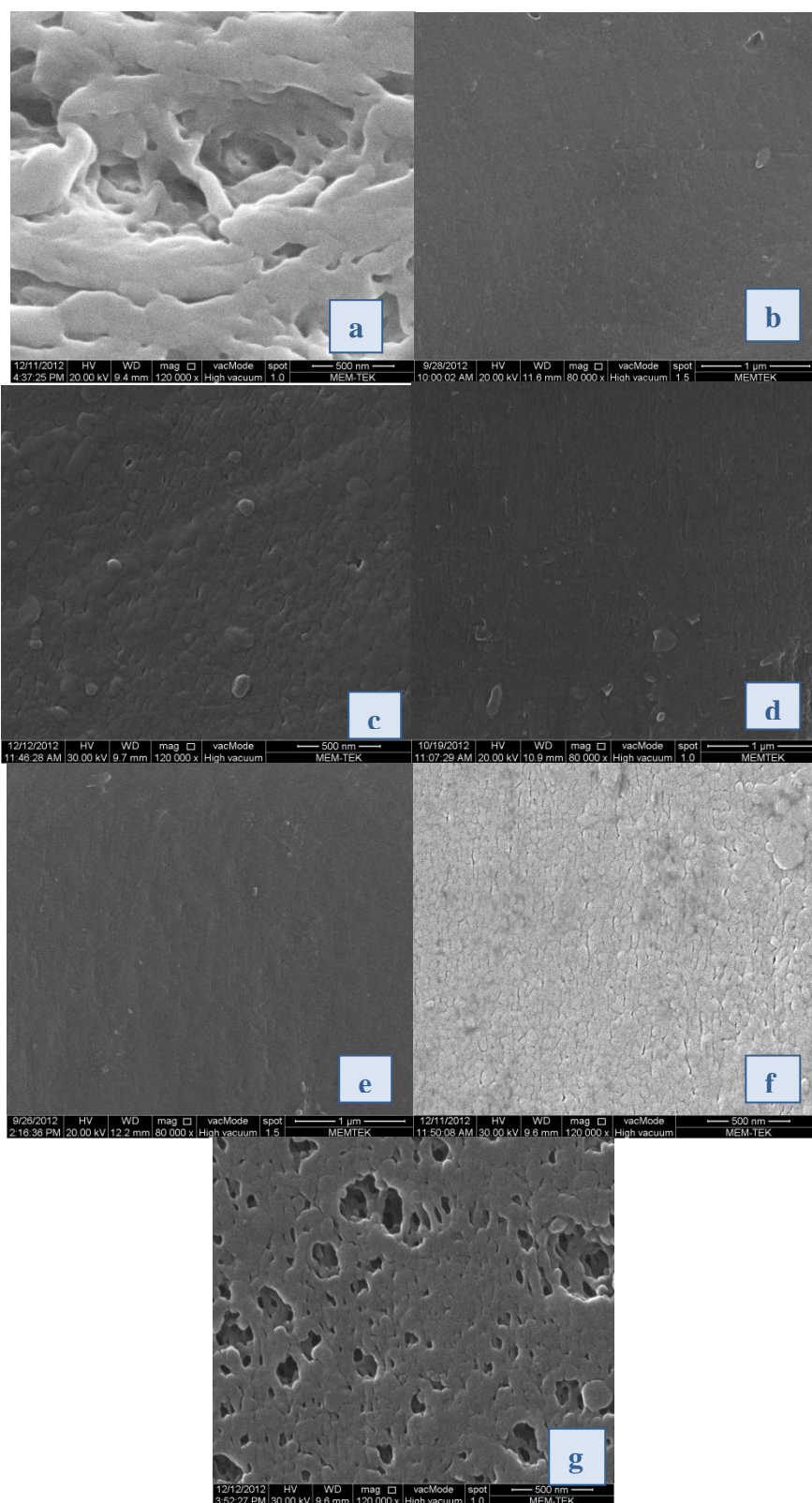


Figure A.11 : Outer surface images of #2 membranes without post treatment. a) Pristine 2, b) 0.2COOH 2, c) 0.4COOH 2, d) 0.8COOH 2, e) 0.2OH 2, f) 0.4OH 2, g) 0.8OH 2.

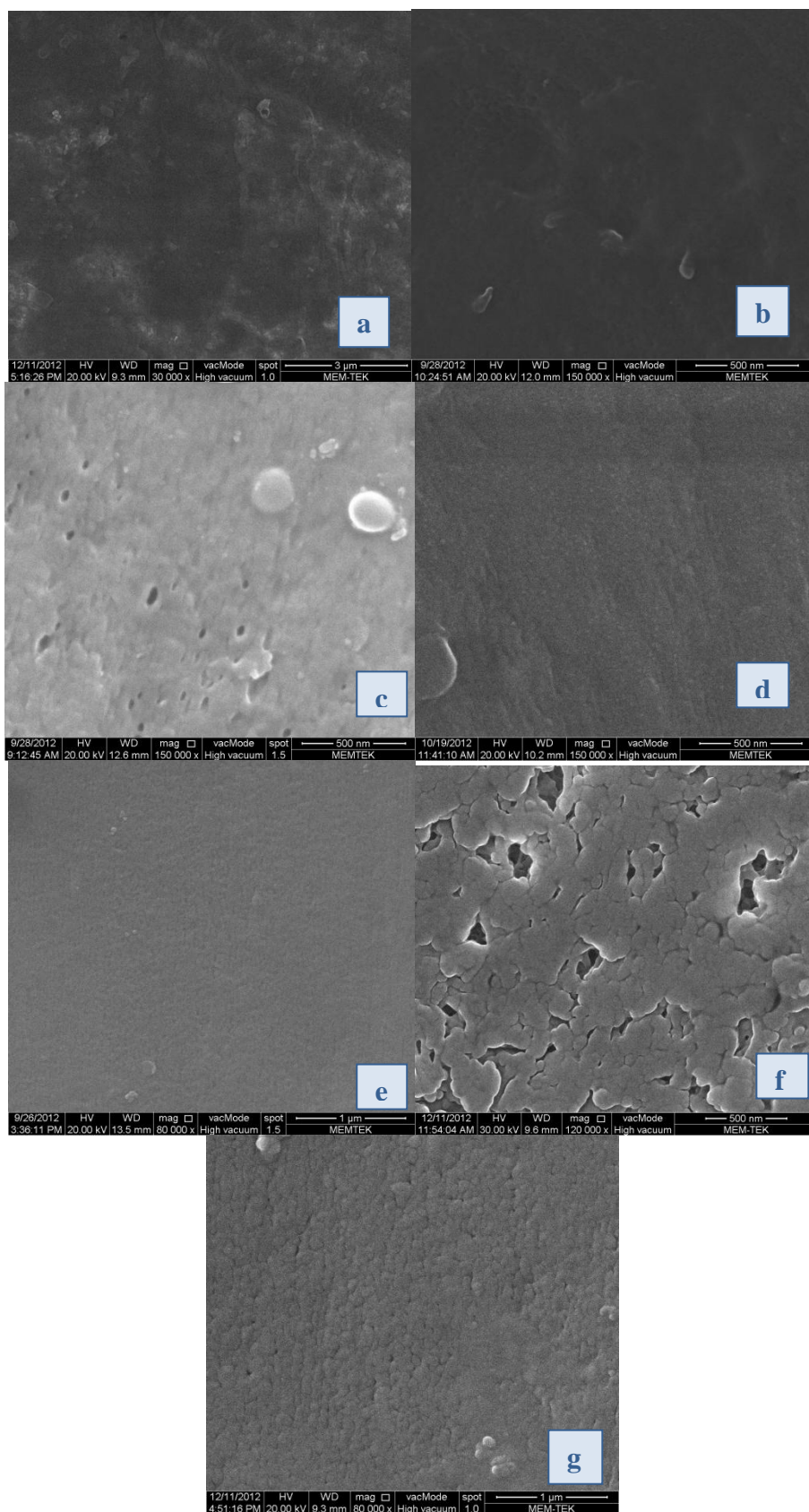


Figure A.12 : Outer surface images of #3 membranes without post treatment. a) Pristine 3, b) 0.2COOH 3, c) 0.4COOH 3, d) 0.8COOH 3, e) 0.2OH 3, f) 0.4OH 3, g) 0.8OH 3.

CURRICULUM VITAE



Name Surname: Reyhan ŞENGÜR

Place and Date of Birth: Bakırköy – İstanbul, 16/09/1987

Address: Bağcılar, İstanbul

E-Mail: reyhansengur@gmail.com

B.Sc.: Marmara University – Environmental Engineering, 2010

M.Sc.: Istanbul Technical University – Nanoscience & Nanoengineering, 2013

Professional Experience and Rewards:

Istanbul Technical University – Department of Nanoscience & Nanoengineering,
Research Assistant (2010 -)

TUBITAK BİDEB 2210 – National scholarship Programme for M.Sc. Students
(2010 -)